



XIV Zababakhin Scientific Talks,
RFNC-VNIITF
March 18-22, 2019
Snezhinsk

Atomistic simulations of defects formation at swift heavy ion irradiation in U-Mo alloy

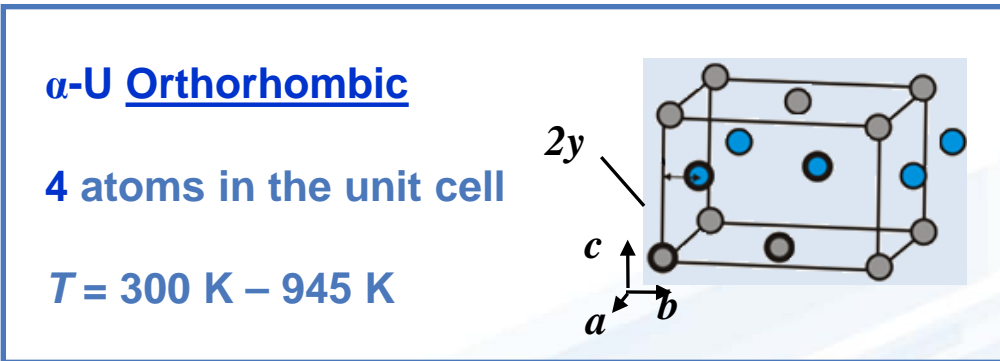
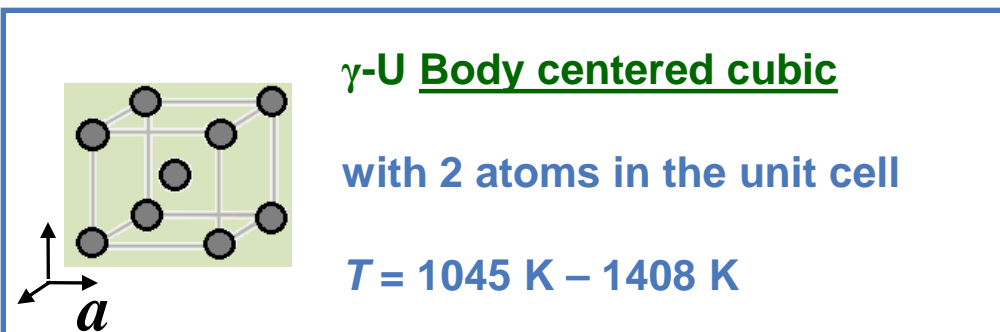
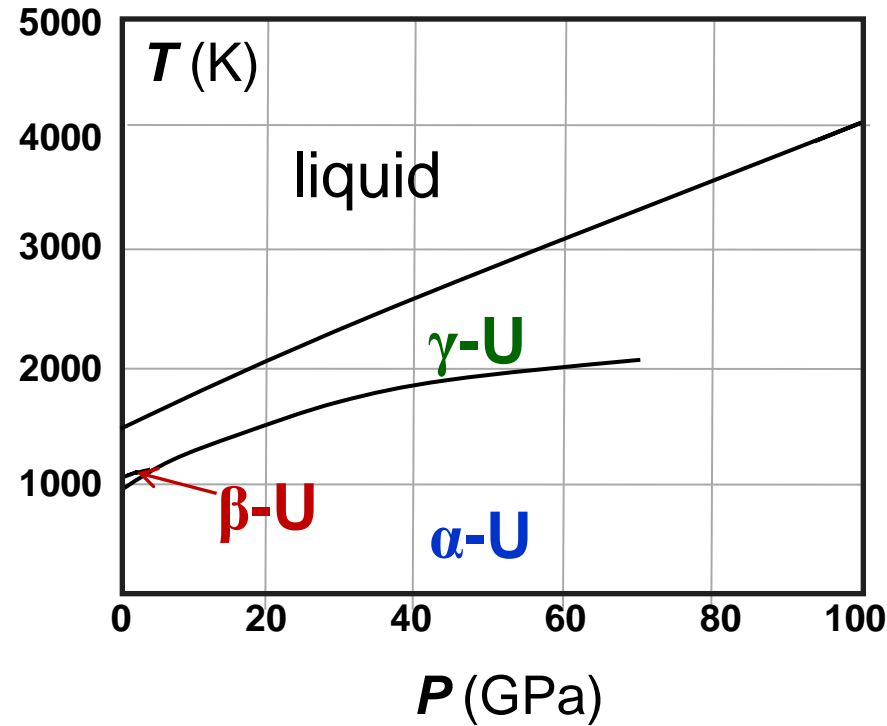
Kolotova L.N., Starikov S.V.

Joint Institute for High Temperatures
Moscow Institute of Physics and Technology

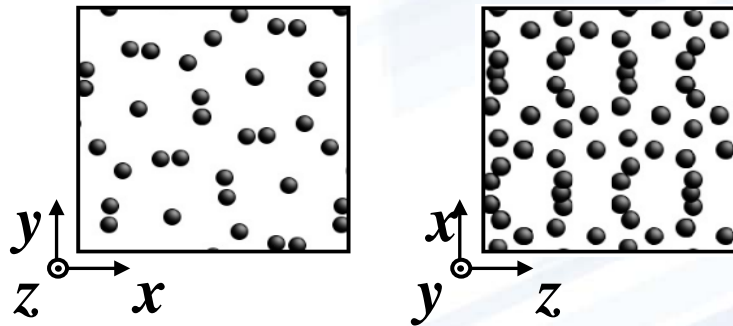
Contents

- Motivation
- U-Mo alloy structures
- U-Mo alloy temperature-concentration diagram
- Defect formation at heating/melting of ionic subsystem
- The threshold stopping power of swift ions dependence on temperature in γ -phase

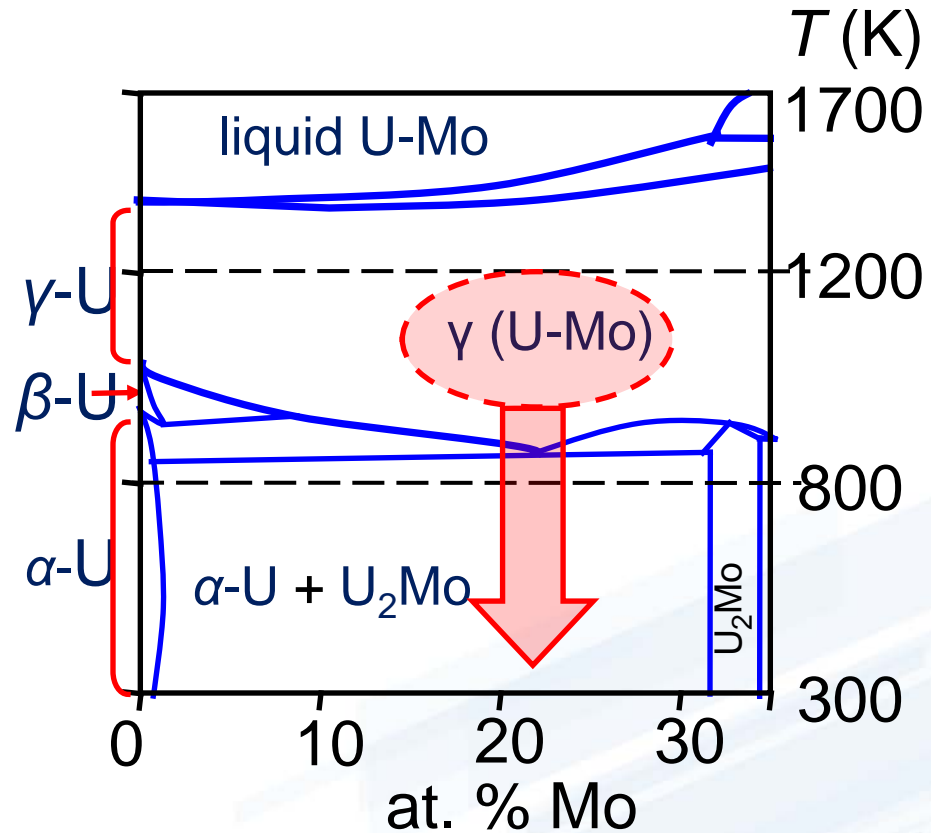
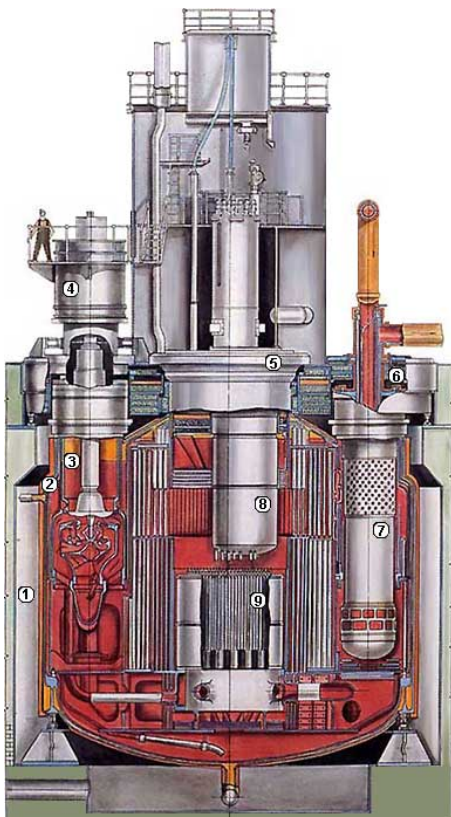
Phase diagram of pure uranium



$\beta\text{-U}$ Tetragonal
with 30 atoms in the unit cell
 $T = 945 \text{ K} - 1045 \text{ K}, P < 3 \text{ GPa}$



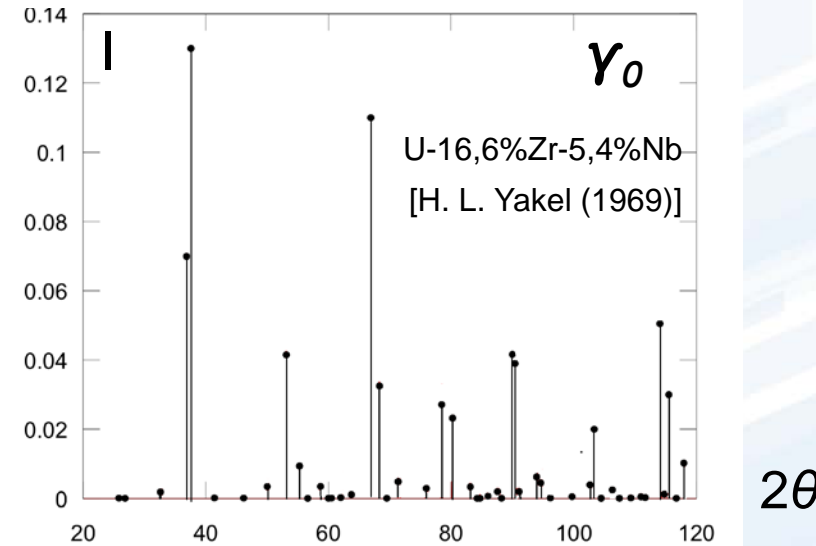
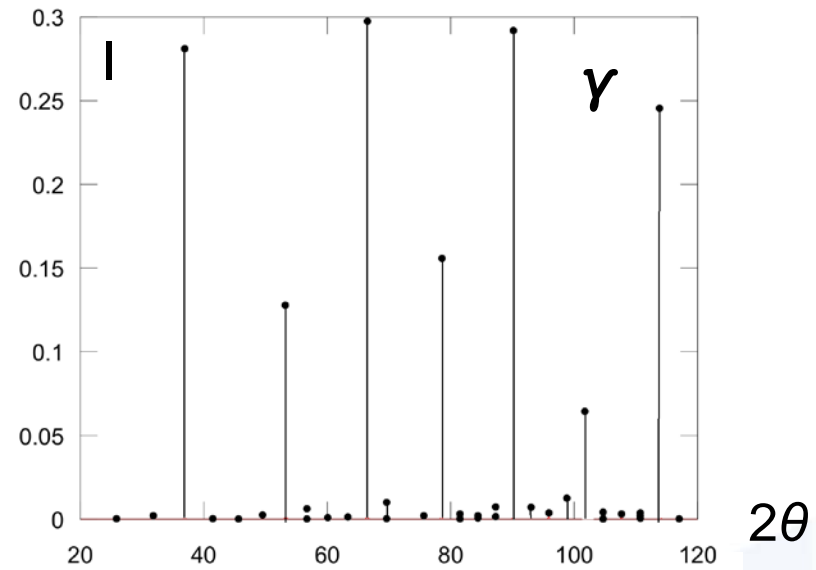
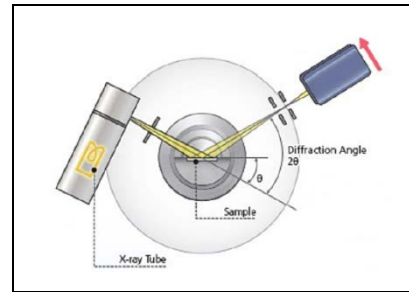
U-Mo alloys



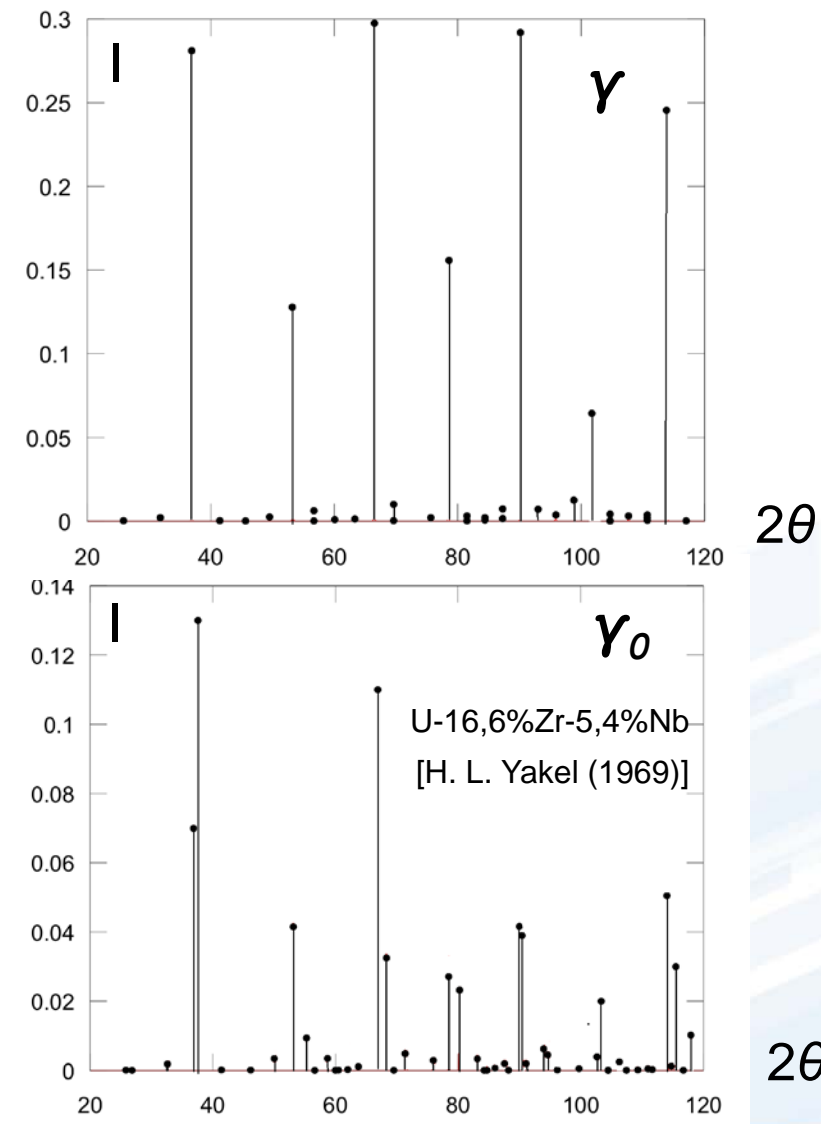
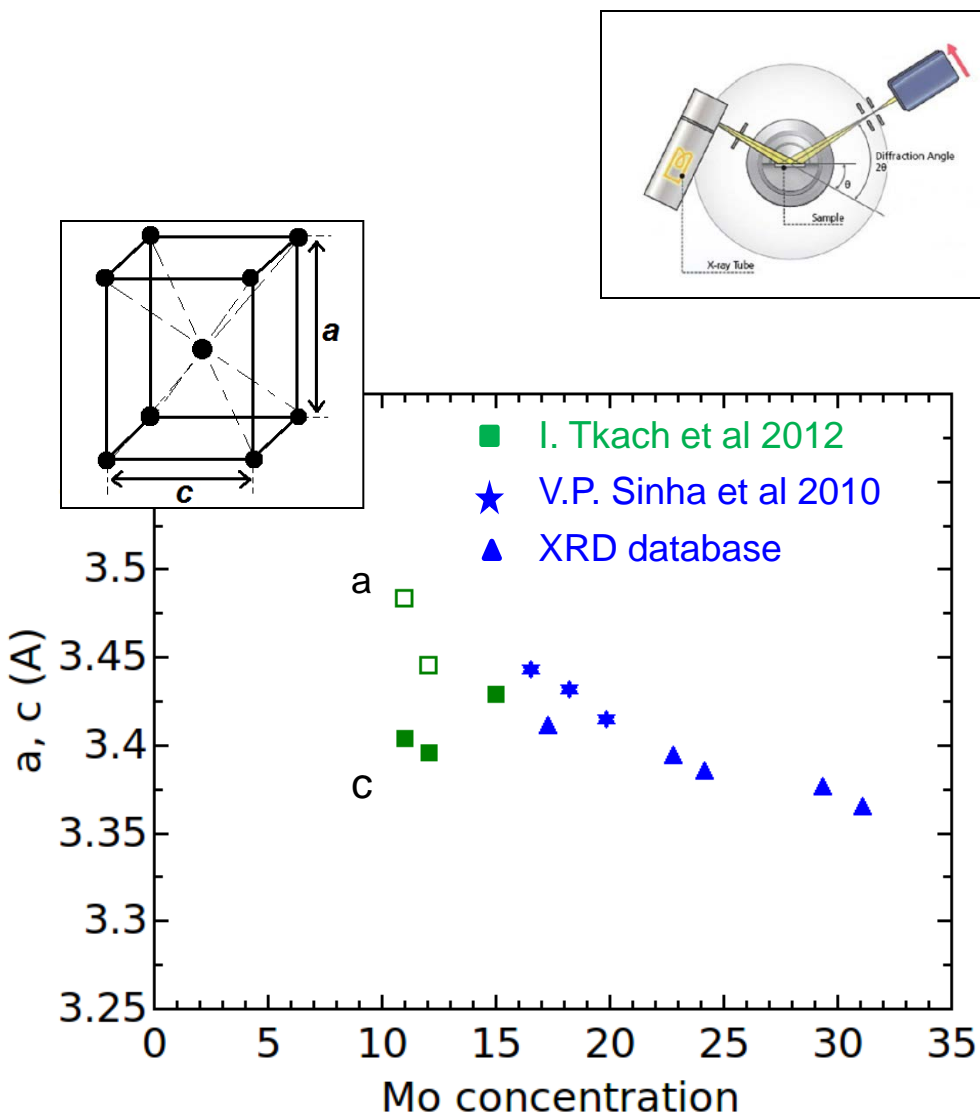
Uranium metal alloys are the most prominent candidates for advanced fast-neutron reactors (Gen IV)

- [1] Kim Y Comprehensive nuclear materials, volume 3: Advanced Fuels/Fuel Cladding/Nuclear Fuel Performance Modeling and Simulation (Elsevier Ltd.) 2012
- [2] Sinha V, Hegde P, Prasad G, Dey G and Kamath H Journal of Alloys and Compounds 506 253–262 2010

Anisotropy of the U-Mo alloy



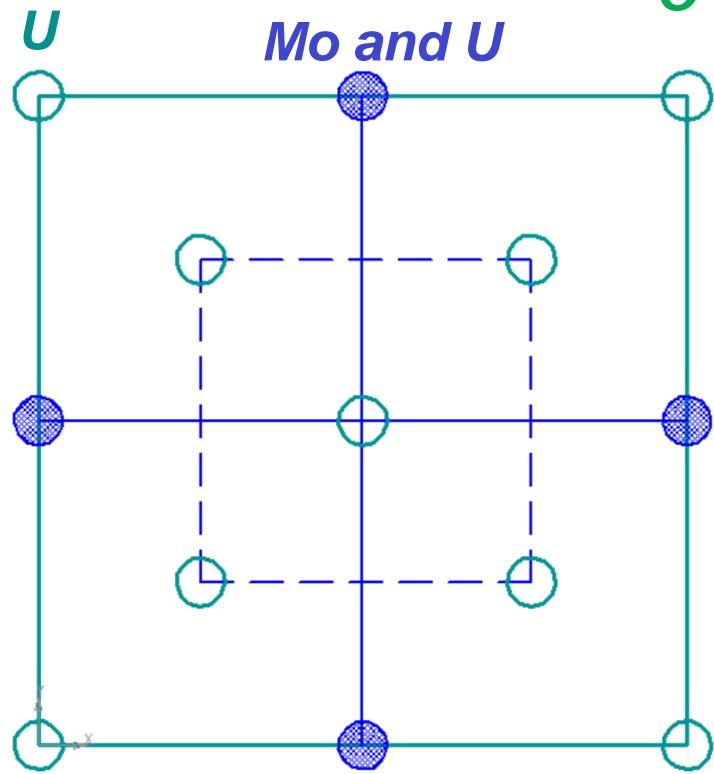
Anisotropy of the U-Mo alloy



U-Mo alloy structures

γ^0 structures

$$c < a = b$$



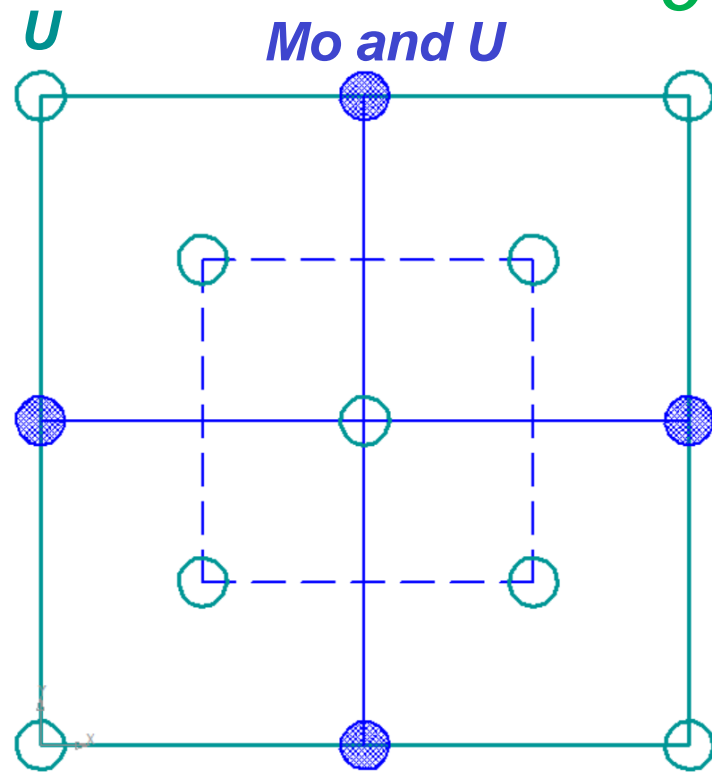
Mo and U atoms ordering

K. Tangri (1961)

B.W. Howlett (1970)

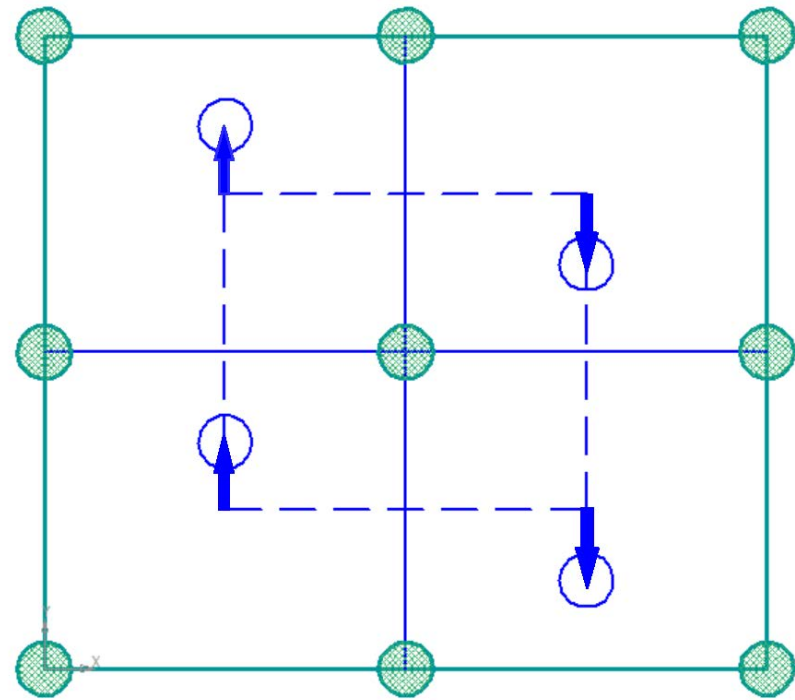
γ^0 structures

$$c < a = b$$



Mo and U atoms ordering

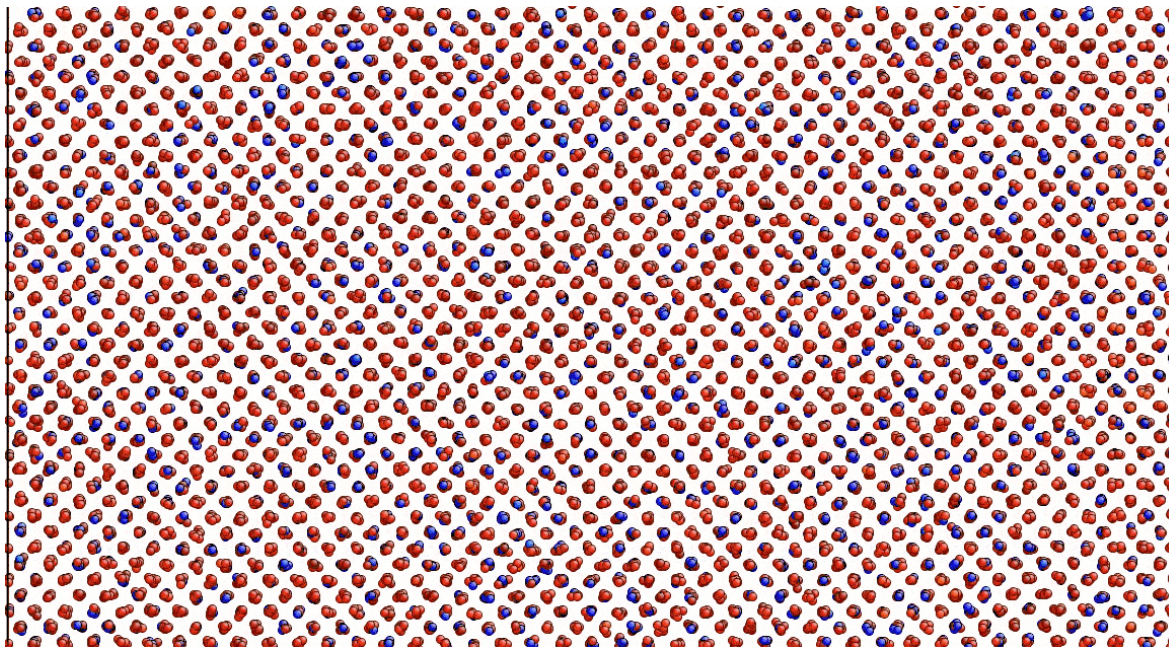
K. Tangri (1961)
B.W. Howlett (1970)



Central atom displacement

H.L. Yakel (1969)
B.W. Howlett (1970)

Preparing the equilibrium γ^0 U-Mo structure



BCC lattice
 $a_0 = 3.45\text{\AA}$

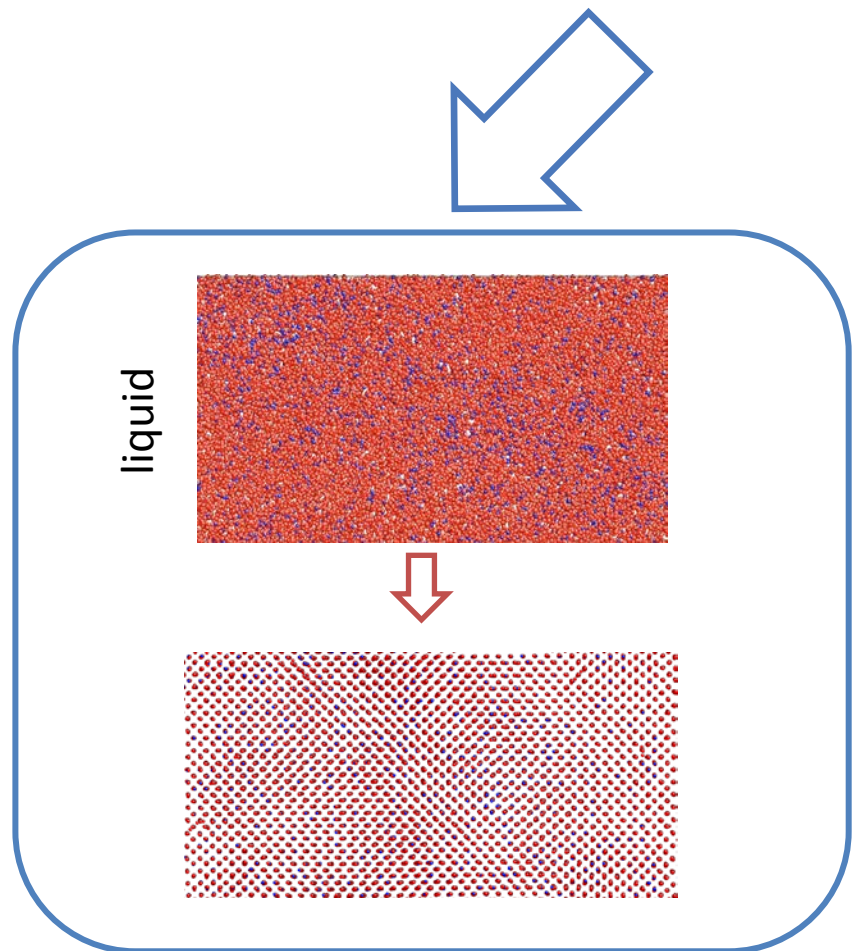
Mo – blue atoms
U – red atoms

ADP potential
[Starikov et al JNM 2018. V. 499. P. 451.]

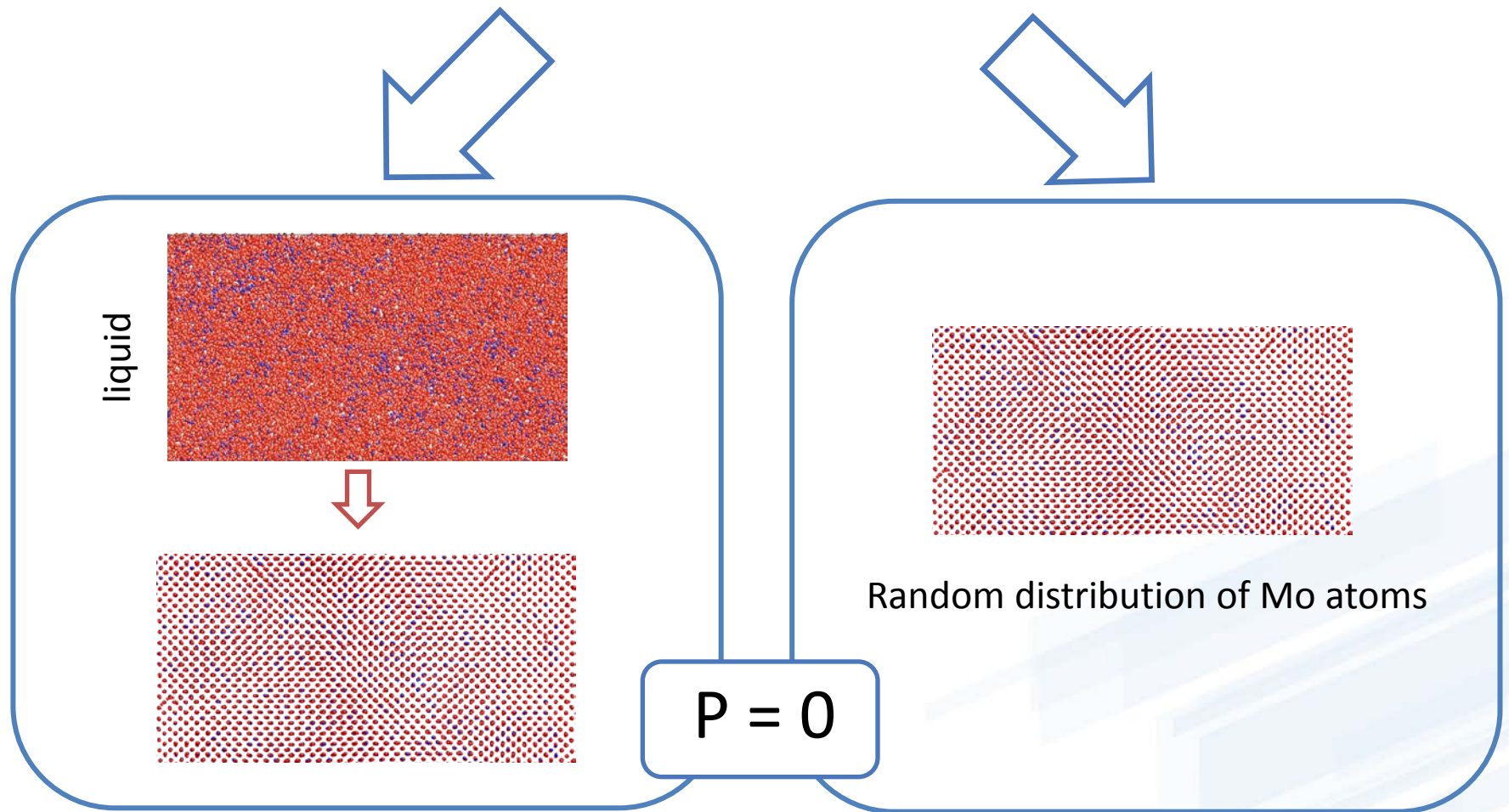
$$\begin{aligned} E_{tot} = & \frac{1}{2} \sum_{i,j(j \neq i)} \Phi_{ij}(r_{ij}) + \sum_i F_i(\bar{\rho}_i) + \frac{1}{2} \sum_{i,\alpha} (\mu_i^\alpha)^2 \\ & + \frac{1}{2} \sum_{i,\alpha,\beta} (\lambda_i^{\alpha\beta})^2 - \frac{1}{6} \sum_i v_i^2 \end{aligned}$$



Preparing the equilibrium γ^0 U-Mo structure



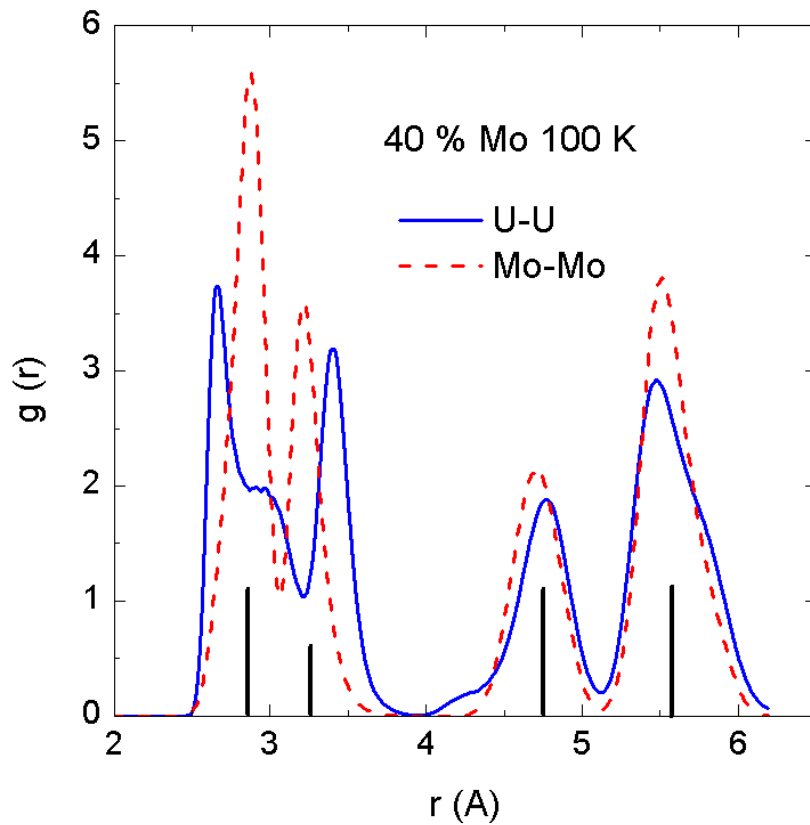
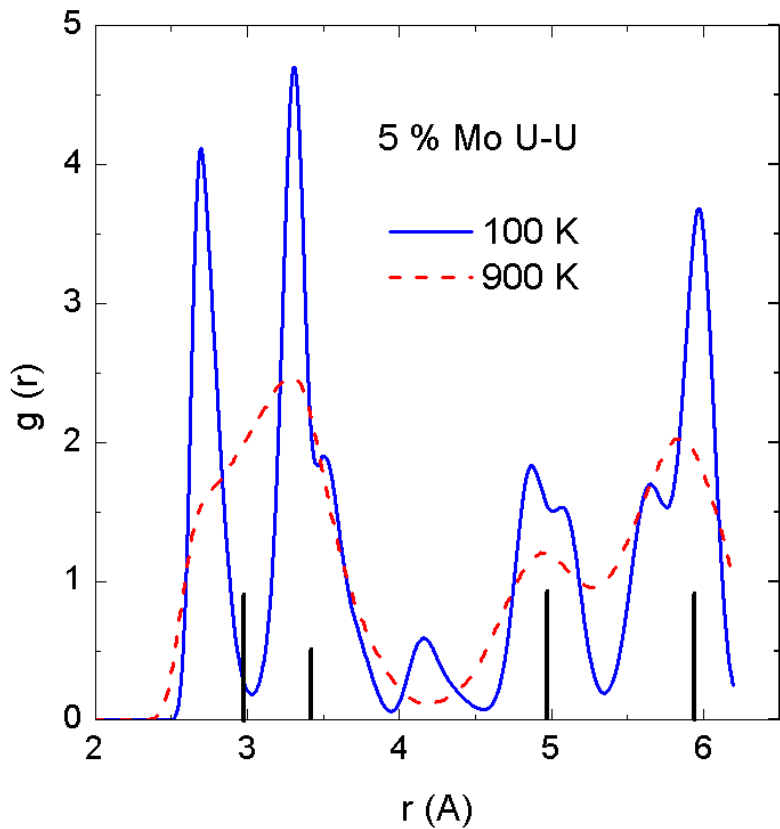
Preparing the equilibrium γ^0 U-Mo structure



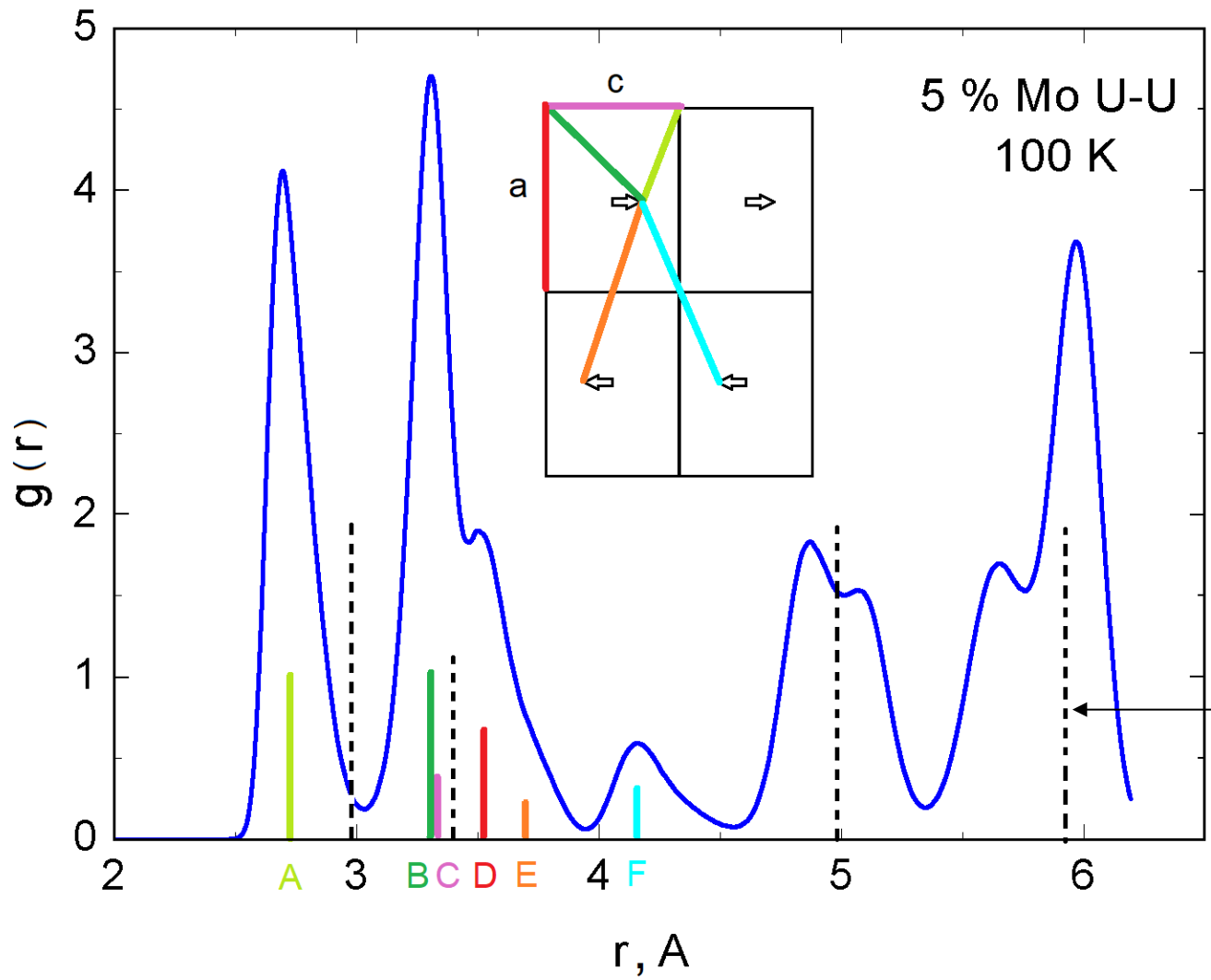
There is no long-range ordering by the type of atoms in crystal lattice. The lattice parameters and the local structure of the alloy are independent of short range order

Radial distribution functions of γ^0 phase

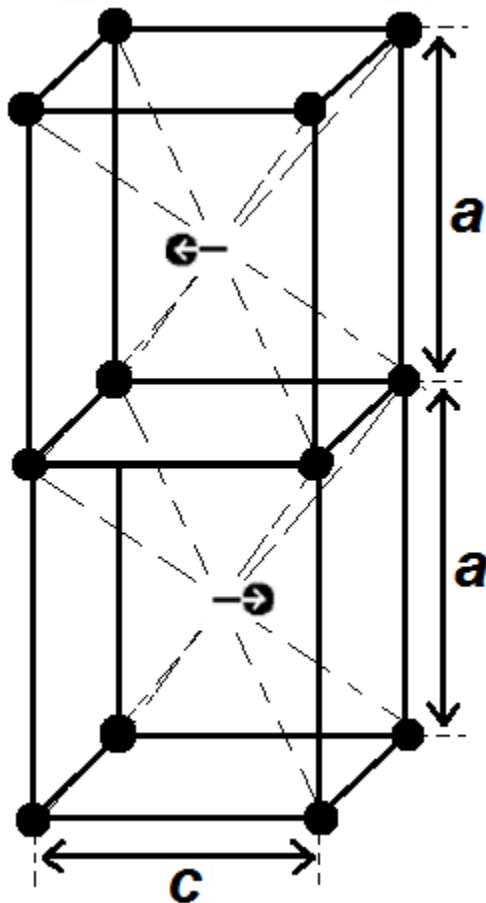
— Ideal BCC
lattice



Radial distribution function of γ^0 phase

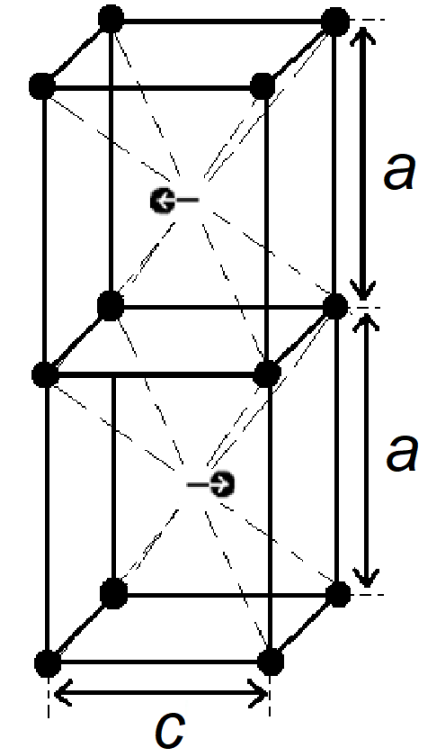
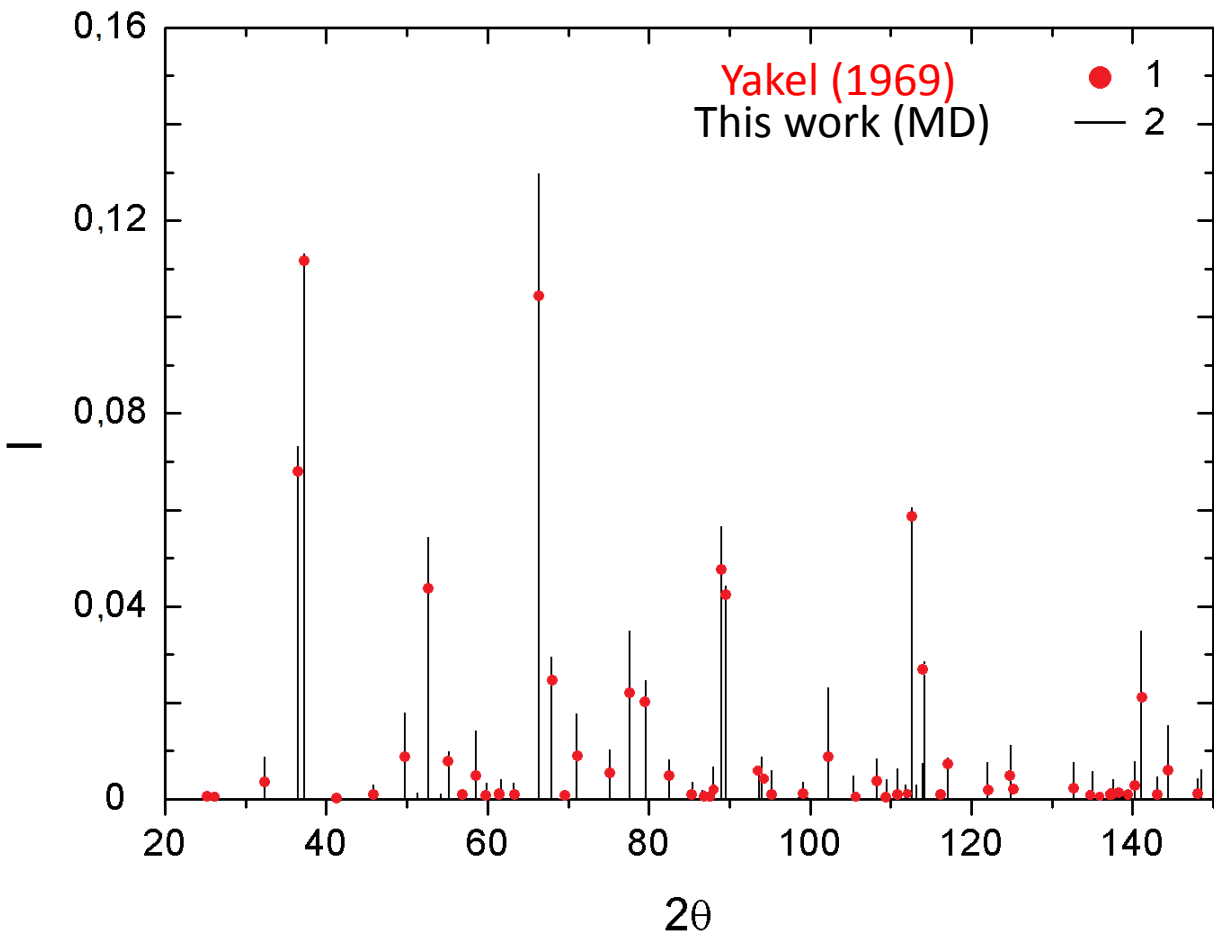


γ^0 structure

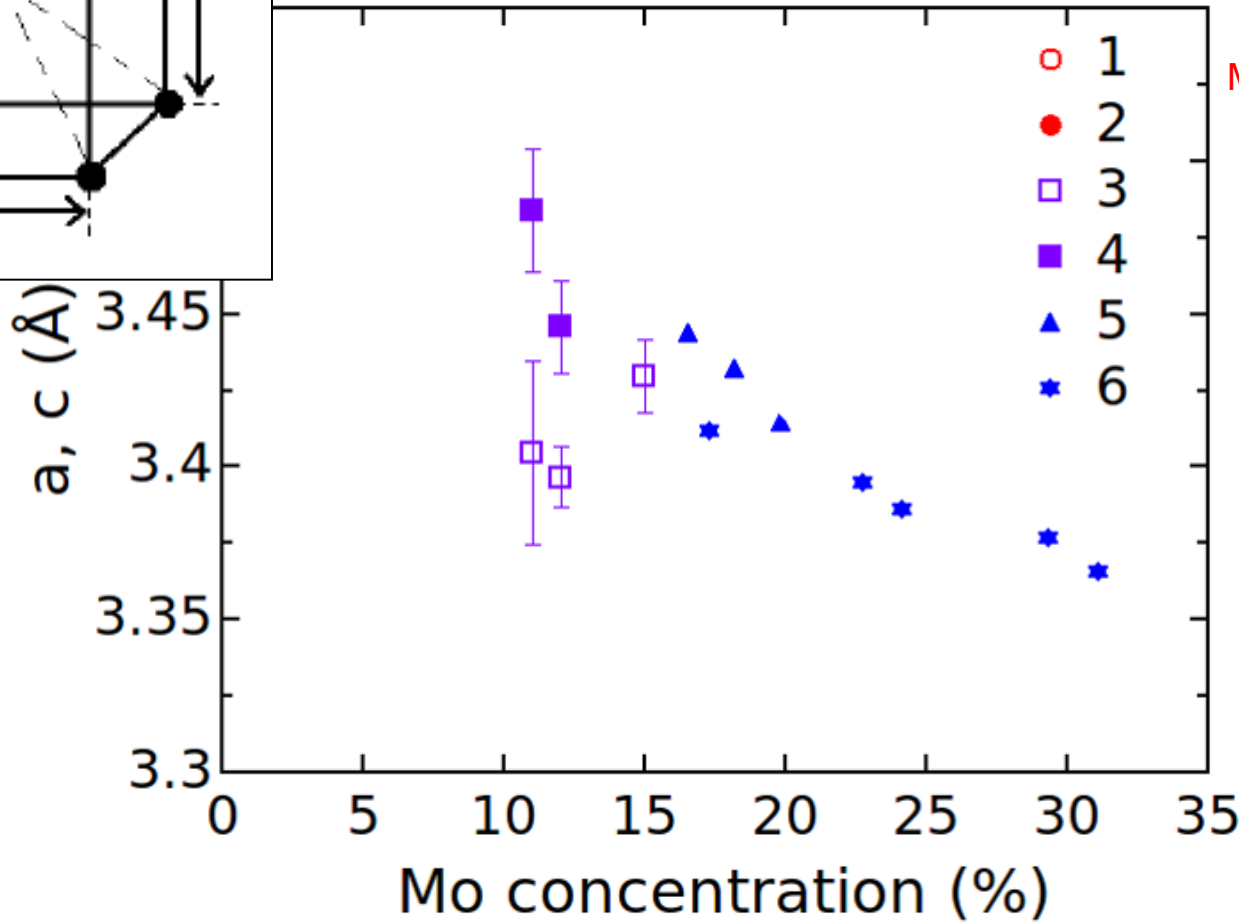
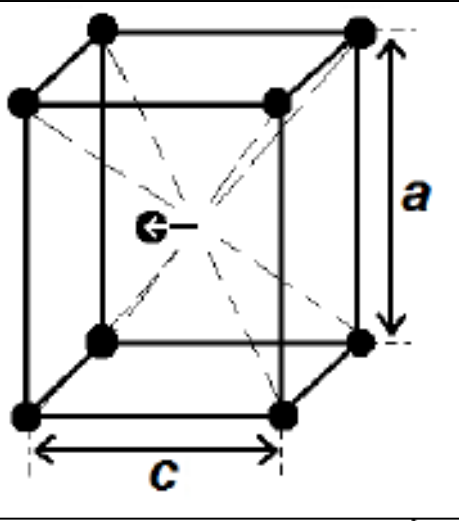


structure γ^0 phase is
the same with Yakel's
work (1969)

XRD of γ^0 phase



Anisotropy of γ^0



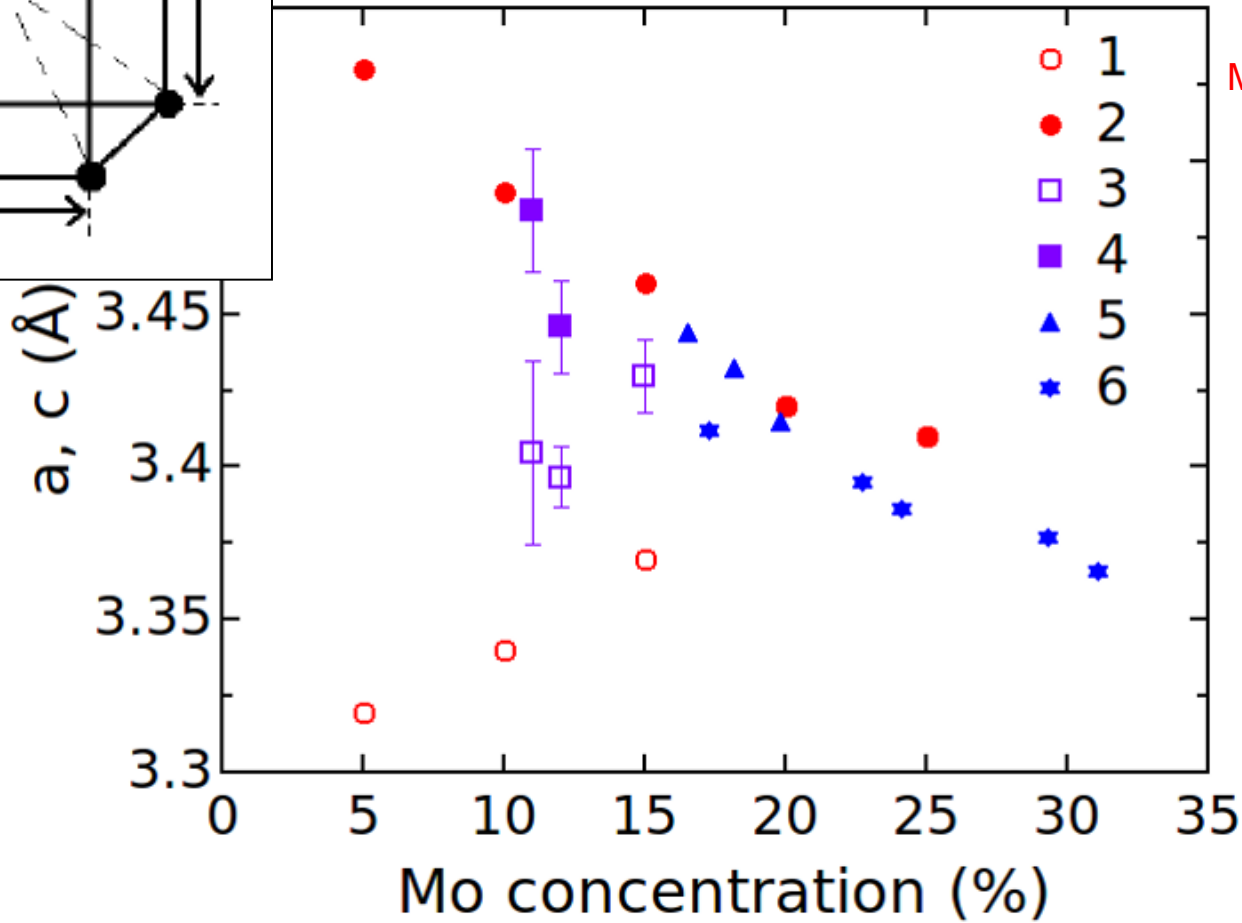
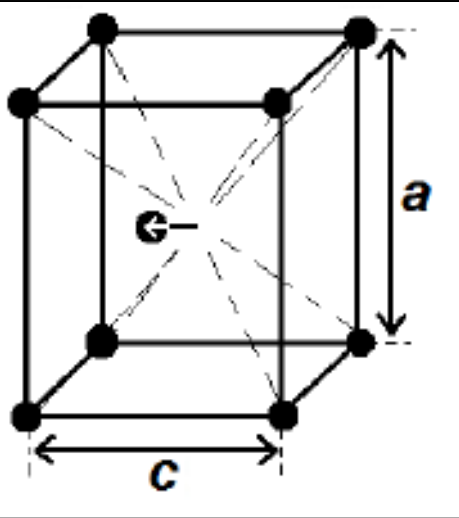
MD calculation, this work

I. Tkach et al 2012

V.P. Sinha et al 2010

XRD database

Anisotropy of γ^0



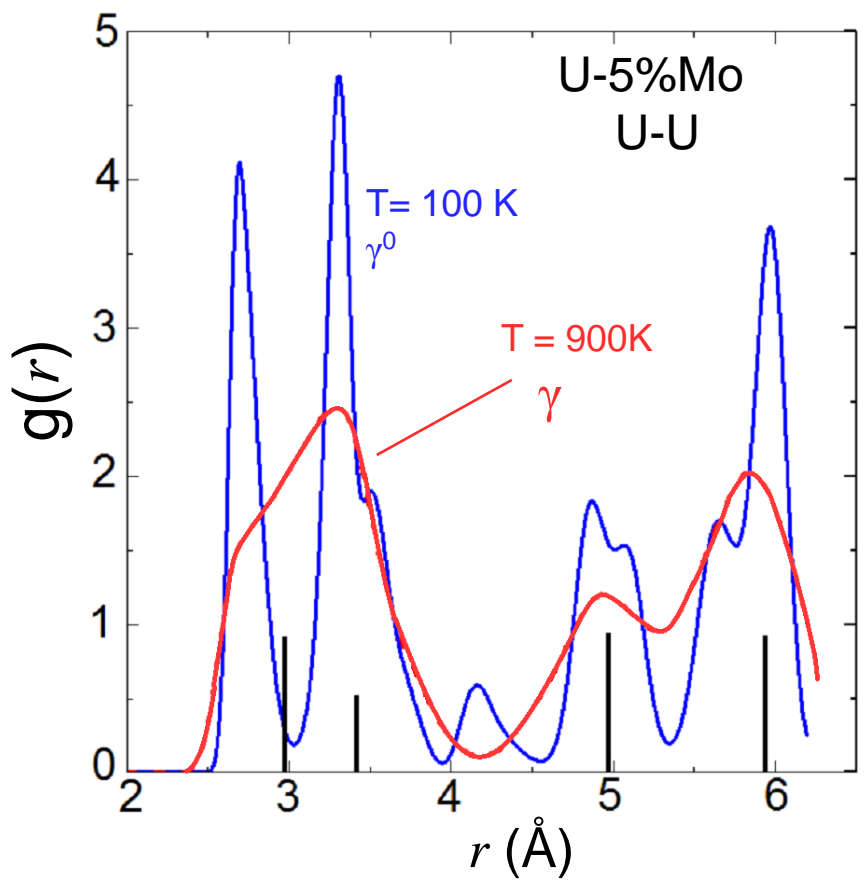
MD calculation, this work

I. Tkach et al 2012

V.P. Sinha et al 2010

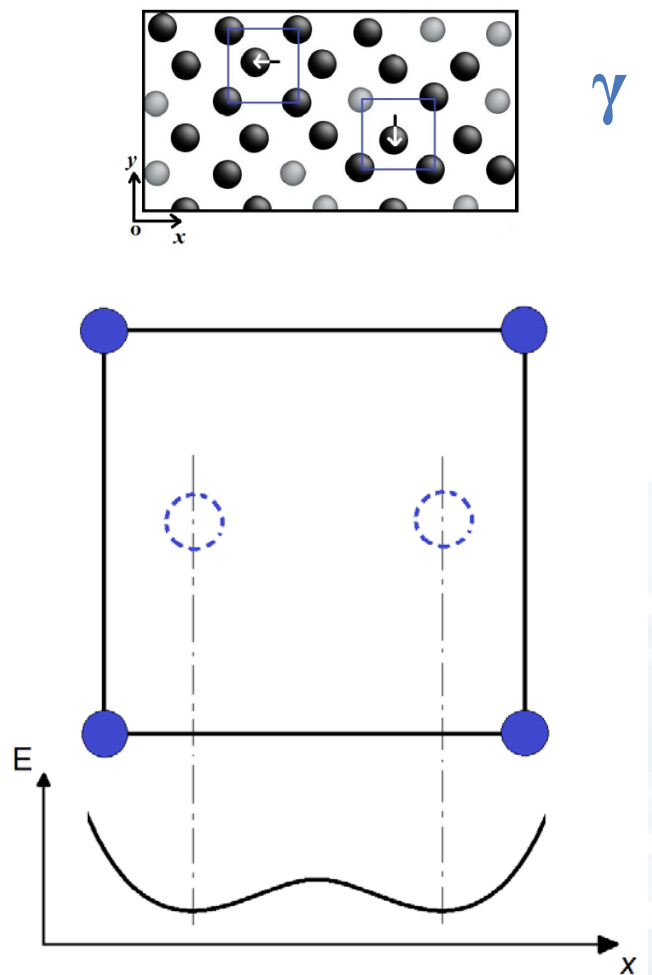
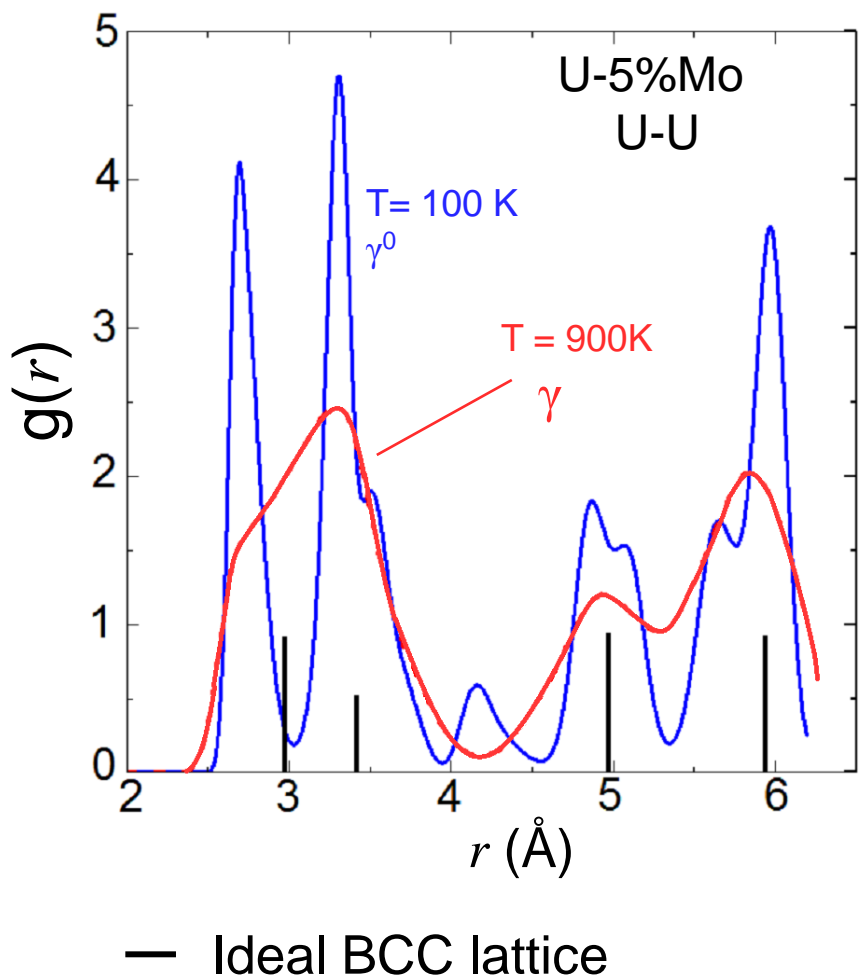
XRD database

Radial distribution function of γ phase

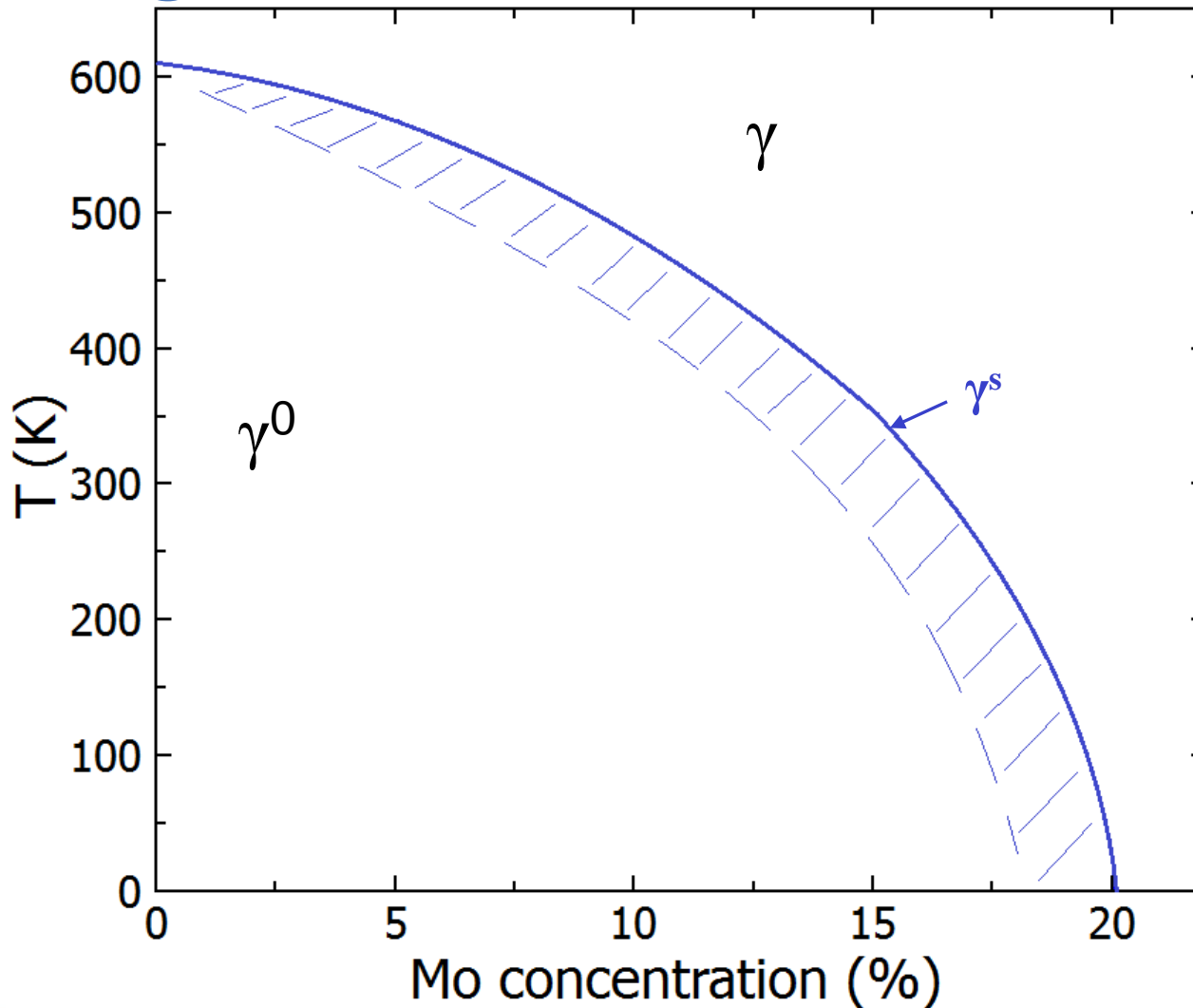


— Ideal BCC lattice

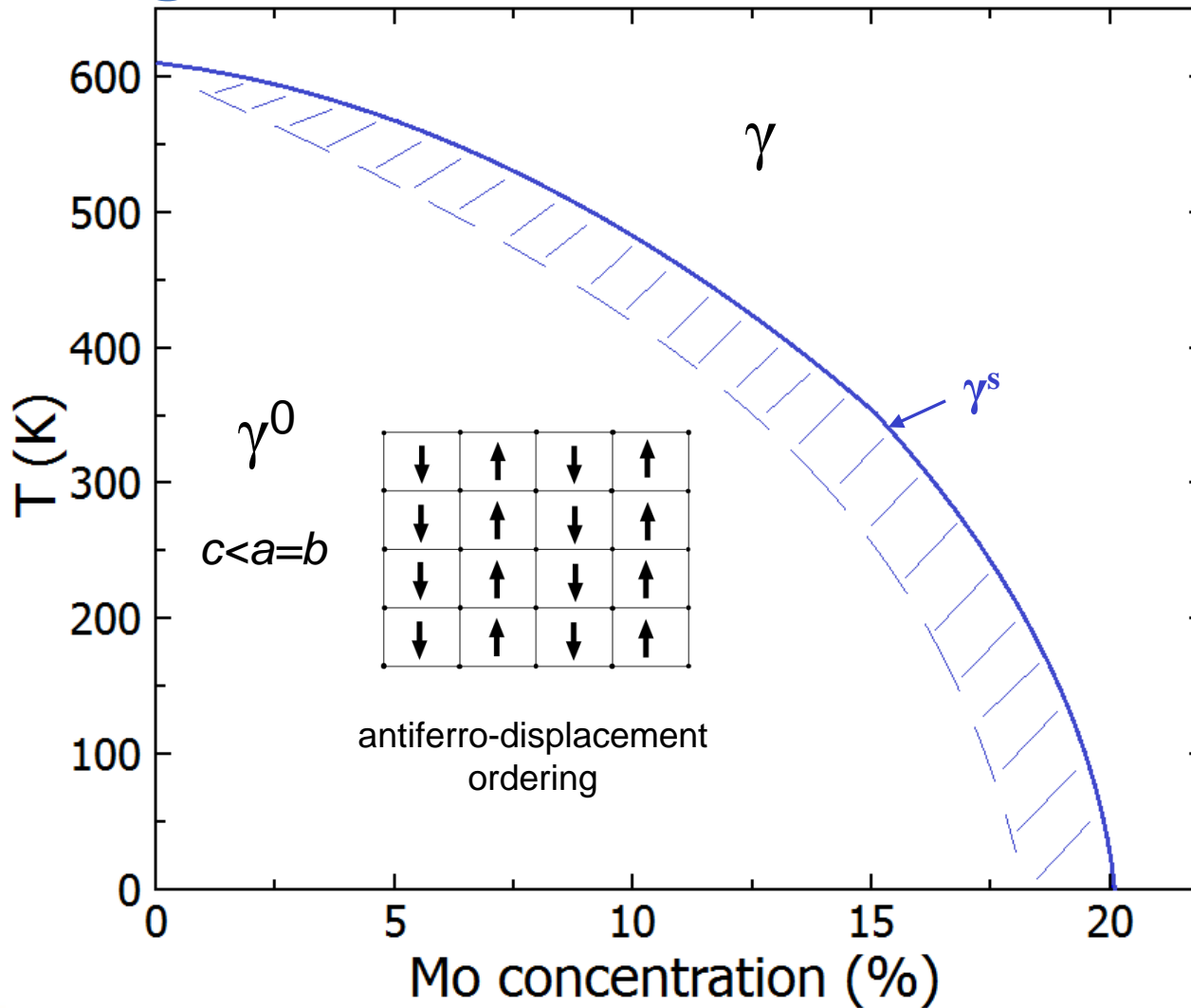
Radial distribution function of γ phase



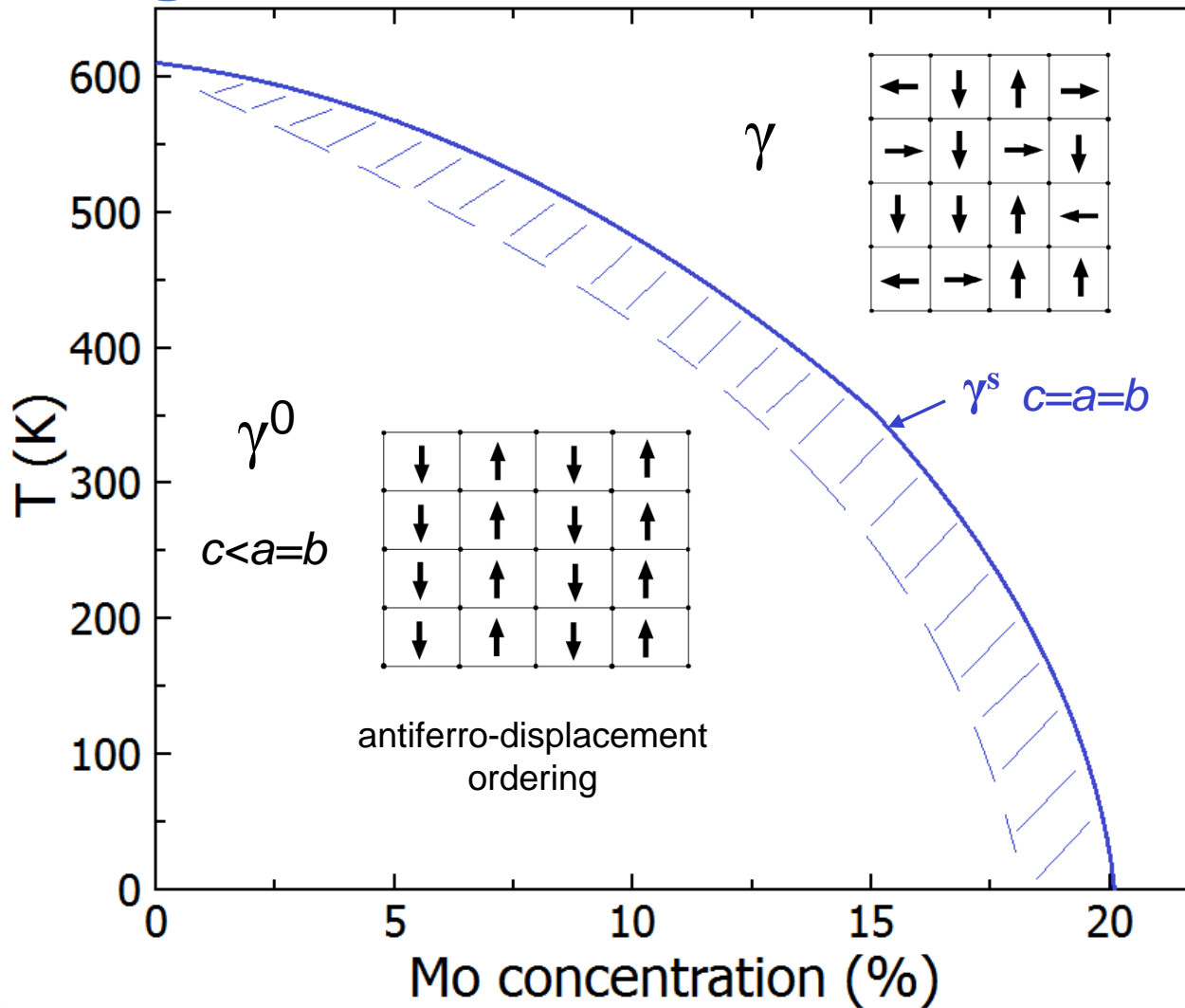
Calculated areas of phase stability on T-x diagram for various structures



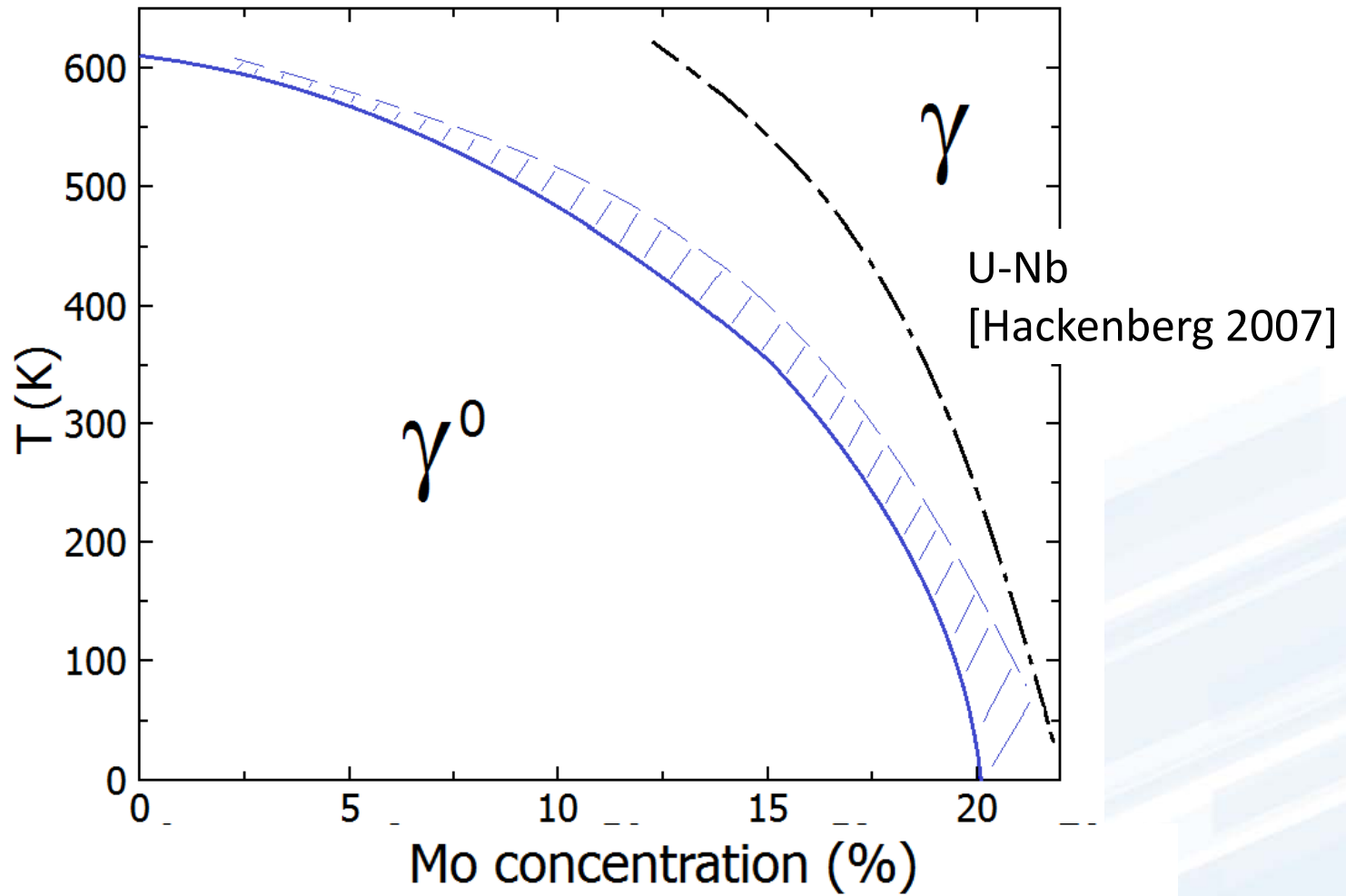
Calculated areas of phase stability on T-x diagram for various structures



Calculated areas of phase stability on T-x diagram for various structures

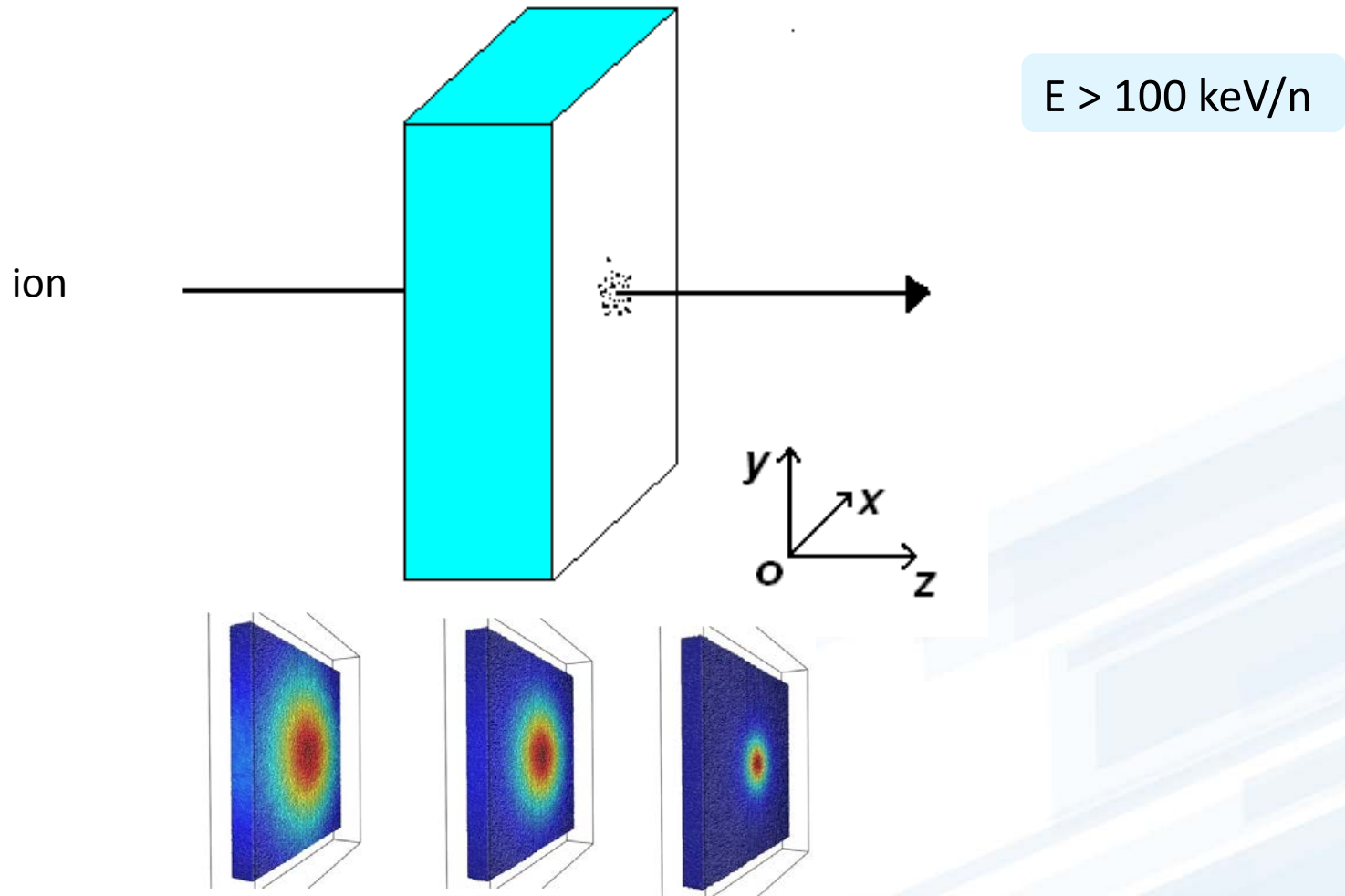


Calculated areas of phase stability on T-x diagram for various structures



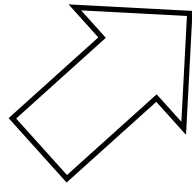
Structure transitions by irradiation effects

Moving of high energy ion through matter



Thermal conductivity equation for ELECTRONS:

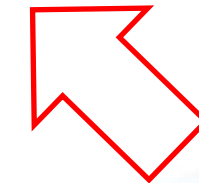
$$C_e \rho_e \frac{\partial T_e}{\partial t} = \nabla (\kappa_e \nabla T_e) - g_p (T_e - T_i)$$



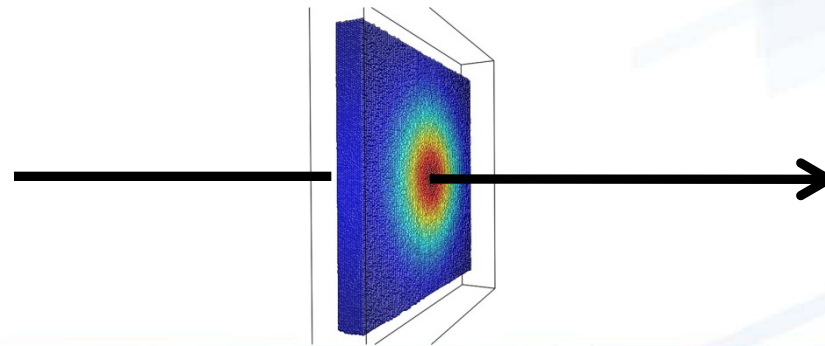
Electron heat capacity



Electron thermal conductivity



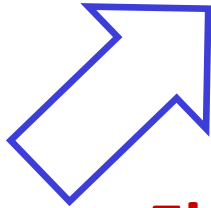
Electron-ion relaxation



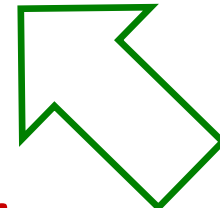
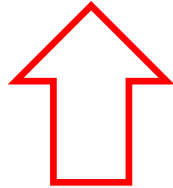
MD simulation for IONS :

$$\vec{F}_i = -\partial U / \partial \vec{r}_i + \vec{F}_{lang} - \nabla P_e / n_i$$

Interionic
potential



Electron-ion relaxation
Langevin thermostat

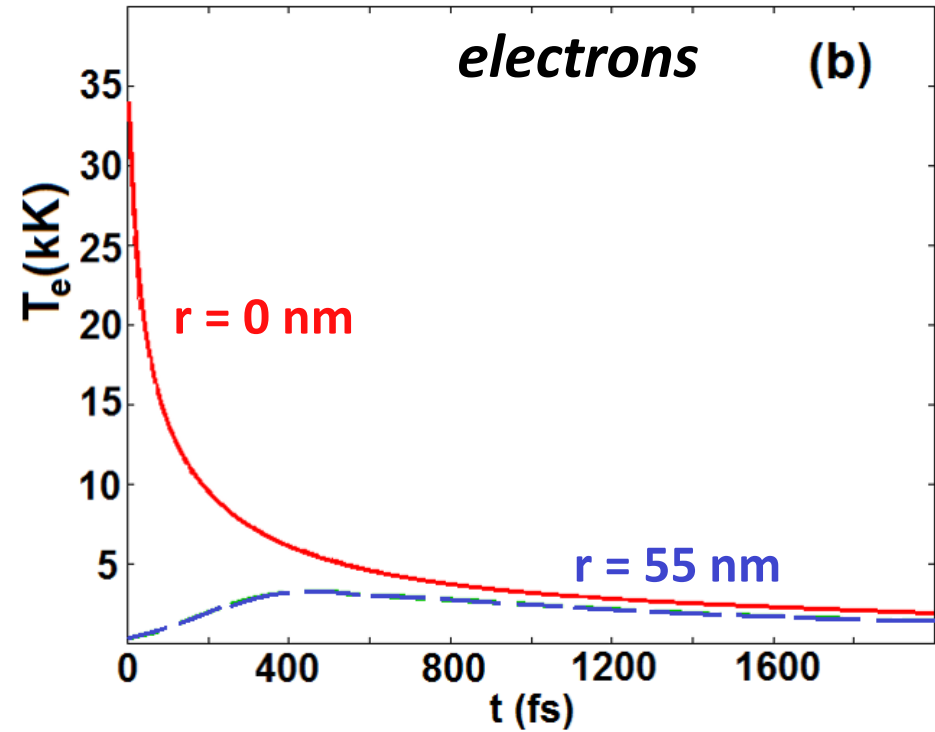
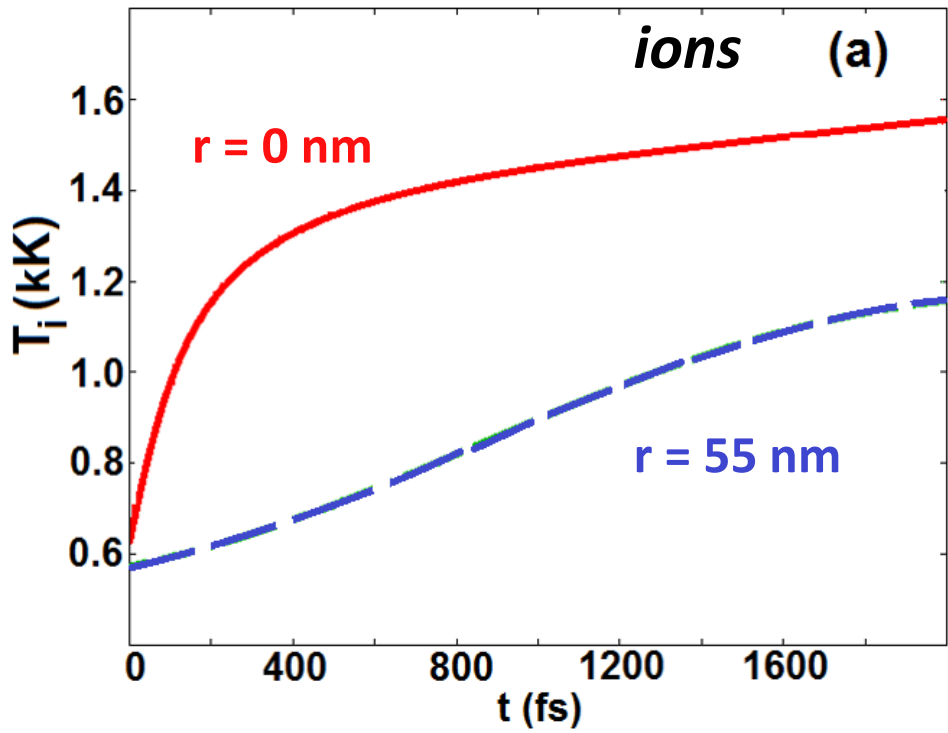


Electron
pressure

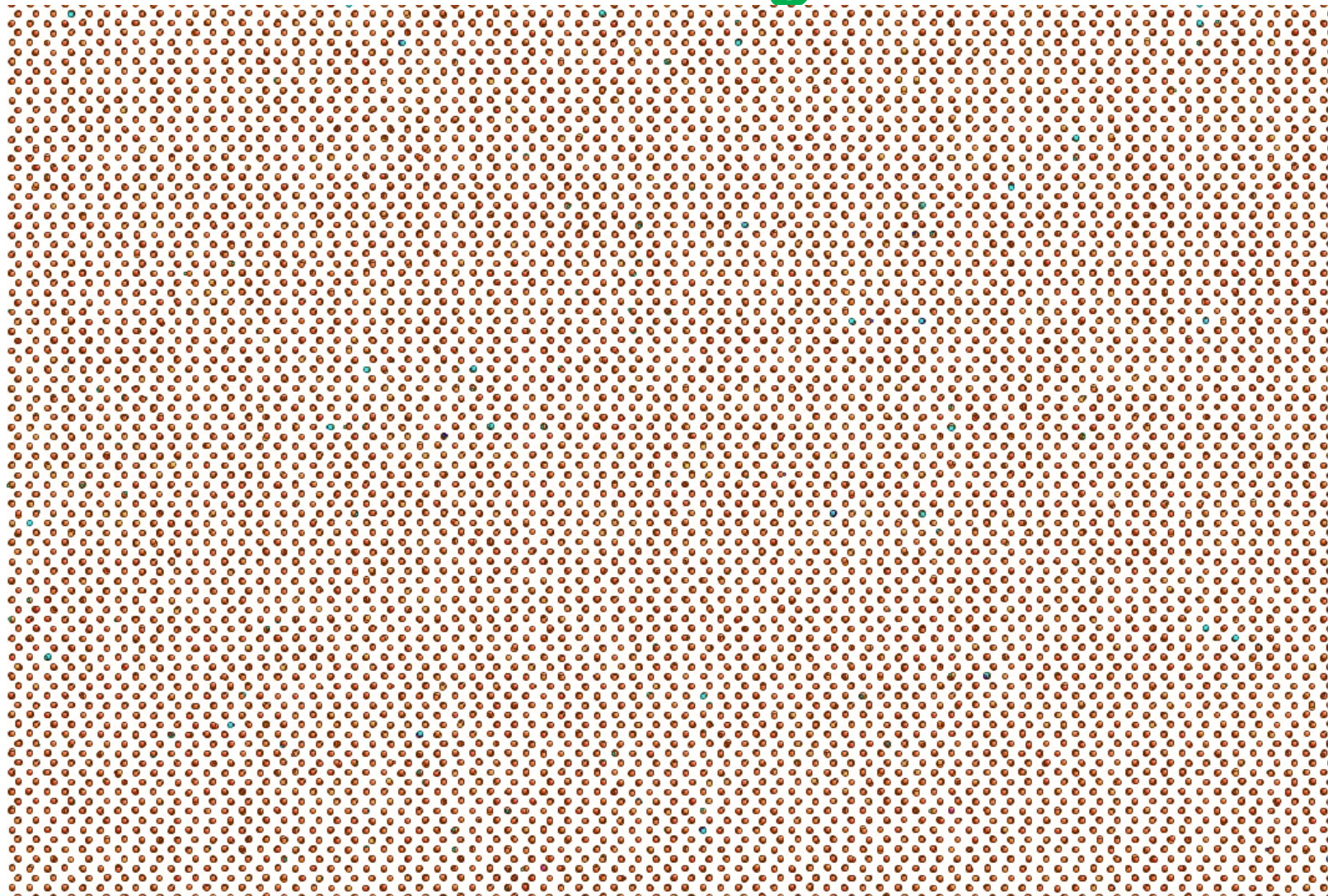
Norman G E, Starikov S V, Stegailov V V et al. 2013 *Contrib. Plasma Phys.* **53** 129-139
Pisarev V V and Starikov S V 2014 *J. Phys.: Condens. Matter* **26** 475401

Thermal spike model

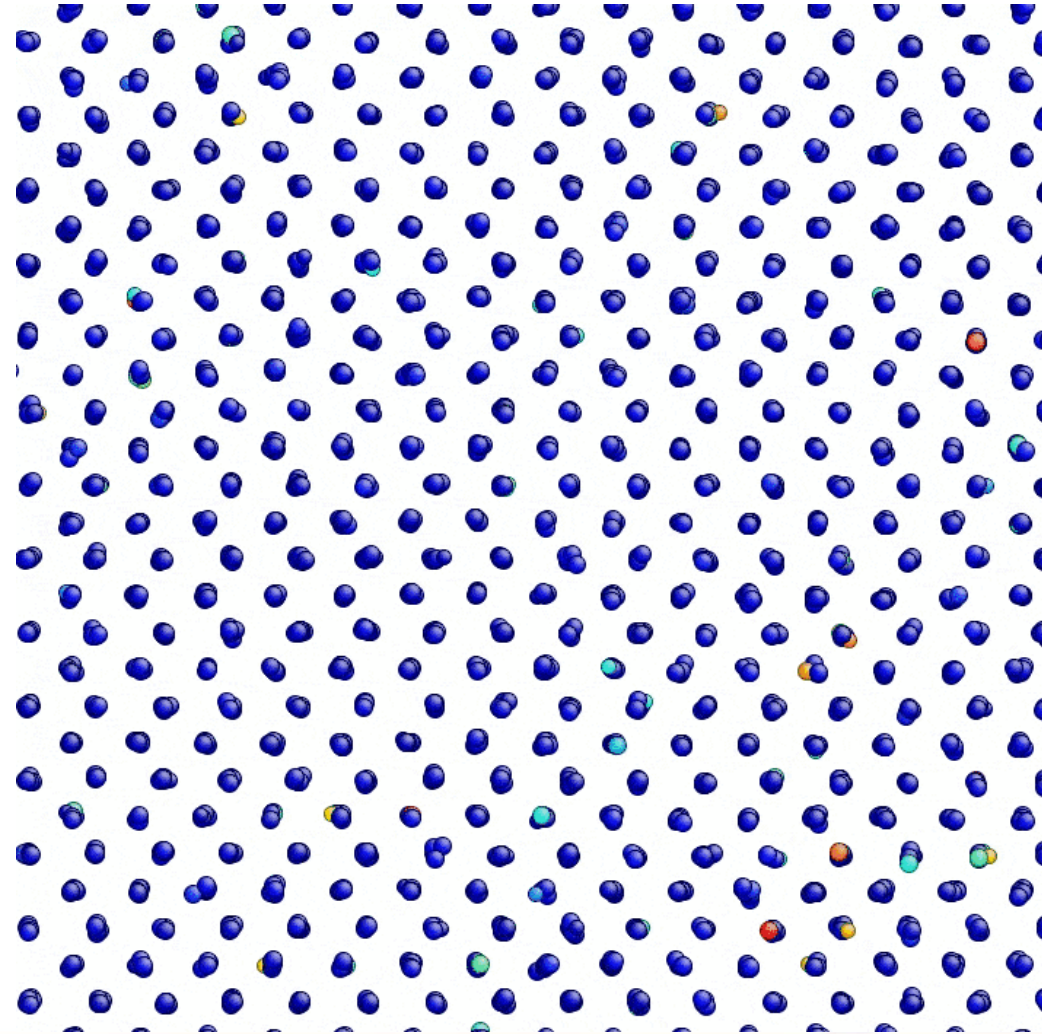
$dE/dz = 27 \text{ keV/nm}$



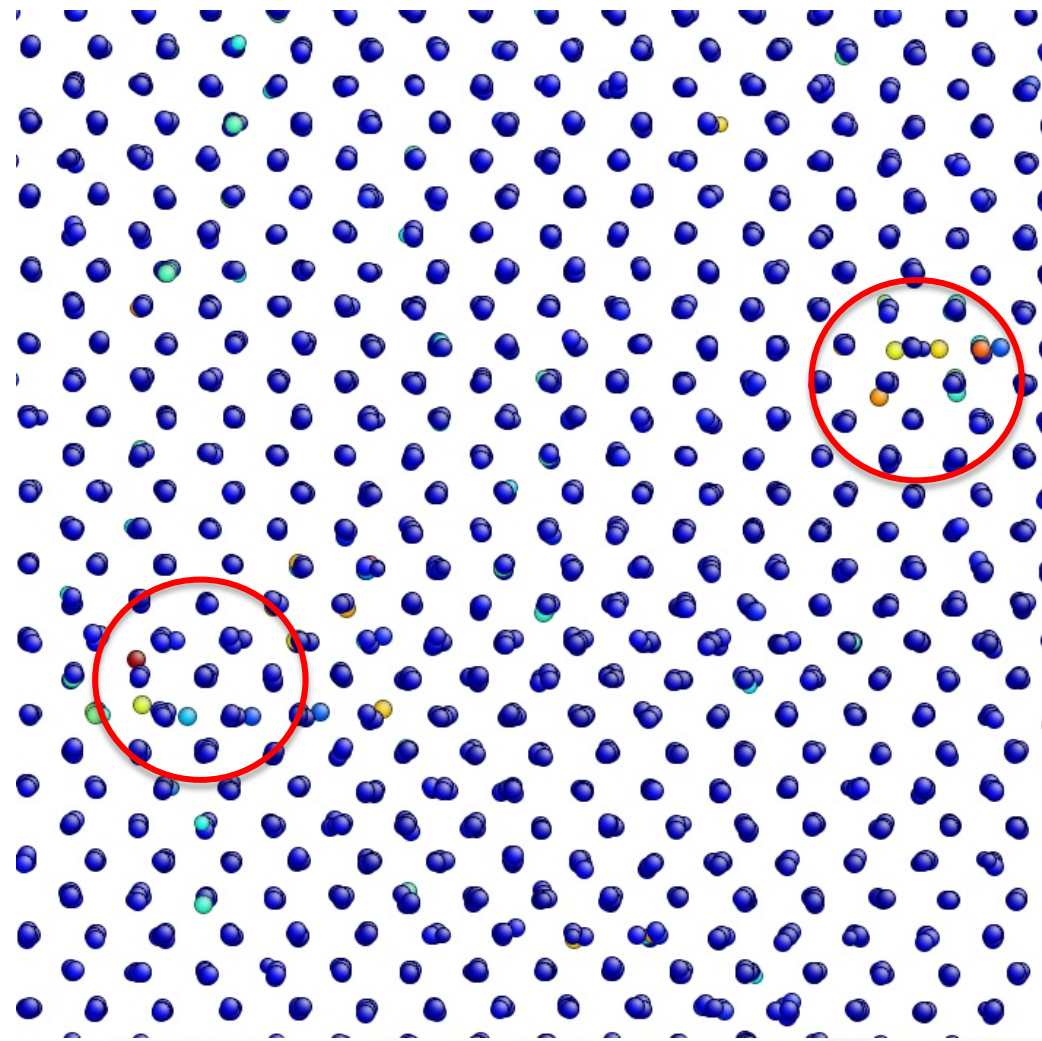
Radiation defects formation after melting



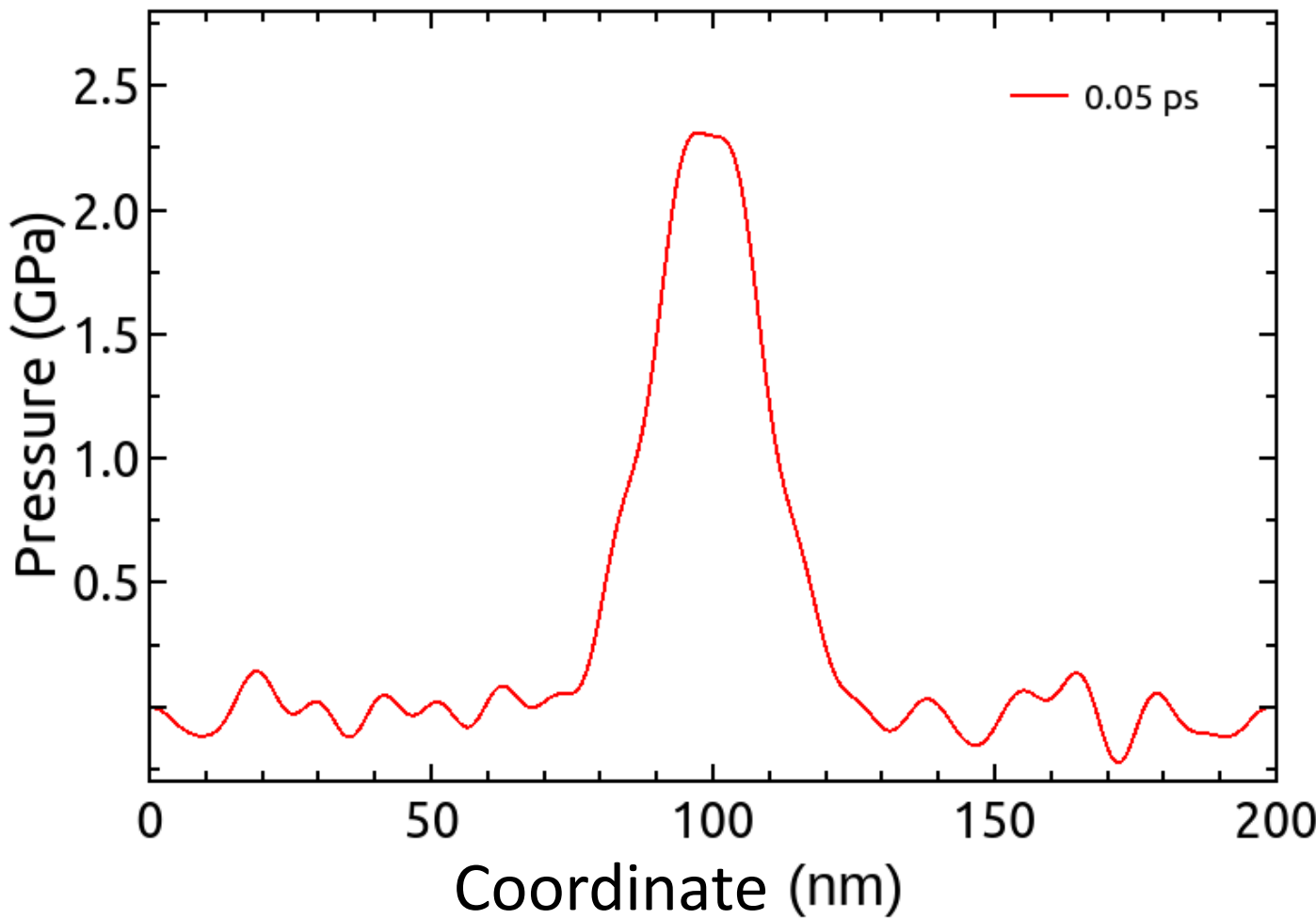
Radiation defects formation without melting



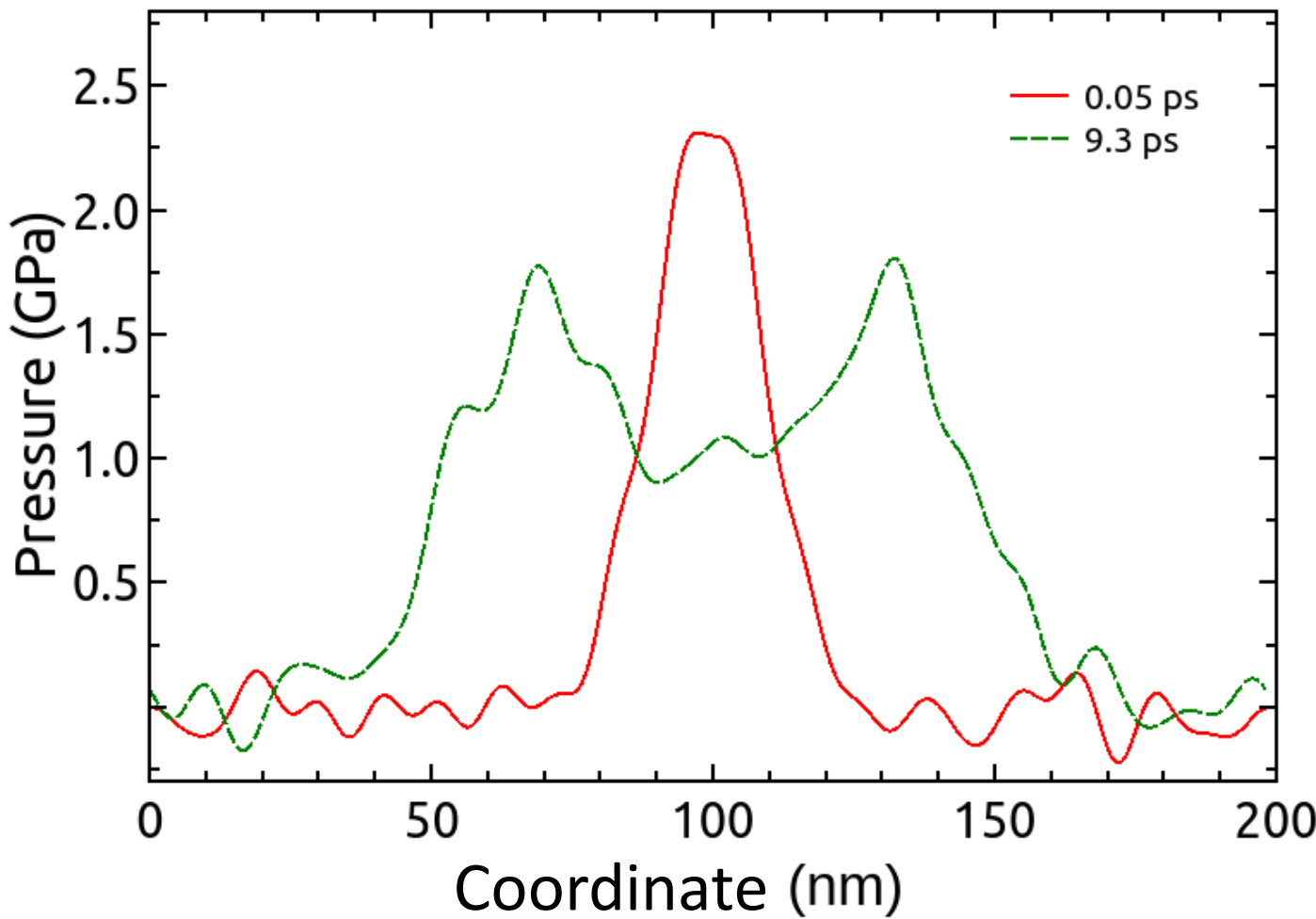
Radiation defects formation without melting



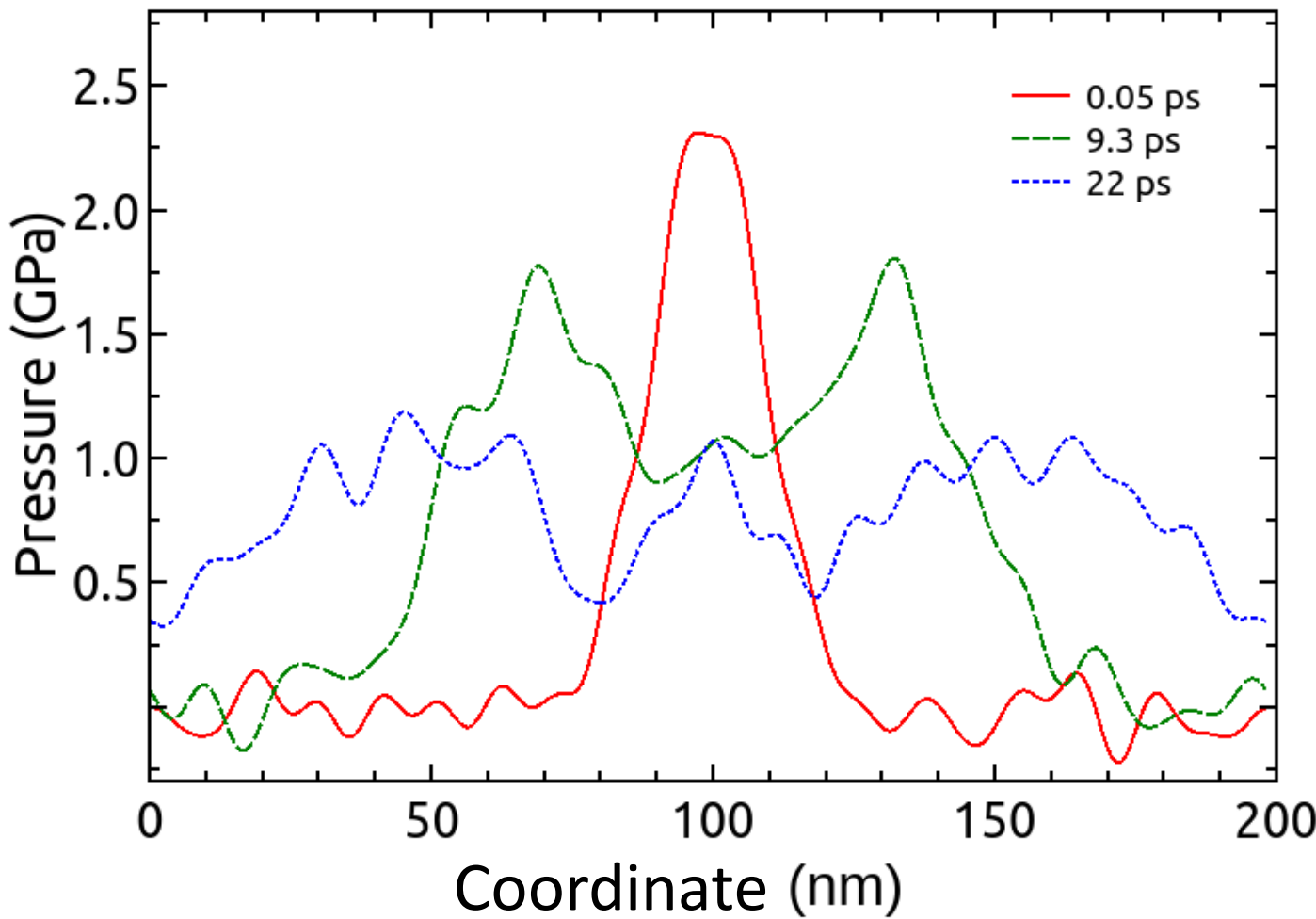
Pressure profiles along the radial direction to the axis of the track



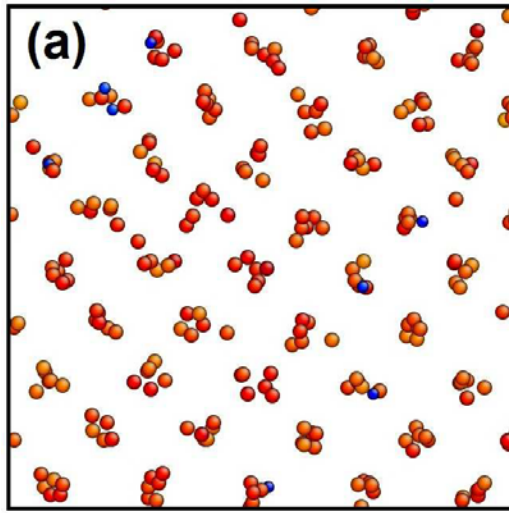
Pressure profiles along the radial direction to the axis of the track



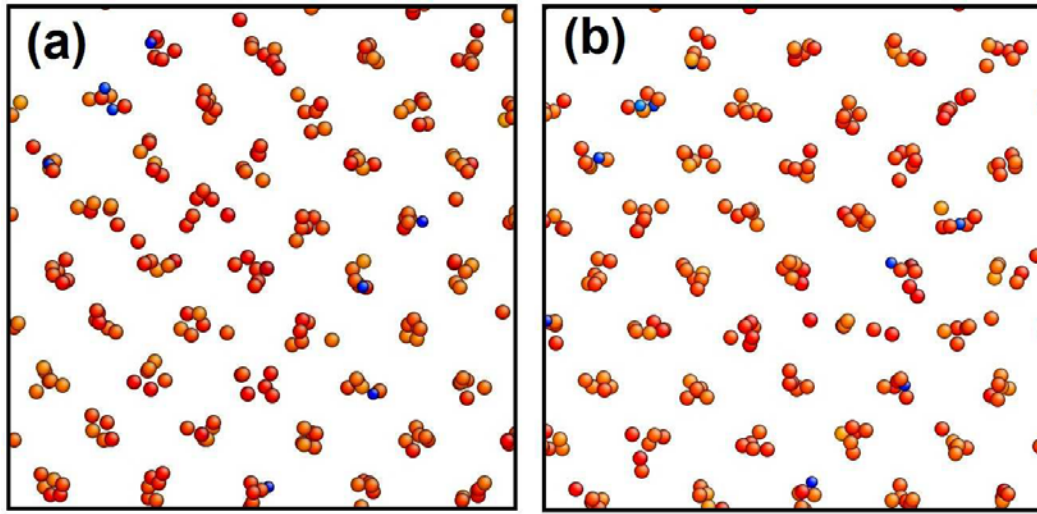
Pressure profiles along the radial direction to the axis of the track



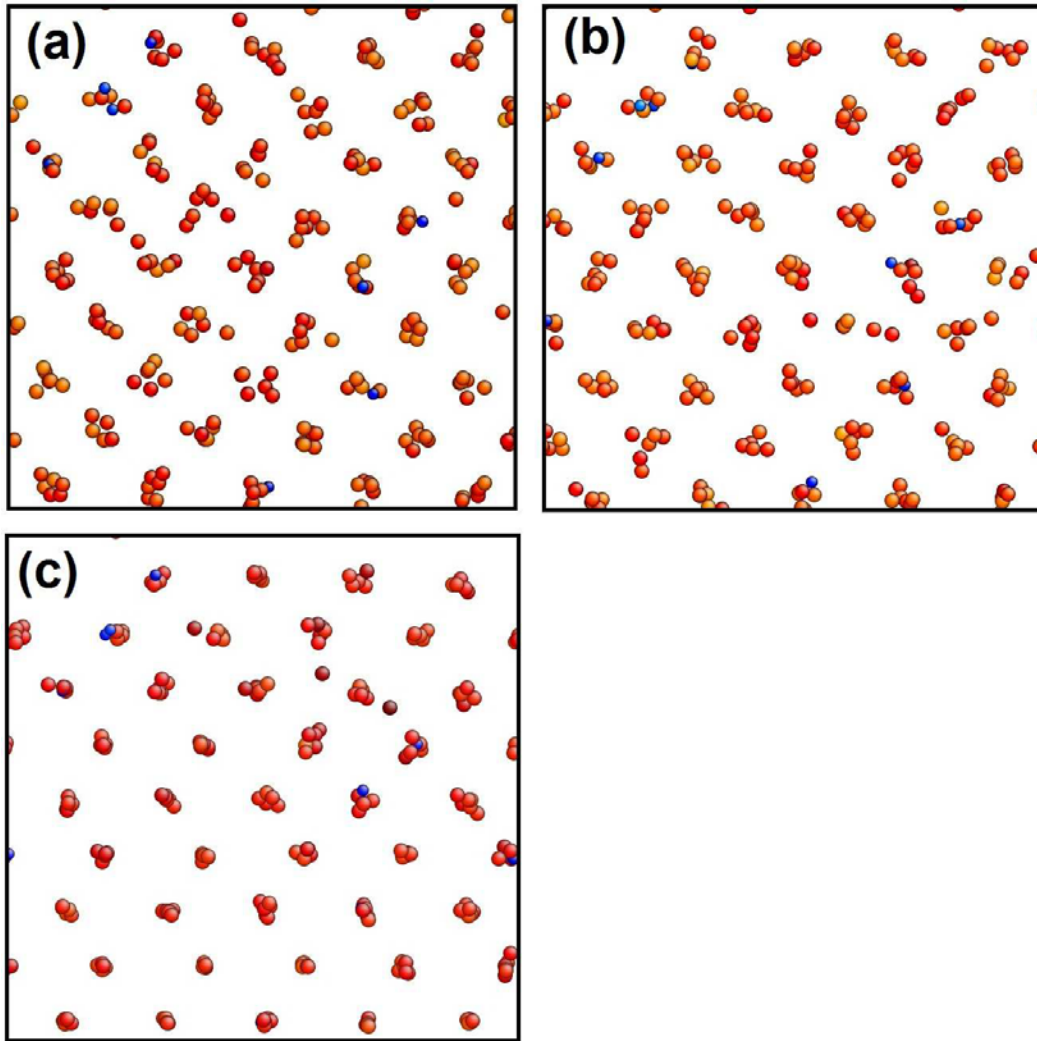
Formation of radiation defects in the atomistic simulation



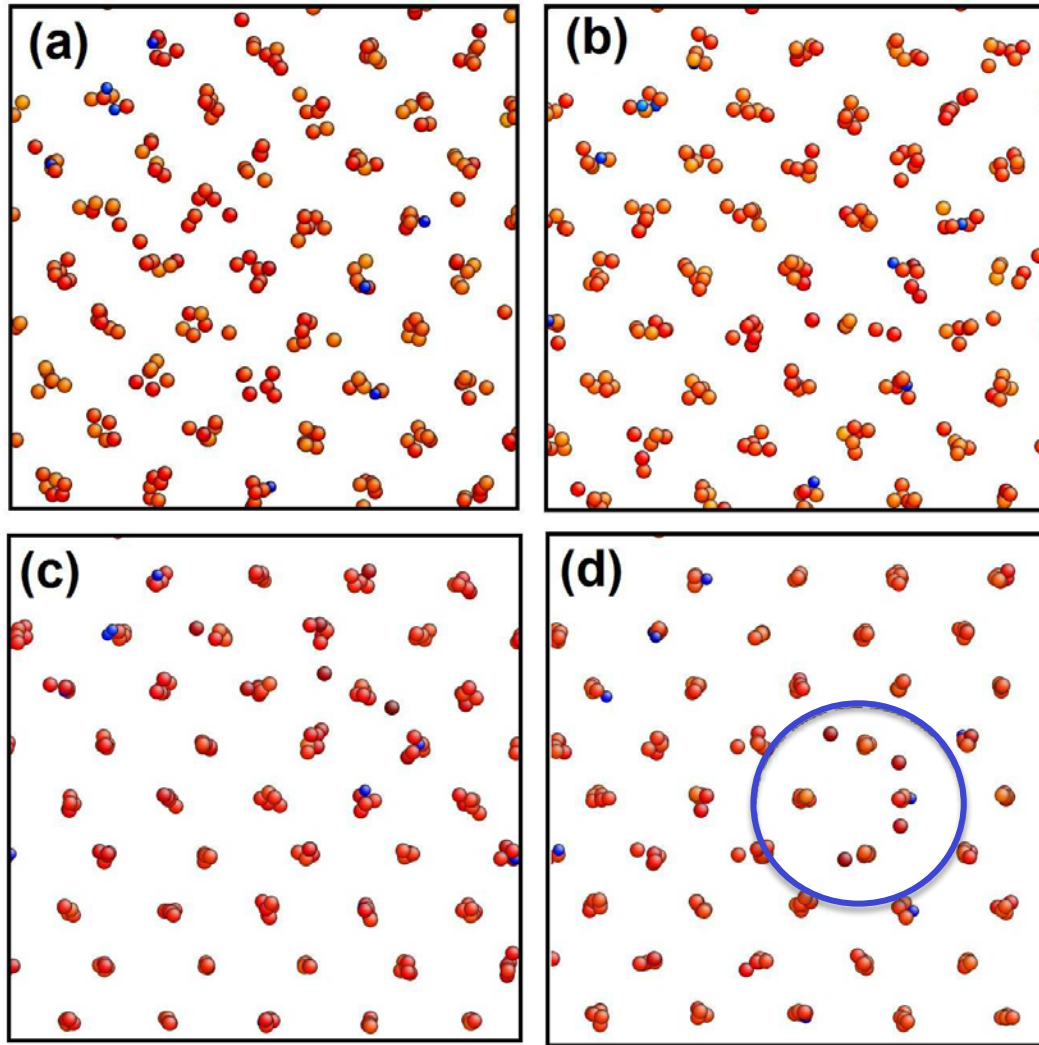
Formation of radiation defects in the atomistic simulation



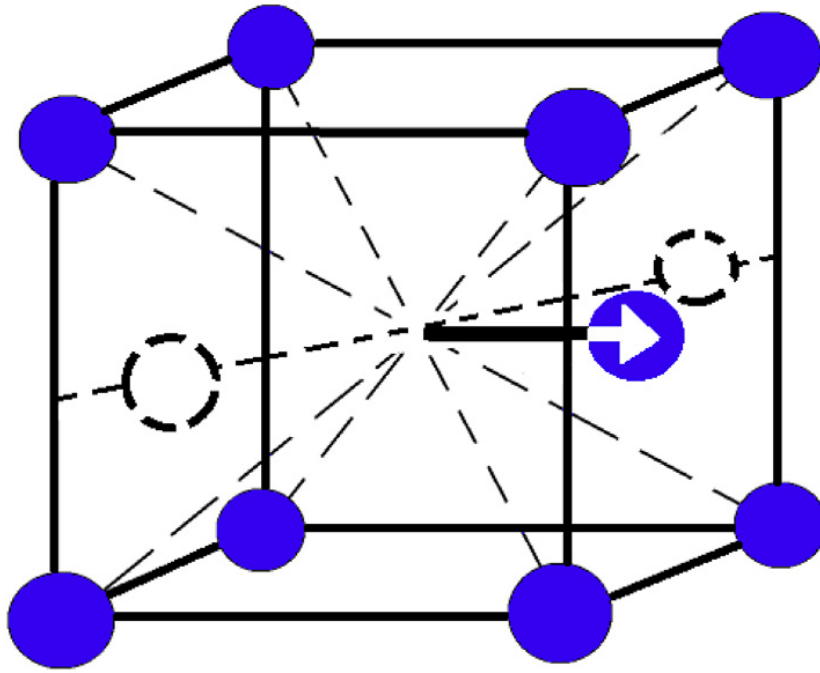
Formation of radiation defects in the atomistic simulation



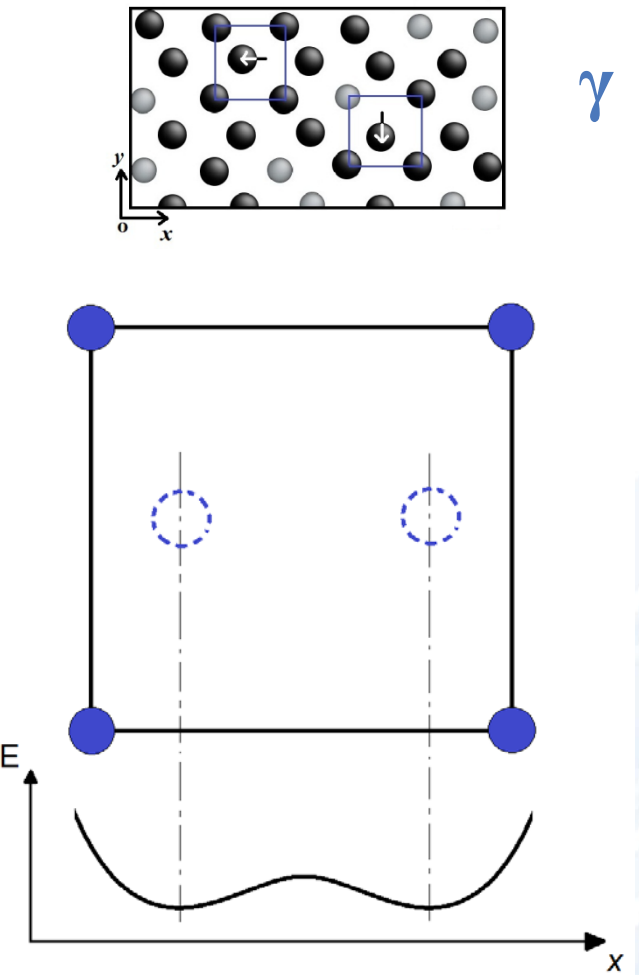
Formation of radiation defects in the atomistic simulation



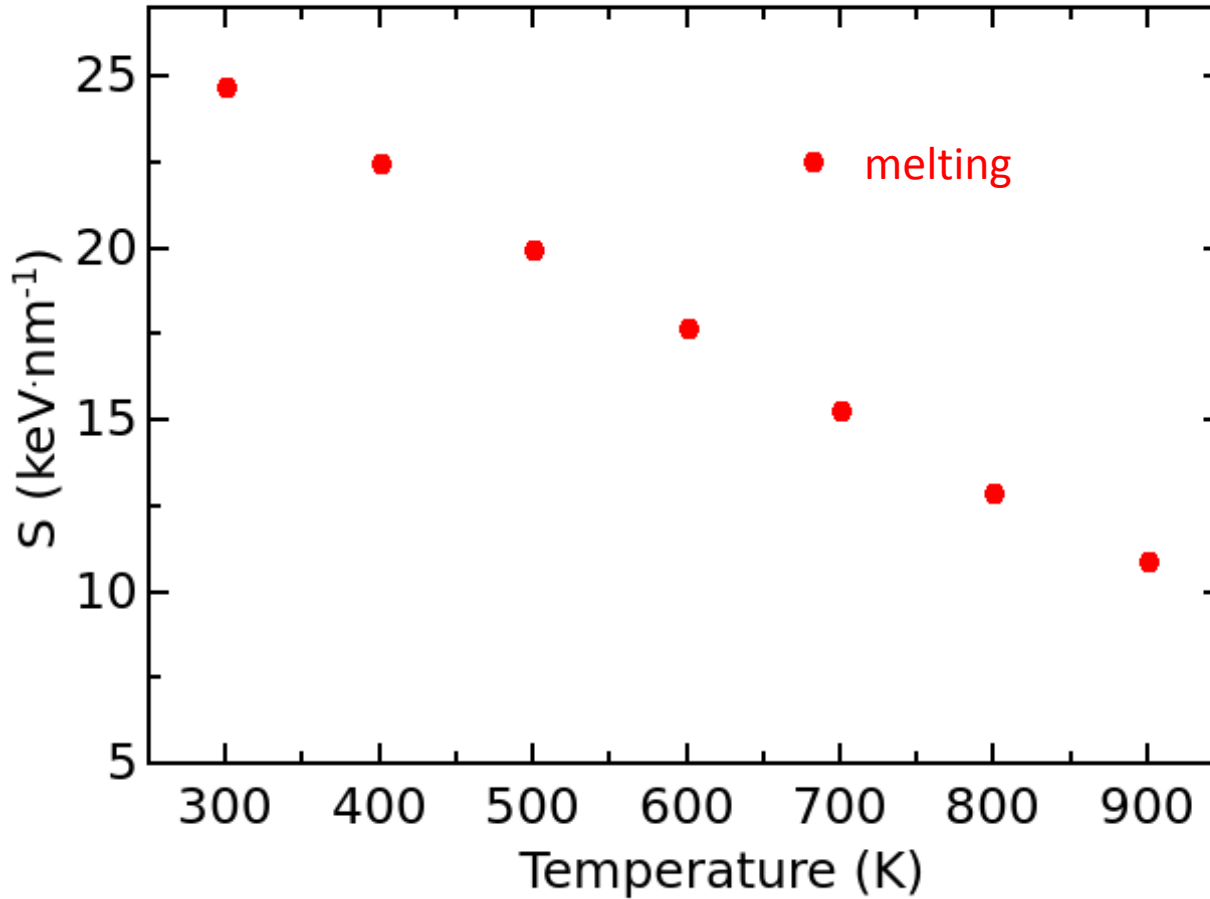
High temperature U-Mo alloy γ structure



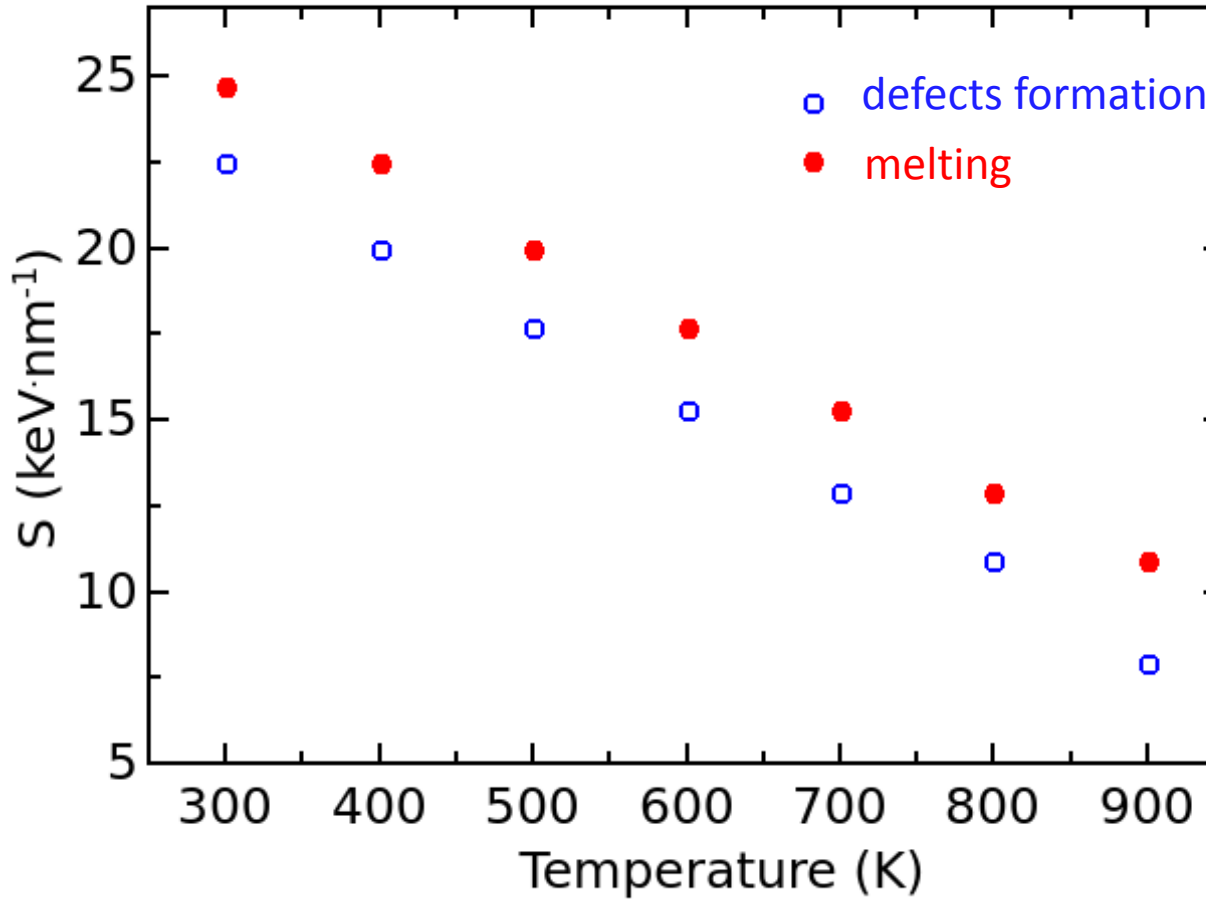
Empty atoms show position of SIA in quasi-bcc lattice of γ -phase (basic cell is shown by blue solid atoms).



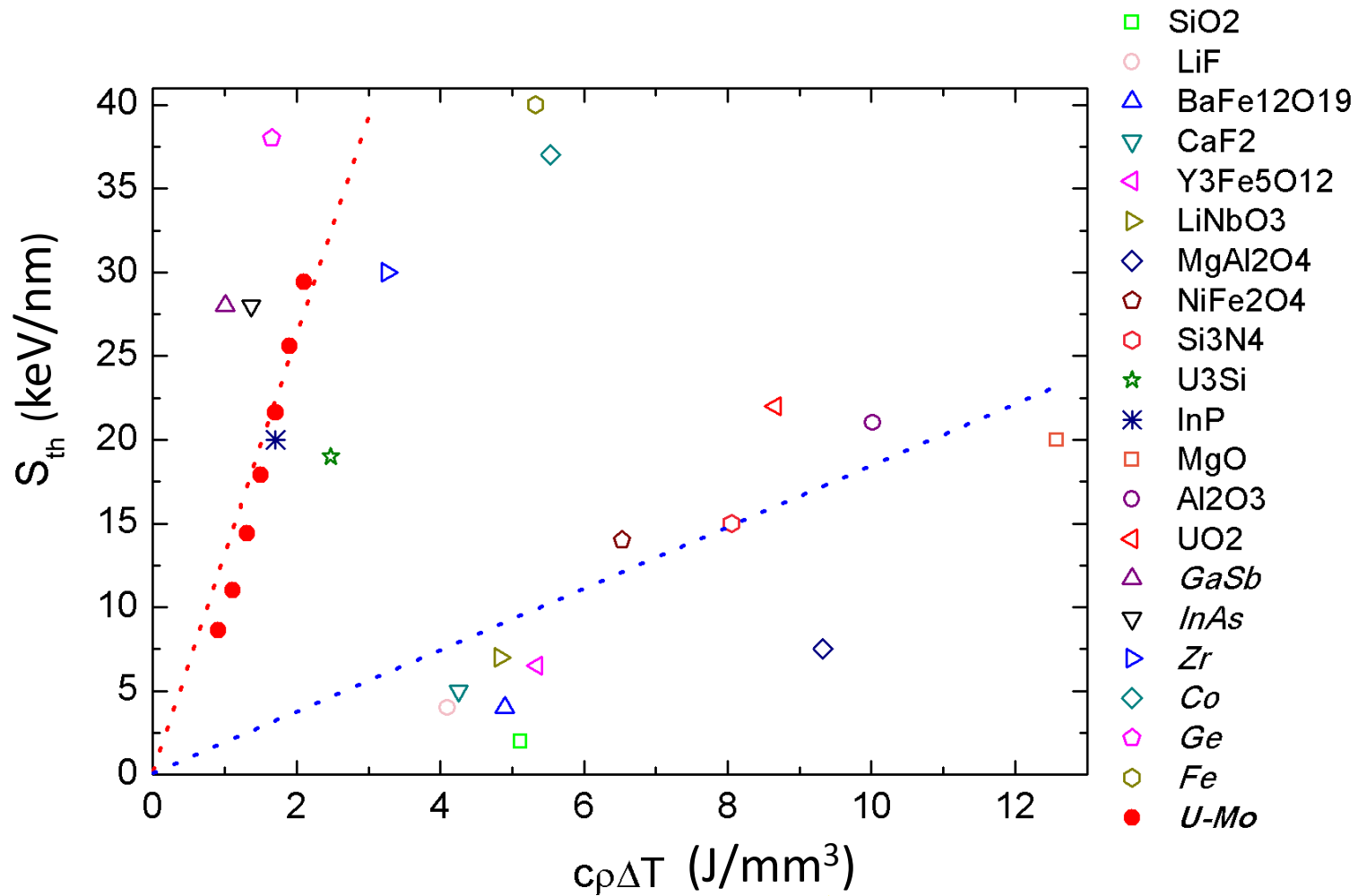
The threshold stopping power of swift ions dependence on temperature



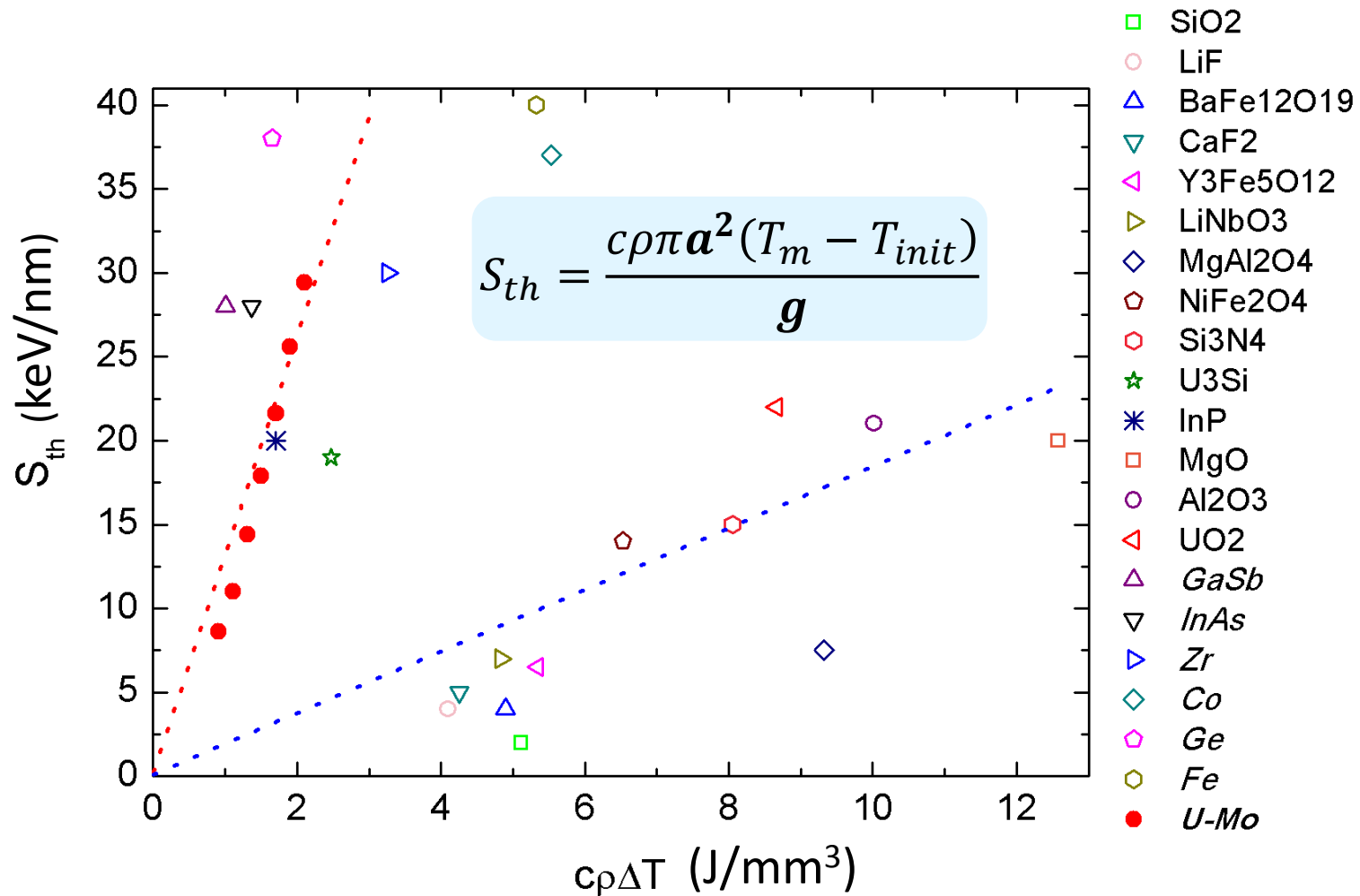
The threshold stopping power of swift ions dependence on temperature



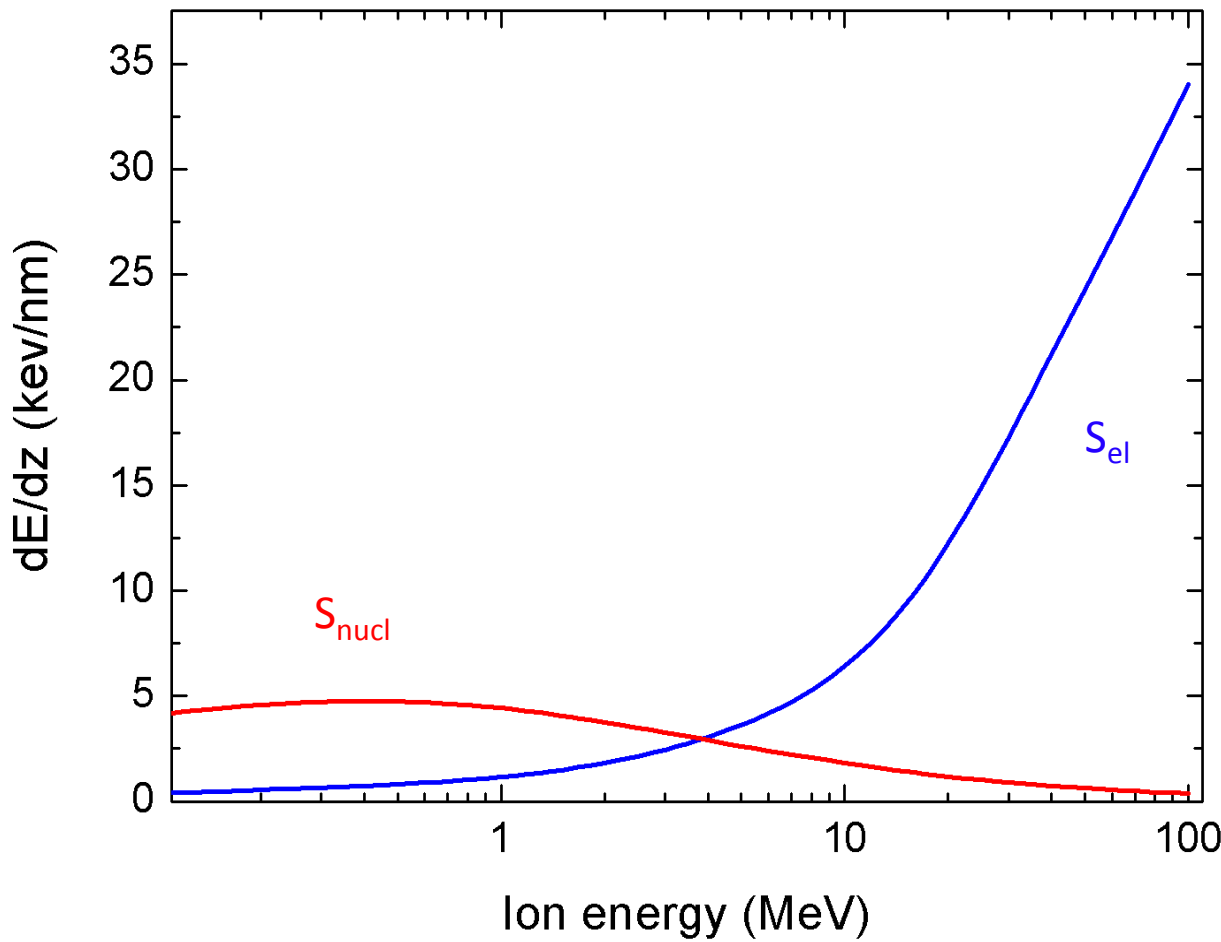
The threshold stopping power of swift ions dependence on temperature



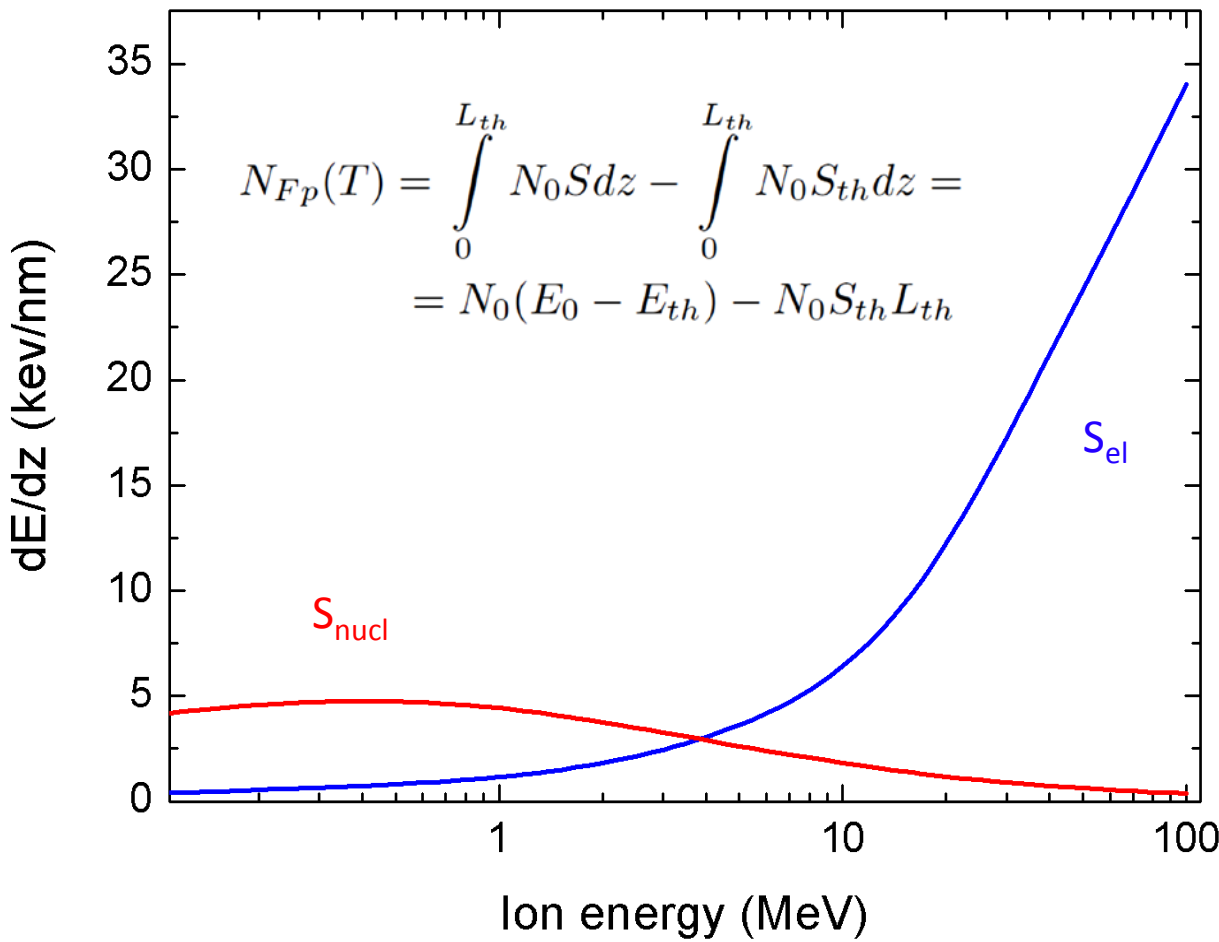
The threshold stopping power of swift ions dependence on temperature



The number of Frenkel pairs dependence on temperature

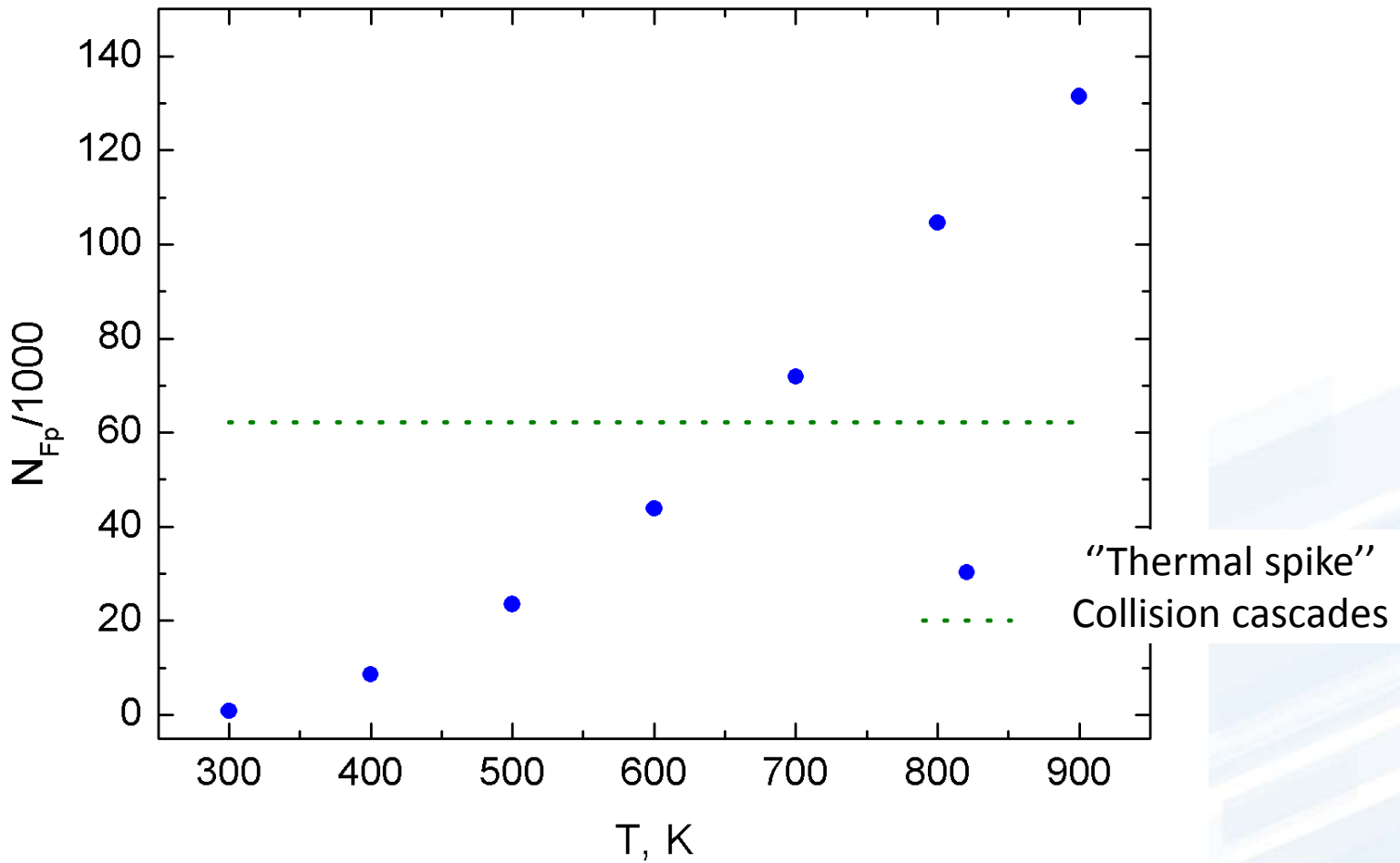


The number of Frenkel pairs dependence on temperature



$$N = N_0(S - S_{th})$$
$$N_0 \approx 2 \text{ keV}^{-1}$$

The number of Frenkel pairs dependence on temperature



TTM parameters

Test

Main

$$C_e(T_e)\rho_e \frac{\partial T_e}{\partial t} = \nabla(\kappa_e \nabla T_e) - g_p(T_e - T_i)$$

$$g_p = 4,5 \cdot 10^{17} \text{ Bm}^{-1}\text{K}^{-1}$$

$$g_p = 6,5 \cdot 10^{17} \text{ Bm}^{-1}\text{K}^{-1}$$

$$\rho_e = 0,625 \text{ e}\text{\AA}^{-3}$$

$$C_e = \gamma T_e$$

$$\gamma = 1,37 \cdot 10^{-9} \text{ эВК}^{-2}\text{e}^{-1}$$

$$\gamma = 4,0 \cdot 10^{-9} \text{ эВК}^{-2}\text{e}^{-1}$$

$$\kappa_e = D_e \rho_e C_e$$

$$D_e = 25 \text{ \AA}^2 \text{ фс}^{-1}$$

$$D_e = 10 \text{ \AA}^2 \text{ фс}^{-1}$$

Ni and W

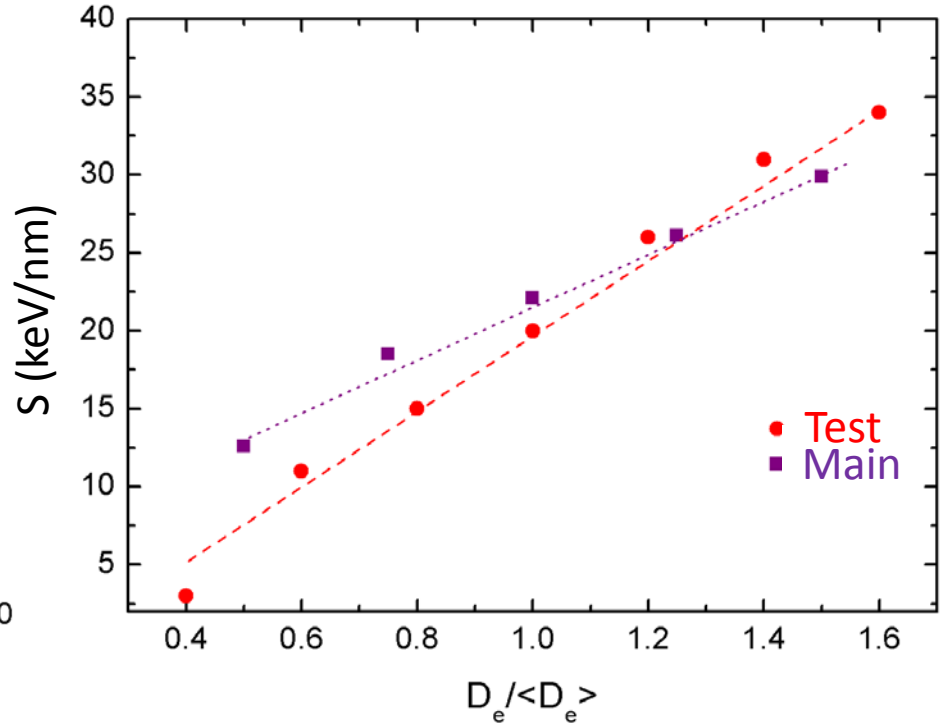
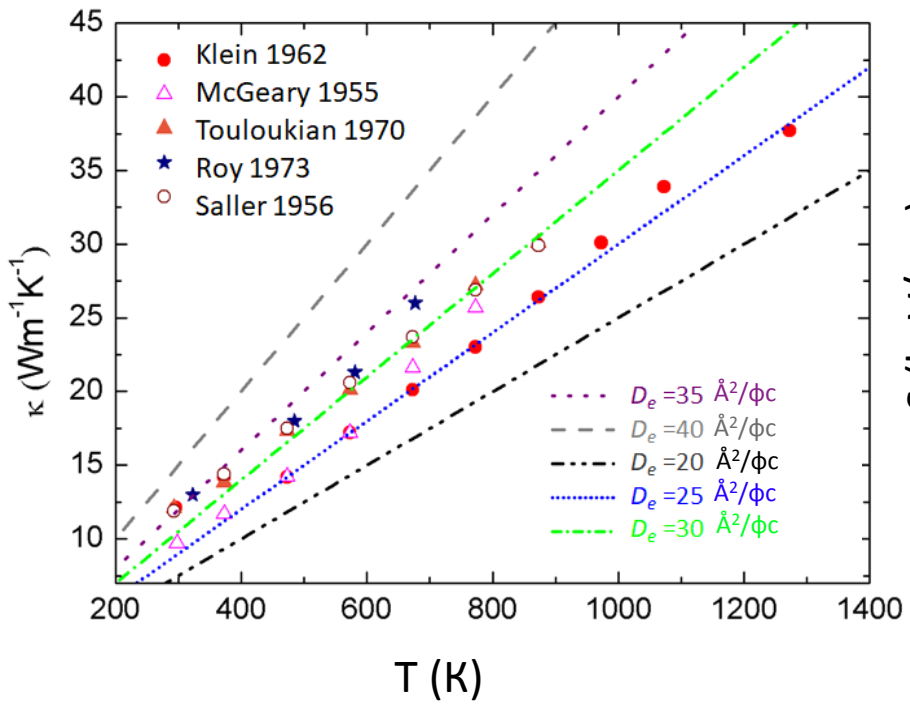
Lin Z, Zhigilei L V et al 2008
J. Phys. Rev. B **77** 075133

$$\vec{F}_j = -\nabla_j U(r_1, \dots, r_n) + F_j^{lang}(T_e - T_i)$$

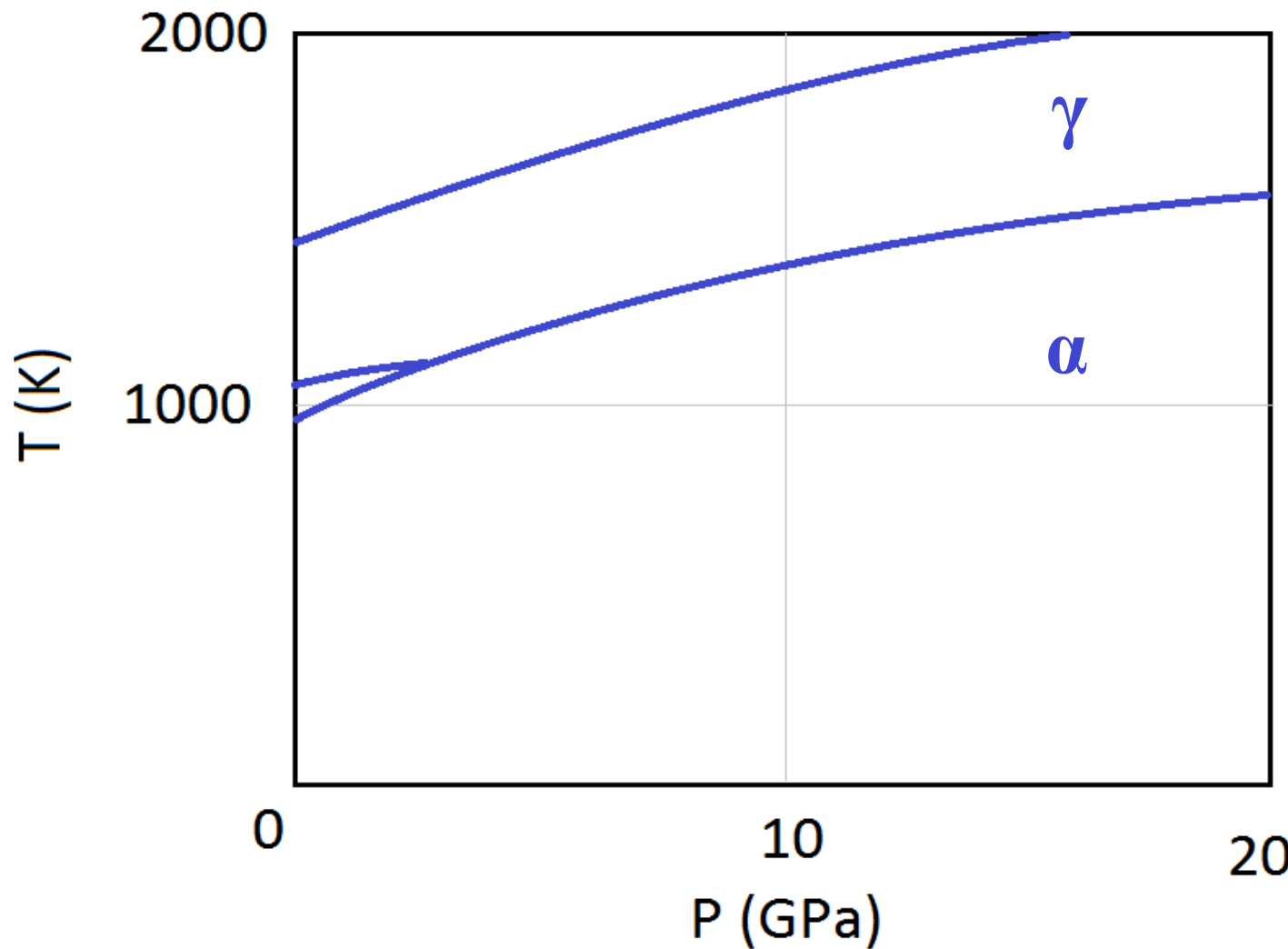
Z. Li, C. Wang et al 2017
J. Phys. Plasmas **24** 022703

TTM parameters

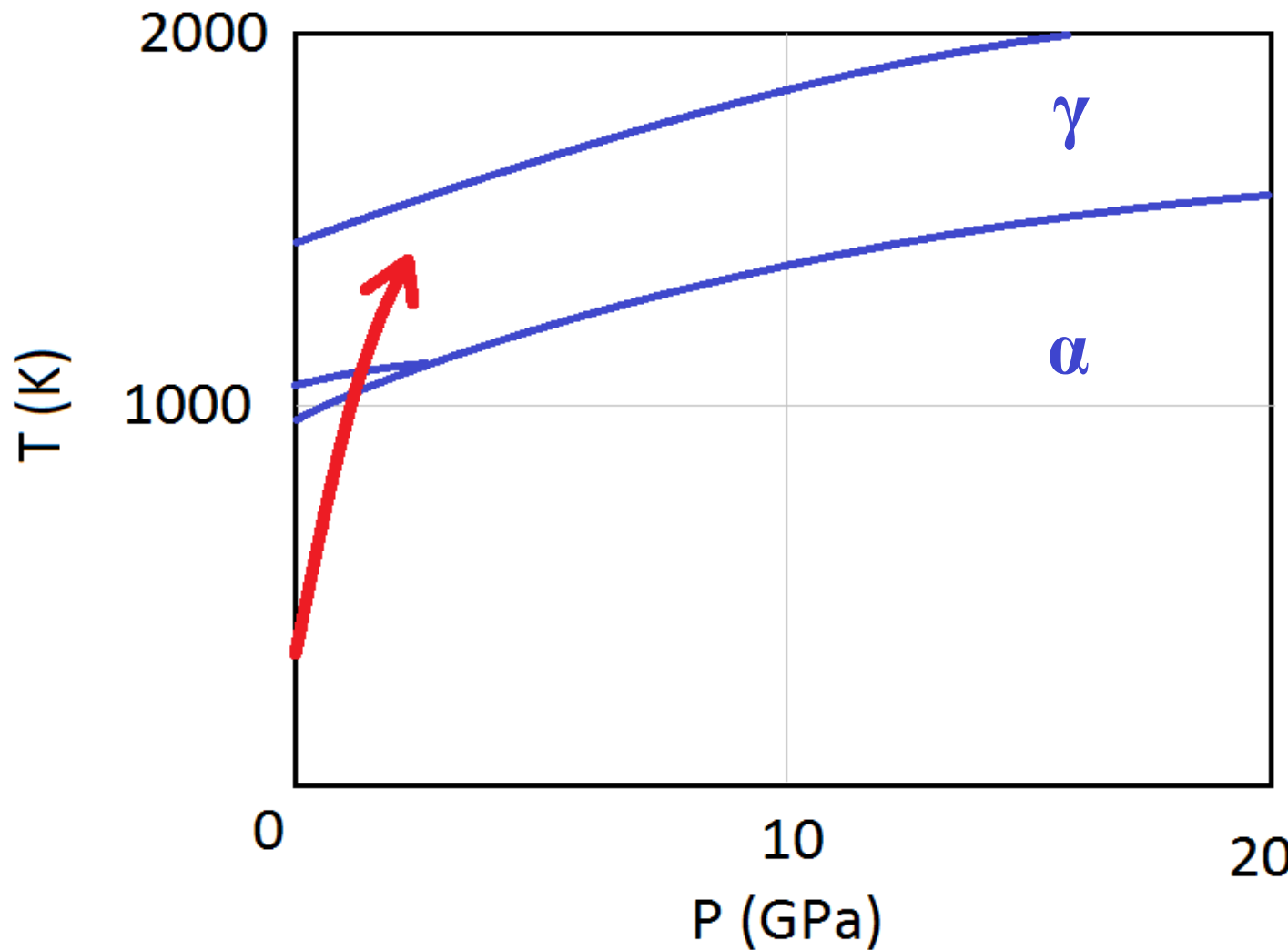
The threshold stopping power



The track formation in α -phase



The track formation in α -phase

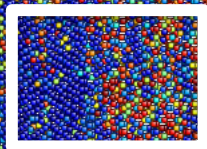


The track formation in α -phase

α

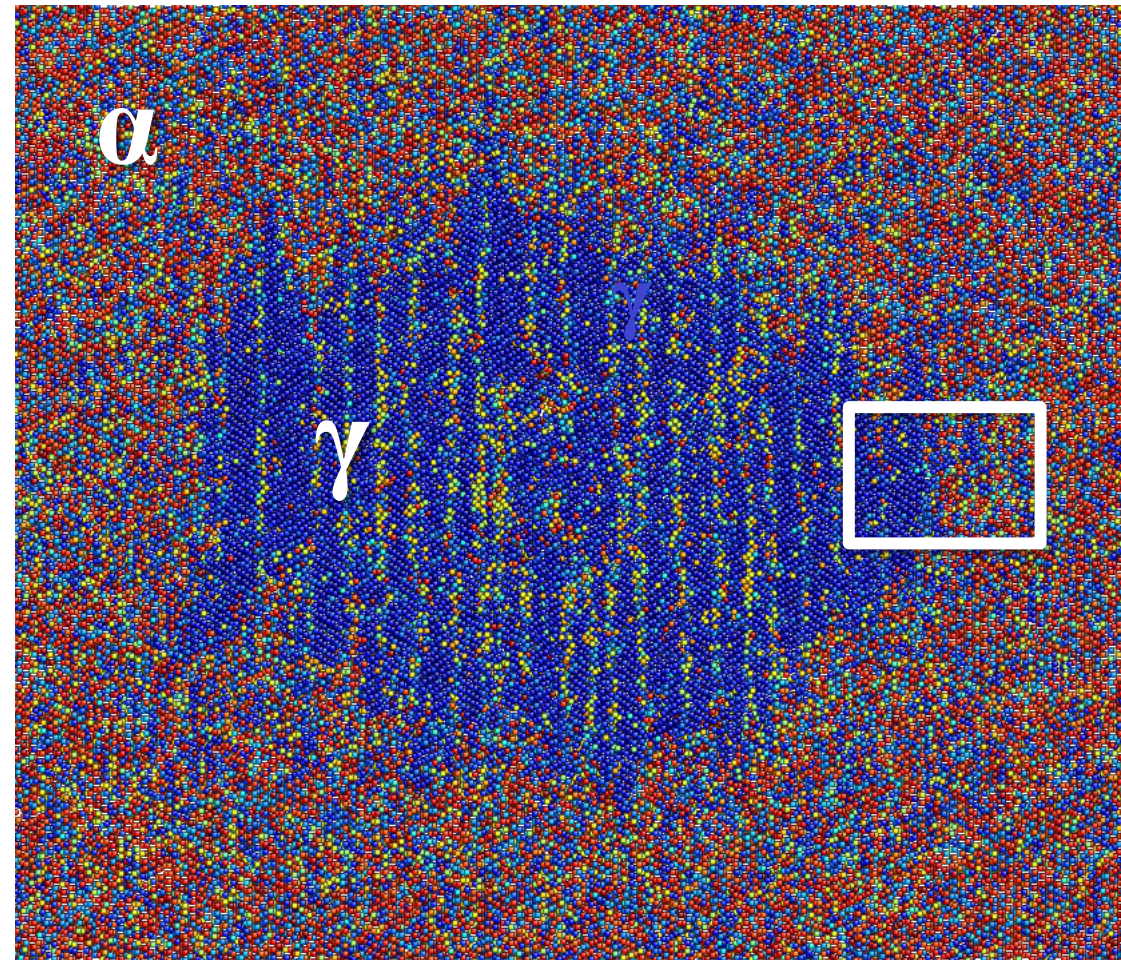
γ

γ



Threshold stopping power

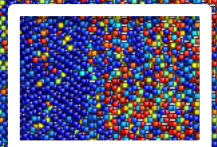
$$dE/dz = 16 \text{ keV/nm}$$



The track formation in α -phase

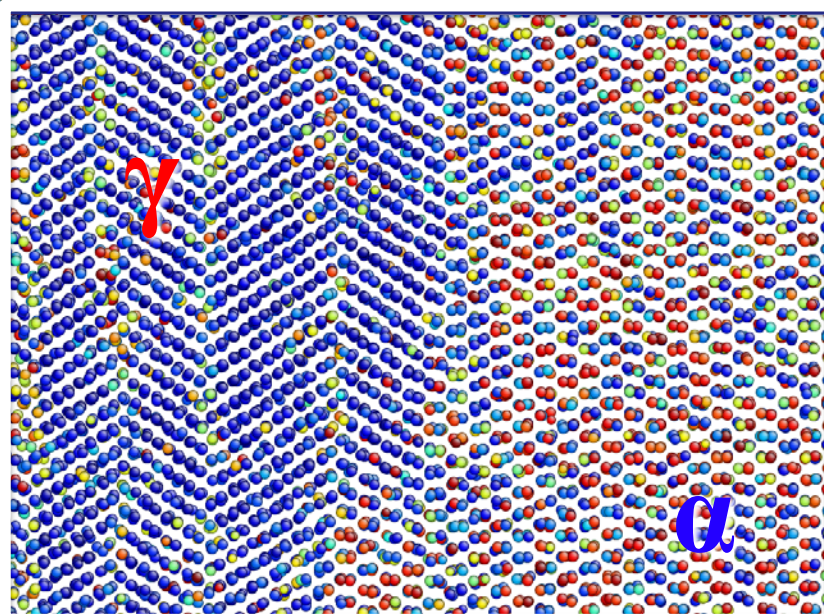
α

γ



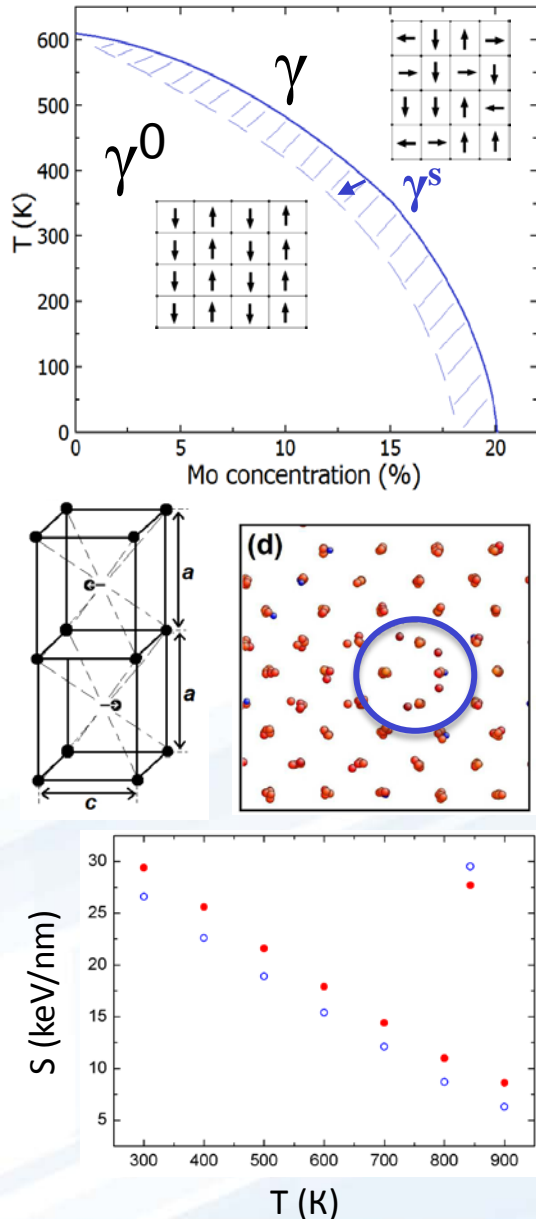
Threshold stopping power

$$dE/dz = 16 \text{ keV/nm}$$

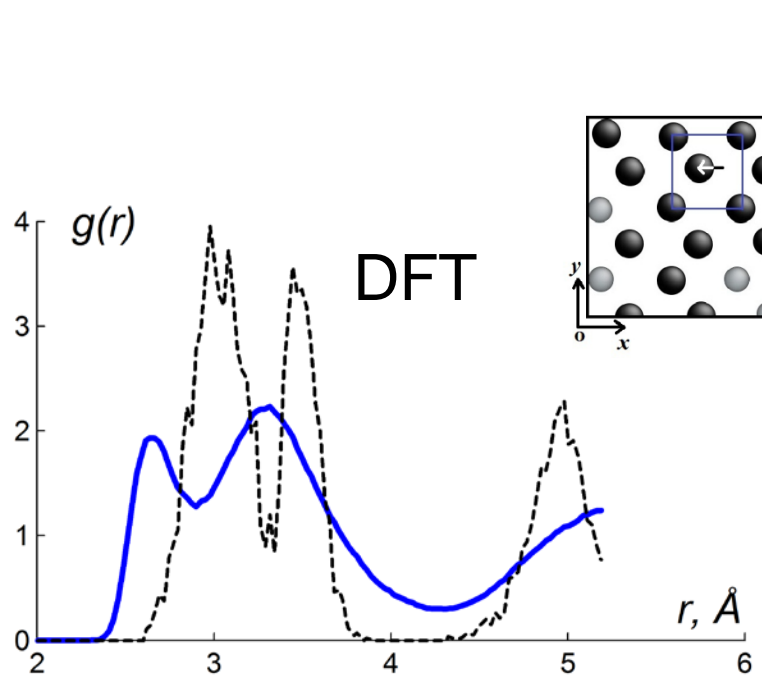


Conclusions

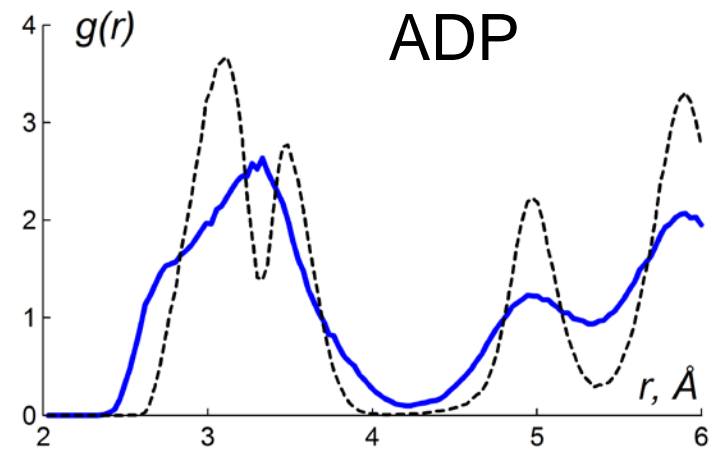
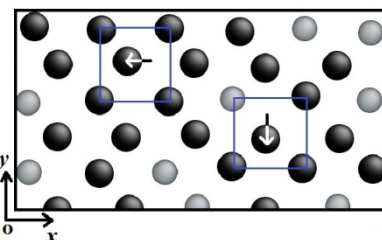
- ✓ The structure of high-temperature γ -phase locally reflects features of γ^0 -phase
- ✓ The martensitic transformation $\gamma \rightarrow \gamma^0$ is quite similar to an atoms rearrangement at ferro- to paraelastic transition of order-disorder type
- ✓ The simulation results indicate that the defects formation in U-Mo may be produced without melting and subsequent crystallization
- ✓ The number of primary radiation defects formed at stage of thermal spike is comparable to the number of primary radiation defects formed in collision cascades, but the number of such defects is weakly dependent on temperature



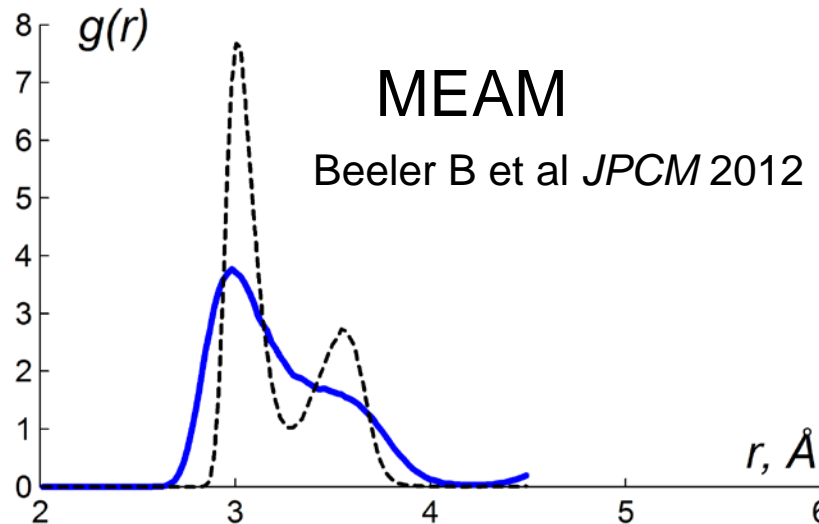
Radial distribution functions of γ -U (T=1000K)



DFT



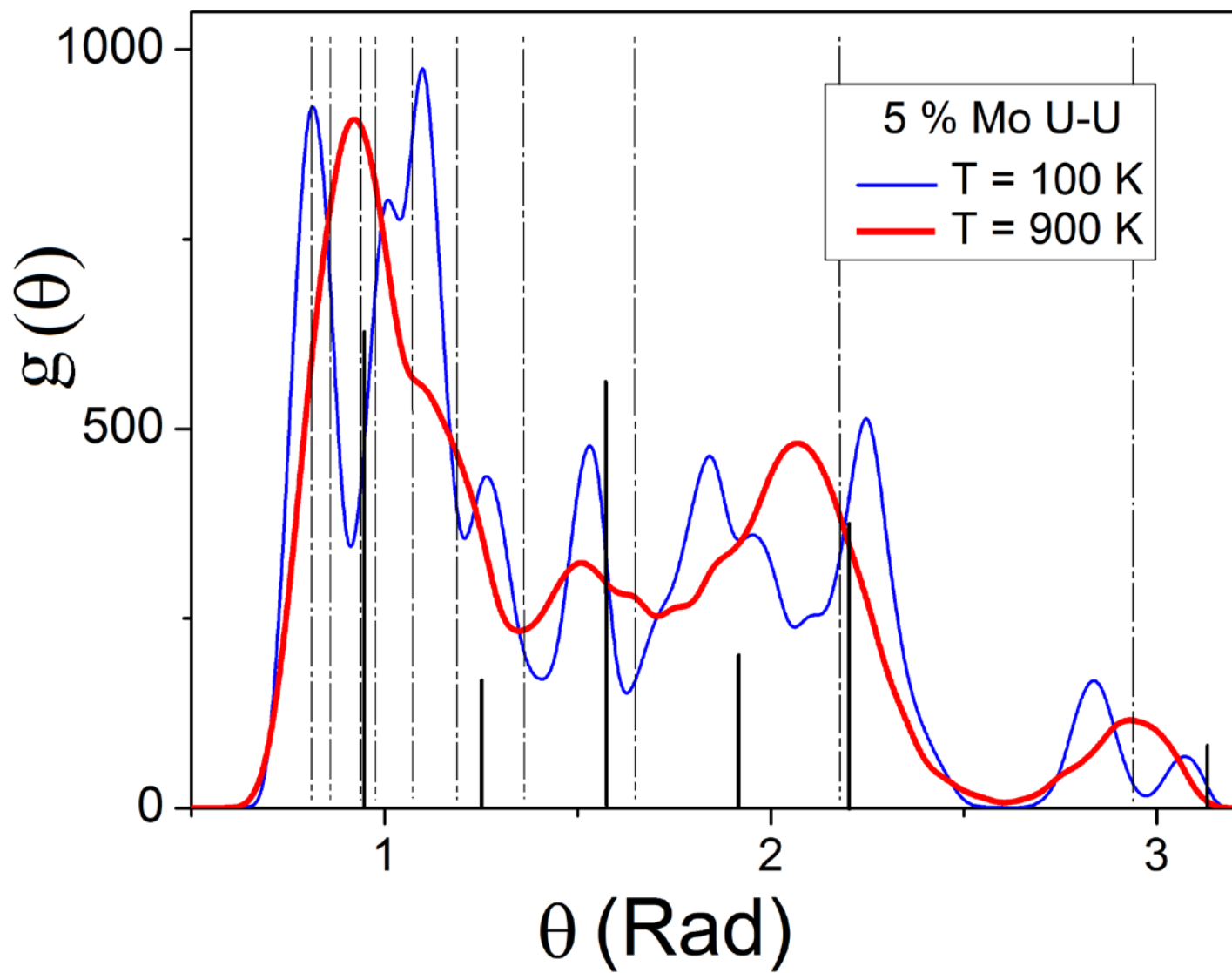
ADP



MEAM

Beeler B et al *JPCM* 2012

— RDF $G(r)$
- - - Averaged RDF $G(<r>)$

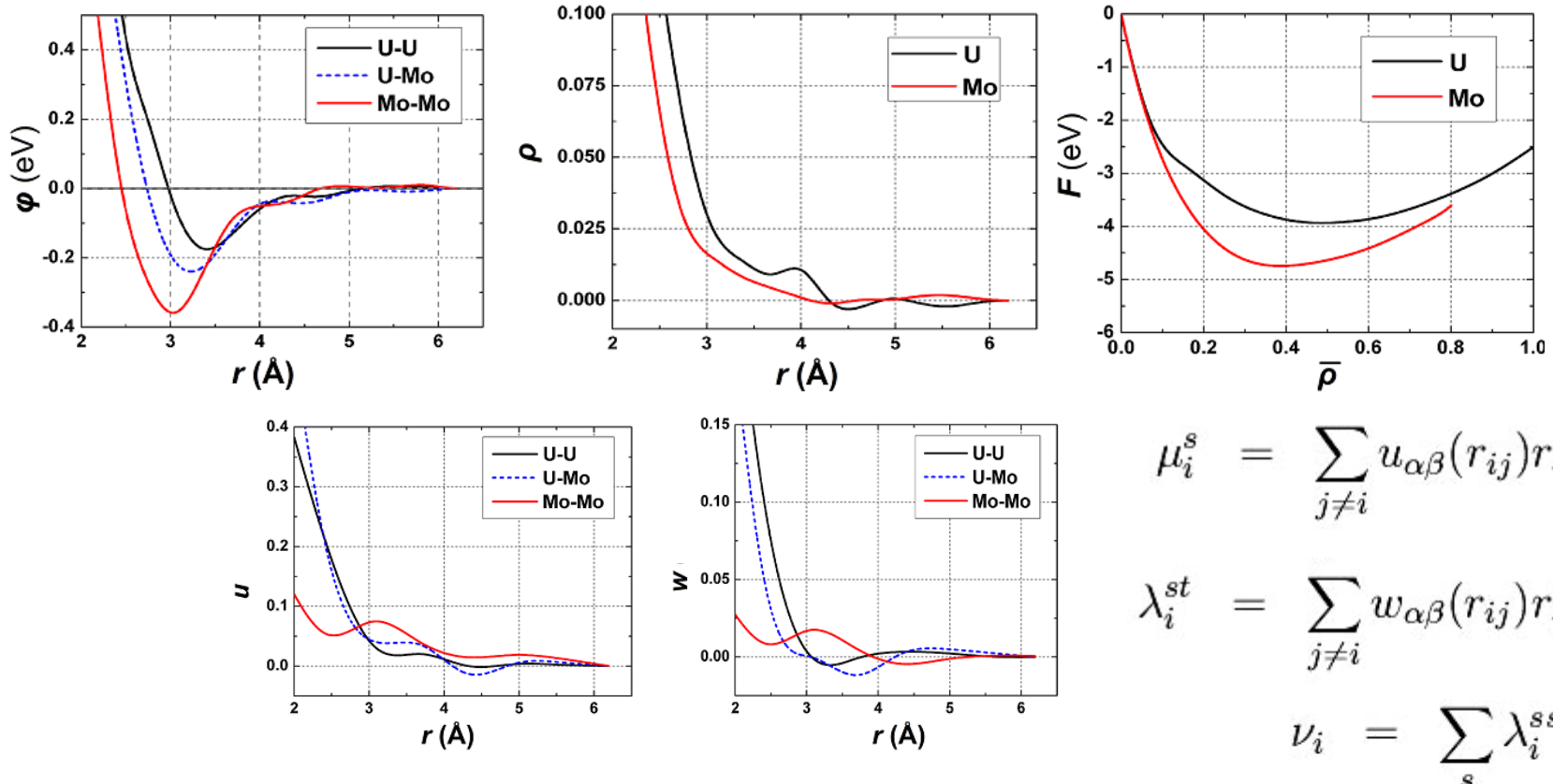


Потенциал для описания системы U-Mo:

ADP — Angular-dependent potential:

$$E_i = F_\alpha \left(\sum_{j \neq i} \rho_\beta(r_{ij}) \right) + \frac{1}{2} \sum_{j \neq i} \phi_{\alpha\beta}(r_{ij}) + \frac{1}{2} \sum_s (\mu_i^s)^2 + \frac{1}{2} \sum_{s,t} (\lambda_i^{st})^2 - \frac{1}{6} \nu_i^2$$

ADP: Y. Mishin, Mehl et al 2005 Acta Mater 53 4029



$$\mu_i^s = \sum_{j \neq i} u_{\alpha\beta}(r_{ij}) r_{ij}^s$$

$$\lambda_i^{st} = \sum_{j \neq i} w_{\alpha\beta}(r_{ij}) r_{ij}^s r_{ij}^t$$

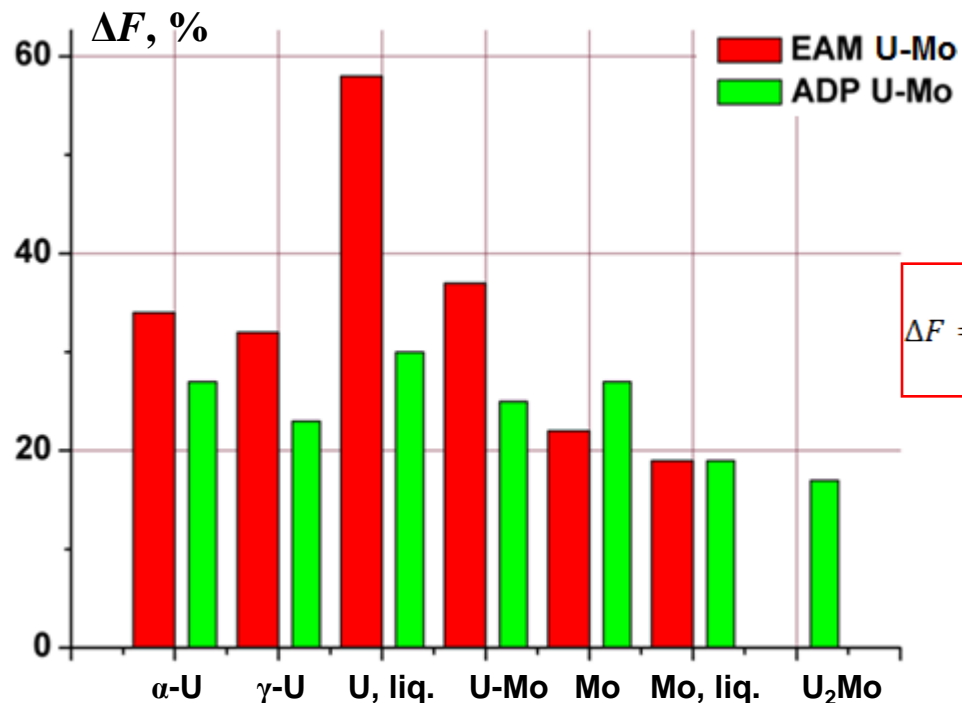
$$\nu_i = \sum_s \lambda_i^{ss}$$

Потенциал для описания системы U-Mo:

ADP — Angular-dependent potential:

$$E_i = F_\alpha \left(\sum_{j \neq i} \rho_\beta(r_{ij}) \right) + \frac{1}{2} \sum_{j \neq i} \phi_{\alpha\beta}(r_{ij}) + \frac{1}{2} \sum_s (\mu_i^s)^2 + \frac{1}{2} \sum_{s,t} (\lambda_i^{st})^2 - \frac{1}{6} \nu_i^2$$

ADP: Y. Mishin, Mehl et al 2005 Acta Mater 53 4029



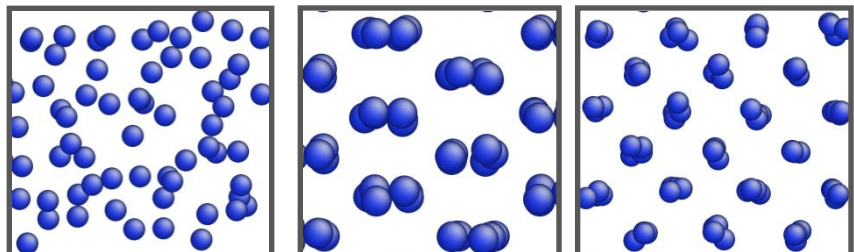
$$\Delta F = \frac{1}{N} \sum_{i=1}^N \sqrt{\frac{(F_{ADP}^i - F_{DFT}^i)^2}{(F_{DFT}^i)^2}} \times 100, \%$$

EAM: Smirnova D. E., Kuksin A. Y., Starikov S. V. et al. // MSM Sci. Eng. 2013. V. 21. P. 035011.

ADP: Smirnova D. E., Kuksin A. Y., Starikov S. V. //JNM. 2015. V. 458. Pp. 304-311.

$$\begin{aligned} \mu_i^s &= \sum_{j \neq i} u_{\alpha\beta}(r_{ij}) r_{ij}^s \\ \lambda_i^{st} &= \sum_{j \neq i} w_{\alpha\beta}(r_{ij}) r_{ij}^s r_{ij}^t \\ \nu_i &= \sum_s \lambda_i^{ss} \end{aligned}$$

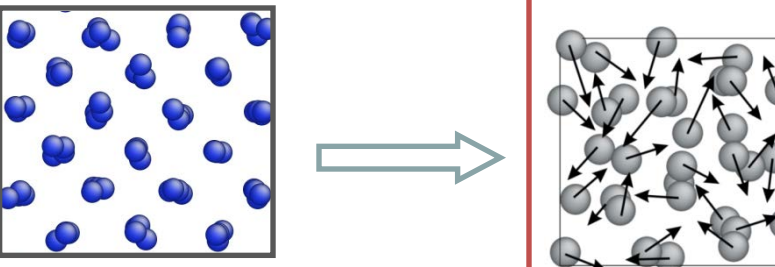
Метод «согласования по силе»:



Расплав U

$\alpha\text{-U}$

$\gamma\text{-U}$



VASP

$$\mathbf{F}_i = -\frac{\partial E}{\partial \mathbf{R}_i}$$

$$E = \frac{\langle \varphi_n | \mathbf{H} | \varphi_n \rangle}{\langle \varphi_n | \varphi_n \rangle}$$

F, E, S

potfit

$$Z_F = \sum_{i=1}^{N_\alpha} \sum_{\alpha=x,y,z} \sqrt{\frac{(F_{ADP}^i - F_{DFT}^i)^2}{(F_{DFT}^i)^2}}$$

Потенциал межатомного взаимодействия (ADP):

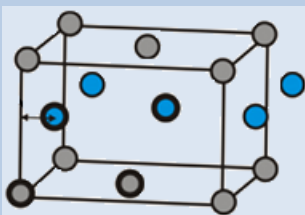
$$E_i = F_\alpha \left(\sum_{j \neq i} \rho_\beta(r_{ij}) \right) + \frac{1}{2} \sum_{j \neq i} \phi_{\alpha\beta}(r_{ij}) + \frac{1}{2} \sum_s (\mu_i^s)^2 + \frac{1}{2} \sum_{s,t} (\lambda_i^{st})^2 - \frac{1}{6} \nu_i^2$$

Верификация потенциала путем расчета большого набора характеристик материала и сопоставления результатов с экспериментальными данными

Force-matching: F. Ercolessi, J.B. Adams 1994 *EPL* **26** 583 **VASP 5.2:** G. Kresse 1996 *Phys. Rev. B* **54** 11169

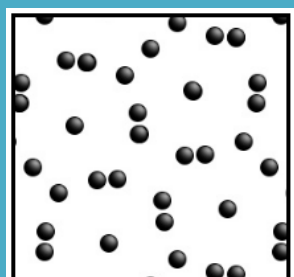
Potfit: P. Brommer, F. Gahler F 2006 *Phil. Mag.* **86** 753 **ADP:** Y. Mishin, Mehl et al 2005 *Acta Mater.* **53** 4029

Verification of created ADP potential (pure U)



$\alpha\text{-U}$	a (Å)	b (Å)	c (Å)	C_{11} (GPa)	C_{22} (GPa)	C_{33} (GPa)	C_{12} (GPa)	C_{13} (GPa)	C_{23} (GPa)
ADP U-Mo	2.849	5.841	4.993	253	199	265	93	90	105
<i>Experiments</i> [*]	2.854	5.870	4.955	215	199	267	46	22	108

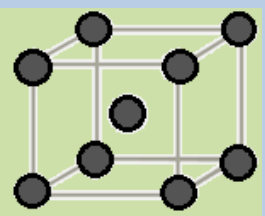
* C. Barrett et al. Phes. Rev. **129** (1963) 625



$\beta\text{-U}$	symmetry	a (Å)	c (Å)	$E_\beta - E_\alpha$ (eV/atom)	T_{tr} (K)
ADP U-Mo	P4 ₂ nm	10.612	5.603	0.089	780
<i>Experiments</i>	P4 ₂ nm	10.590	5.634	> 0	1045
<i>Calculations (GGA)</i>	P4 ₂ nm	10.460	5.660	0.099	—

Experiment: C. Tucker and P. Senio, Acta Crystallographica **6** (1953) 753760

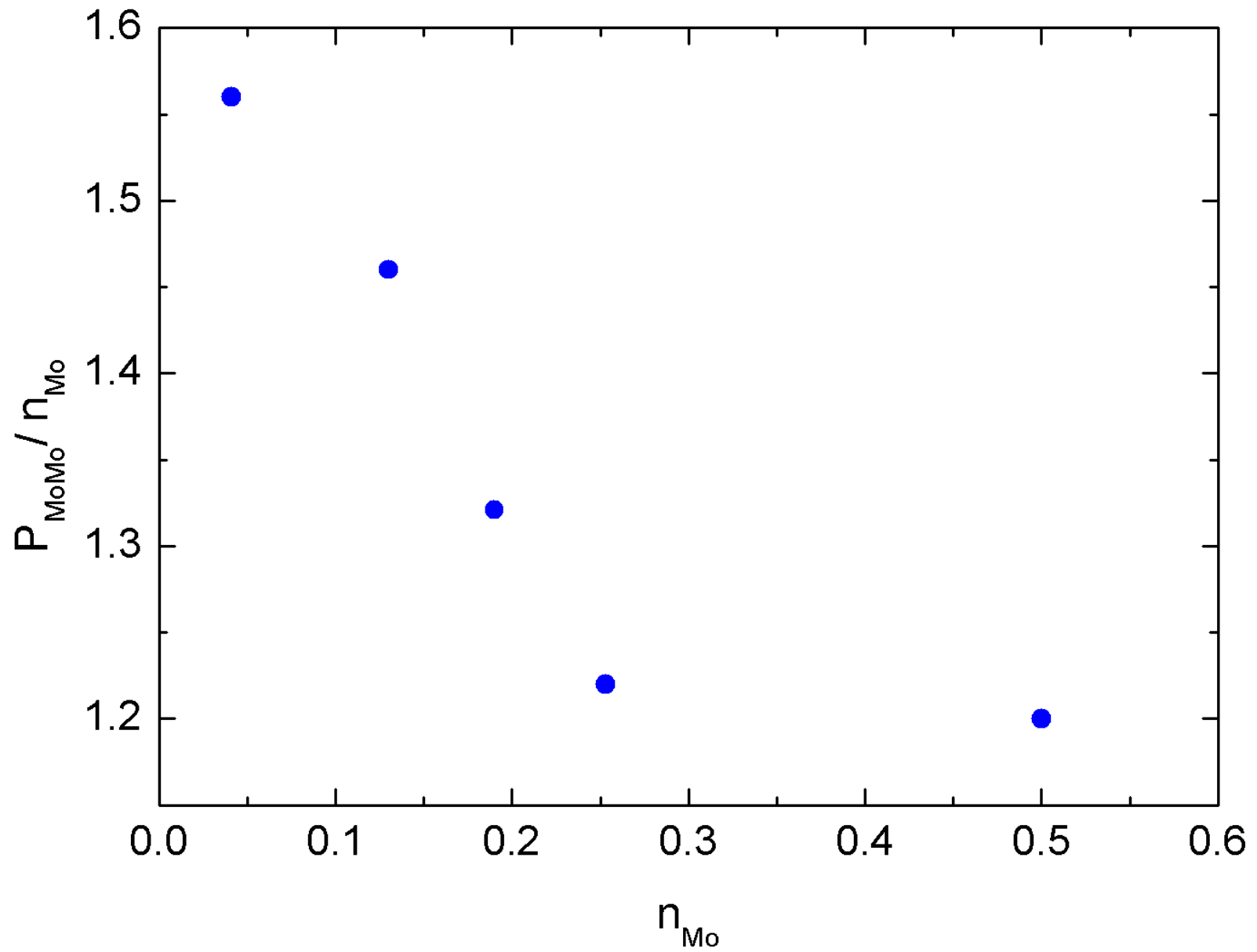
GGA: Y. Li et al. JNM **475** (2016)

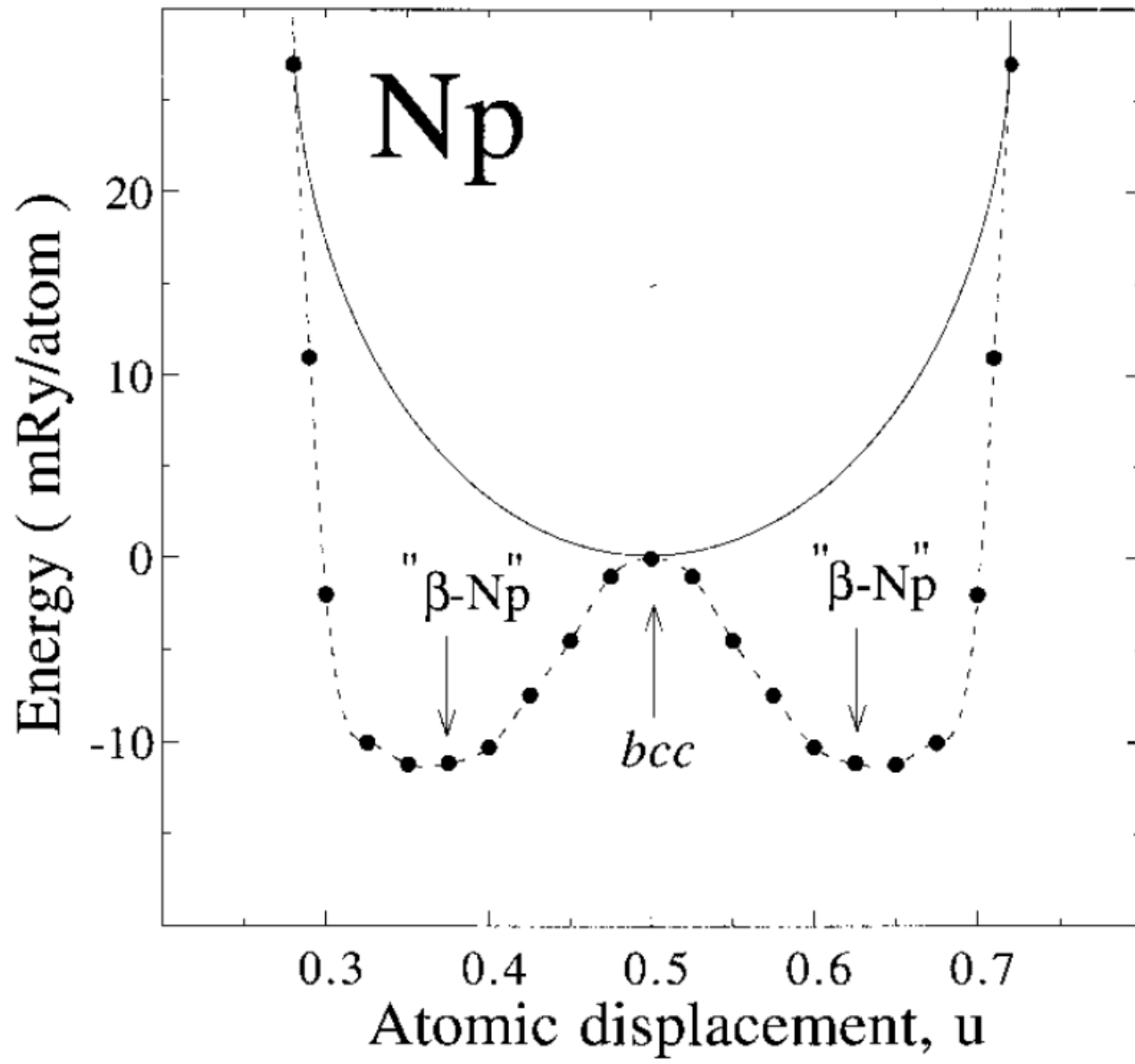


$\gamma\text{-U}$ ($T=1000\text{K}$)	a (Å)	B (GPa)	$E_{bcc} - E_\alpha$ (eV/atom)	T_{melt} (K)	E_{vac}^t (eV)
ADP U-Mo	3.52	120	0.072	1330	2.1
<i>Experiments</i>	3.47	113	> 0	1408	0.9 – 1.45
<i>Calculations (GGA)</i>	3.43	136	0.28	—	1.2

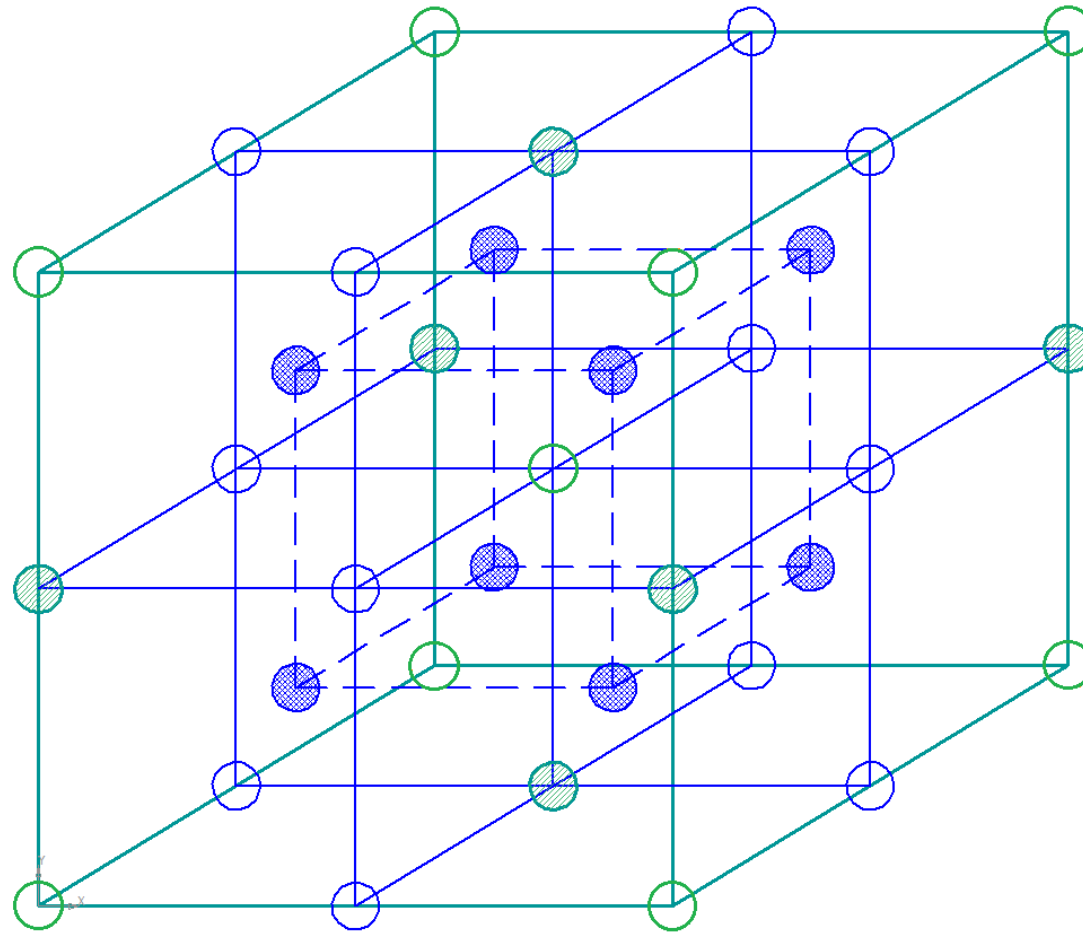
Experiment: C.-S. Yoo et al. Phys. Rev. B. **57** (1998) 10359.

GGA: Y. Li et al. JNM **475** (2016)

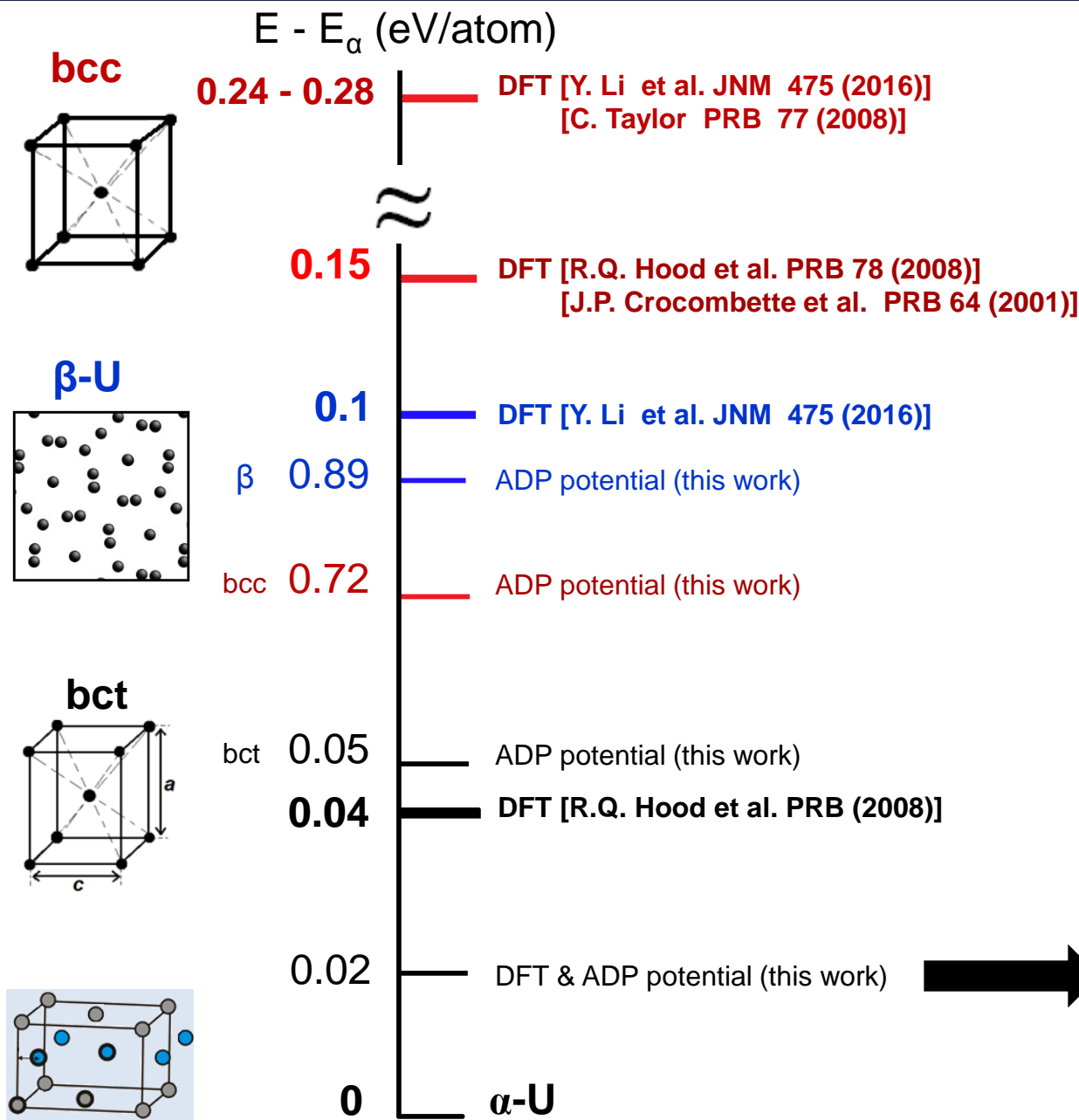




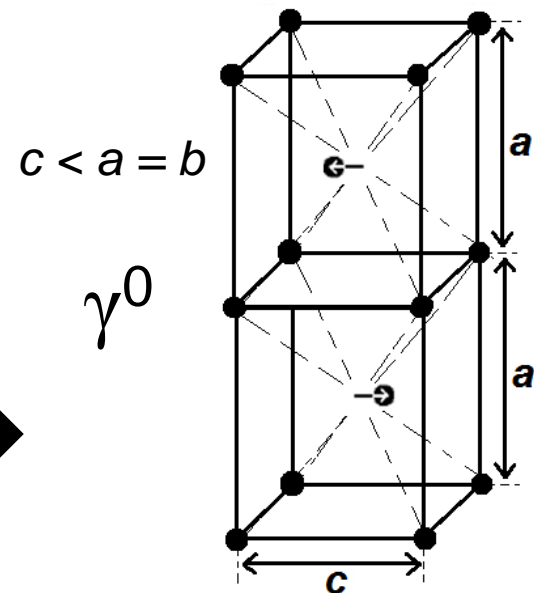
γ^s structure

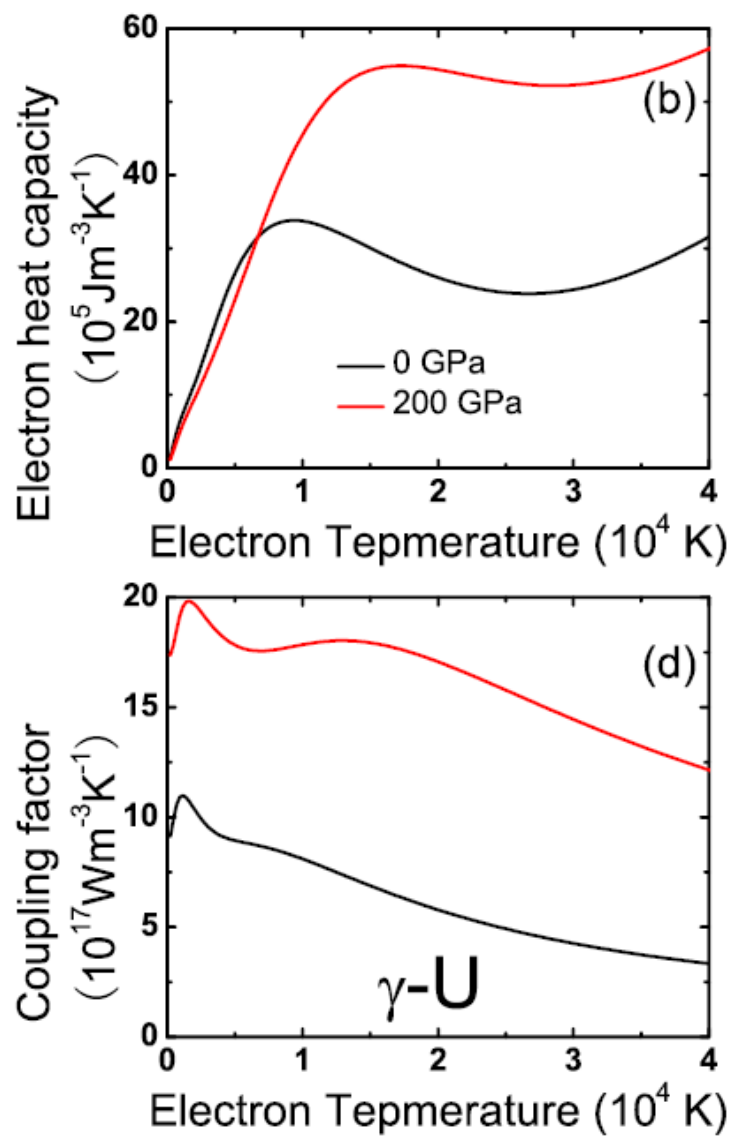


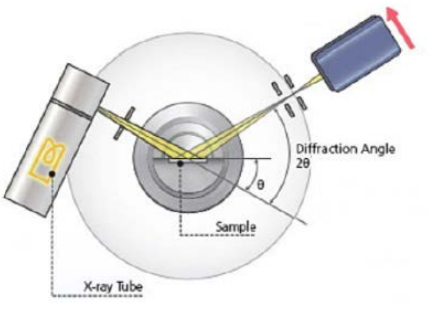
Energy hierarchy of phases in pure uranium



Experimentally observed phase for the alloys
 [K. Tangri and G.I. Williams, JNM 4 (1961)]
 [B.W. Howlett, JNM 35 (1970)]
 [H.L. Yakel, JNM 33 (1969)]
 [N.T. Chebotarev et al. Atomnaya Energiya 48 (1980)]







- 1) В обратном пространстве задается сетка расчетных точек.
- 2) Интенсивности рассеяния рассчитываются в узлах сетки. Если расчетная точка не совпала с узлом обратной решетки (где интенсивность велика), то весомого вклада в пункте 3 она не даст.
- 3) Происходит суммирование по узлам с равными углами рассеяния.
- 4) 2-3 повторяются на заданных шагах интегрирования, происходит усреднение.

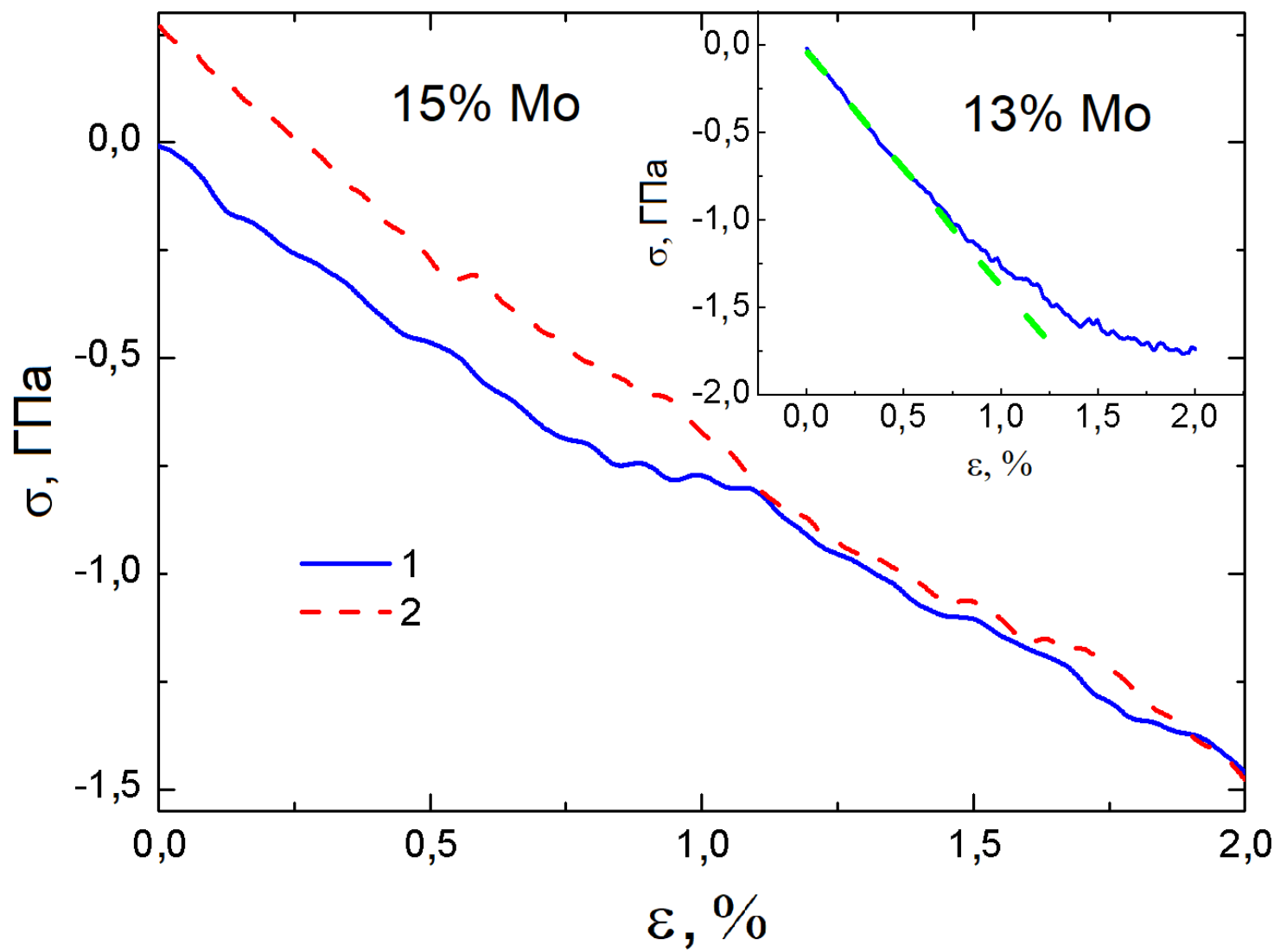
$$\mathbf{A} = 2\pi \frac{[b, c]}{(a, b, c)}, \mathbf{B} = 2\pi \frac{[c, a]}{(a, b, c)}, \mathbf{C} = 2\pi \frac{[a, b]}{(a, b, c)}, \quad \mathbf{K}_{hkl} = h\mathbf{A} + k\mathbf{B} + l\mathbf{C}$$

$$\mathbf{k} - \mathbf{k}' = \mathbf{K}_{hkl}$$

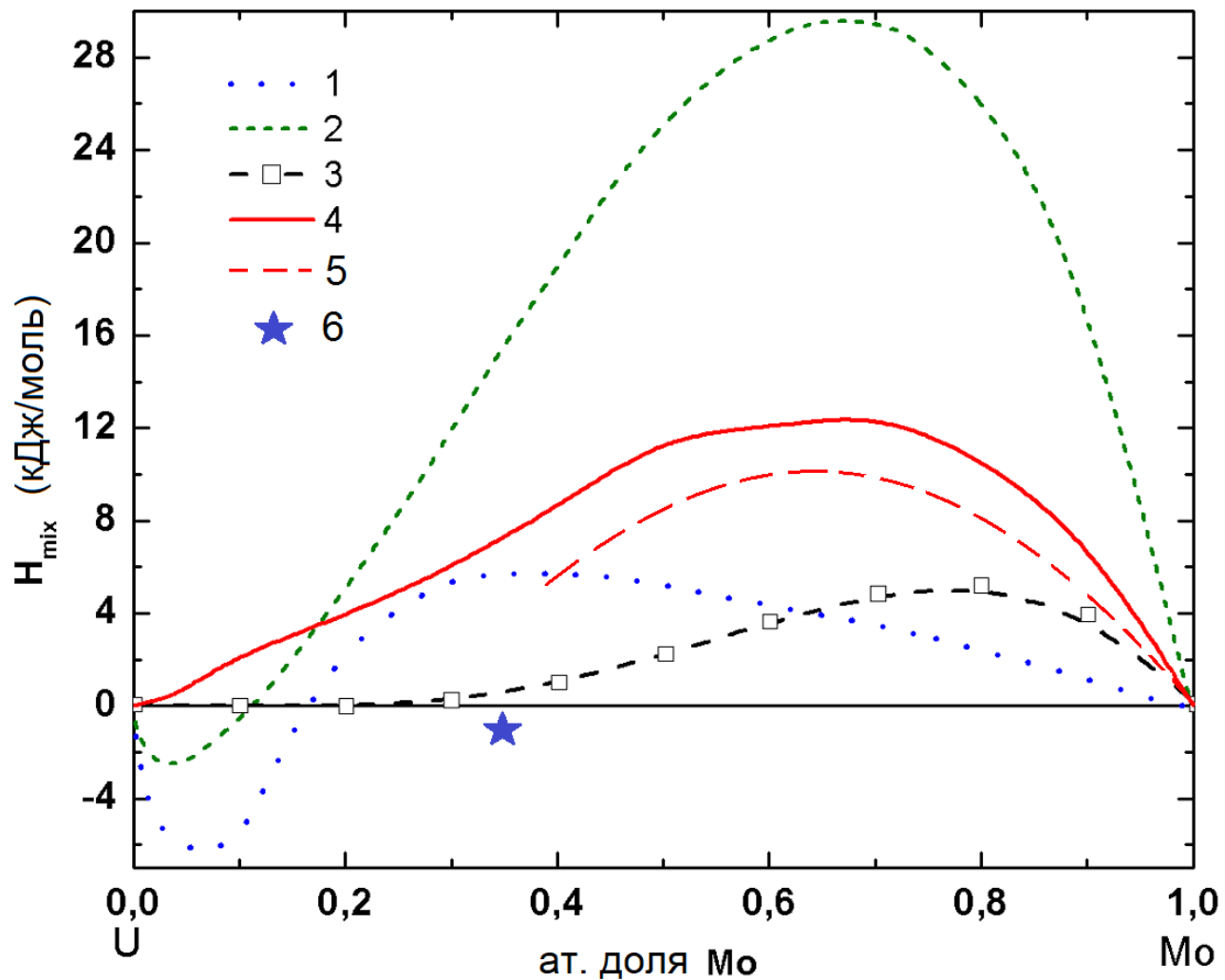
$$I = P(\theta) F F^*$$

$$F = \sum_{j=1} f_j(\theta) \exp \{-2i\pi \mathbf{r}_j \cdot \mathbf{K}_{hkl}\} = \sum_{j=1} f_j(\theta) \exp \{-2i\pi(x_j h + y_j k + z_j l)\},$$

$$\mathbf{r}_j = x_j \mathbf{a} + y_j \mathbf{b} + z_j \mathbf{c} \qquad \qquad \sin(\theta) = \frac{\lambda |\mathbf{K}|}{2} = \frac{\lambda}{2d_{hkl}},$$



Enthalpy of mixing of U-Mo alloy



Conclusions

- ✓ The simulation results indicate that the defects formation in U-Mo may be produced without melting and subsequent crystallization
- ✓ The threshold stopping power of swift ions dependence on temperature was obtained
- ✓ The number of primary radiation defects formed at stage of thermal spike is comparable to the number of primary radiation defects formed in collision cascades, but the number of such defects is weakly dependent on temperature

